$\mathcal{N} = 1$ supersymmetric Yang-Mills theory and adjoint QCD on the lattice

Dissertation

zur Erlangung des akademischen Grades
doctor rerum naturalium (Dr. rer. nat.)

vorgelegt dem Rat der Physikalisch-Astronomischen Fakultät
der Friedrich-Schiller-Universität Jena

von M.Sc. Juan Camilo López Vargas
geboren am 24.04.1990 in Medellin

Gutachter

1. Dr. habil. Georg Bergner (Friedrich-Schiller-Universität Jena)

2. Prof. Dr. Agostino Patella (Humboldt-Universität zu Berlin)

3. Dr. David Schaich (University of Liverpool)

Tag der Disputation: 08.10.2020

Abstract

In this work we study the low-energy physics of Yang-Mills theory coupled to adjoint matter by means of lattice Monte Carlo simulations. A main ingredient of our computations is the Yang-Mills gradient flow, which is a gradient flow in field space. The kernel of the flow operator smoothens the fields in such a way that correlators of local operators can be computed avoiding divergences and extra multiplicative renormalisations. The flow kernel can also be related, under some specific conditions, to a renormalisation group transformation. This property allows to compute the scaling dimensions of operators, with respect to variations of the energy scale. We exploit these two properties of the gradient flow in order to study non-perturbative properties of Yang-Mills with adjoint fermions.

First, we study the case when the Yang-Mills field is coupled to a single adjoint fermion. This model is the $\mathcal{N} = 1$ supersymmetric Yang-Mills theory. It is the only QCD-like supersymmetric theory in the sense that it has no scalars, is asymptotically free, has a low-energy mass-gap, is confining and shows fermion condensation. We study these properties at zero and finite temperatures for the $SU(2)$ and $SU(3)$ gauge groups. With the gradient flow we are able to confirm the formation of a non-vanishing chiral condensate at zero temperature and its melting at higher temperatures. We also observe that chiral symmetry restoration and deconfinement occur at the same critical temperature. We moreover investigate $SU(3)$ supersymmetric Yang-Mills on $\mathbb{R}^3 \times \mathbb{S}^1$ with periodic boundary conditions for the fermions at different compactification radii. We compare the fate of confinement with the thermal case, and measure the trace of the energy-momentum tensor, which gives us information about the Witten index.

The second part of this work is devoted to N_f adjoint QCD, i.e. Yang-Mills theory coupled to N_f adjoint fermions. Depending on the number of flavours, adjoint QCD may lie inside the conformal window and thus become a strongly interacting conformal field theory in the infrared. In this context we use the gradient flow and the lattice in order to measure the scaling of the mass anomalous dimension, as the energy scale is lowered. The goal is to see signals of conformal behaviour and to determine the value of the anomalous dimension at the critical point, which is important within the scope of beyond the Standard Model theories.

Zusammenfassung

Wir untersuchen die Eigenschaften von Yang-Mills-Theorien mit Fermionen in der adjungierten Darstellung bei niedrigen Energien mittels Monte-Carlo Gitter-Simulationen. Hierbei spielt die sogenannte Gradient-Flow-Methode (GF), oder Gradientenfluss, eine prominente Rolle. Zum einen werden Quantenfelder durch den Kern des GF-Operators so geschmiert, dass Korrelatoren von lokalen Operatoren endlich bleiben und im Fall der Eichfelder keine zusätzliche Renormierung nötig ist. Zum anderen kann der Kern des Gradientenflusses unter speziellen Umständen als Teil einer Renormierungsgruppentransformation (RG) betrachtet werden. Somit ermöglicht die GF-Methode die Berechnung der Skalierung verschiedener Operatoren als die Energieskala verändert wird.

Zunächst beschäftigen wir uns mit der supersymmetrischen Yang-Mills-Theorie bzw. Yang-Mills-Theorie mit einem einzigen adjungierten Majorana Fermion. Dieses Modell ist der Quantenchromodynamik (QCD) sehr ähnlich, da es keine elementaren Skalarfelder beinhaltet, es asymptotisch-frei ist und es ein Mass-Gap zeigt. Es besteht außerdem das Quark-Confinement und die spontane Brechung der chiralen Symmetrie bei niedrigen Energien. Wir untersuchen diese Eigenschaften bei verschiedenen Temperaturen für die Eichgruppen $SU(2)$ und $SU(3)$. Mithilfe der GF-Methode bestätigen wir die Entstehung eines nicht-verschwindenden Fermionen-Kondensats bei $T = 0$ und sein Schmelzen bei höheren Temperaturen. Darüber hinaus finden wir, dass die Phasenübergänge zum Deconfinement und zur Wiederehestellung der chiralen Symmetrie an derselben kritischen Temperatur geschehen. Im Fall der $SU(3)$ Eichgruppe beschäftigen wir uns außerdem mit der Theorie definiert auf dem Zylinder $\mathbb{R}^3 \times \mathbb{S}^1$ und mit periodischen (d.h. nicht-thermischen) Randbedingungen für die Fermionen. Wir erkunden das Confinement im Vergleich zum thermischen Fall und messen die Spur des Energie-Impuls-Tensors, welcher Rückschlüsse auf die Realisierung der Supersymmetrie anhand des Witten-Index ergibt.

Der zweite Teil dieser Arbeit ist der Yang-Mills-Theorie mit mehr als einem Fermion gewidmet, der sogenannten adjungierten QCD. Je nach der Anzahl an Fermionen kann die Theorie im Infrarotbereich stark wechselwirkend sowie konform bzw. skaleninvariant werden. Wir verwenden die GF-Methode, um die Skalierung der anomalen Dimension des Massenoperators zu untersuchen, wenn die Energieskala variiert wird. Das Ziel ist Hinweise auf skaleninvariantes Verhalten zu erkennen und den kritischen Wert der anomalen Dimension im Limes der unendlichen Gradientenfluss-Zeit zu bestimmen, welcher im Rahmen der Erweiterungen des Standardmodells relevant ist.

Contents

Chapter 1

Introduction

Emergent collective phenomena are perhaps as intriguing as the question about what the fundamental bricks of Nature are. The sought after a logical explanation of how matter and time arise and evolve, has played a pivotal role in all societies throughout millennia. It underlies both the ancient natural philosophy and the more recent discovery of the Higgs boson. Already the earlier Greek and Indian-Buddhist philosophers imagined the Universe as being composed of different invisible and indivisible *atoms* moving in *void*. Comparatively, we talk today of a very precise and finite number of elementary particles. However, and in spite of this similitude, our world-view has since then substantially changed. Our comprehension of the elementary bricks of Nature distinguishes itself greatly from the ancient atomism, not because we can actually *measure* the particles but because of two fundamental facts: interactions and emergence. Both are essential ingredients of the current most successful framework to describe the Universe at small scales: Quantum Field Theory (QFT). We currently see particles as particular states of quantum fields, which are objects with infinite strongly interacting fluctuating degrees of freedom.

We confront ourselves with *emergence*, when we meet the laws of thermodynamics for the first time. They are universal, they require no specific knowledge about the microscopic degrees of freedom of a given material. Something similar happens in hydrodynamics. We learn that a small number of parameters suffices to describe a system, and we don't need to characterise every single of the millions of atoms that constitute it. The microscopic world thus influences the phenomena occurring at larger scales in a very particular way. As we go from smaller to larger scales only some information prevails, while much gets washed out. Being able to put the theory of scales into a solid theoretical framework has been one of the greatest achievements in the history of physics: The Renormalisation Group (RG). The RG is a systematic way to go from the micro to the macro, which has been pioneered by Kenneth G. Wilson in the 1970s [1]. The RG allows us to ask what microscopic features are relevant and which become irrelevant as we change the scale. Moreover it addresses the question about the limits where the scaling ceases: the fixed points. If we could zoom in all the way down to scales smaller than the

smallest known particle, perhaps, at some point, the picture doesn't change anymore and all we would see is the fabric of the space-time. If we could zoom out and see the Universe as a whole, perhaps we would see that the clusters of galaxies just build self-similar structures, whose picture doesn't change as we move to larger distances. These extremal situations are fixed or scale-invariant points. In between the points there is a seemingly hierarchical structure: elementary particles, atoms, molecules, proteins, cells, humans, societies, planets, the visible Universe. Each of these realms can then be described by a scale-dependent effective model. Thanks to the RG, the concepts of statistical continuum limit and universality were properly understood. Universality means that two (or more) systems, which at small distances are very different from each other, have the same properties at larger scales. This led to a deep understanding of second order phase transitions in condensed matter physics. The concept behind the continuum limit is that the emergent large-scale physics of condensed matter systems can be modelled through QFT. In the 1970s QFT was also able to accurately explain the output of experimental particle physics. However, the problem of infinities appearing in the computations had a merely operational solution. With the RG it was understood that the infinities appeared as the signal of a lacking characteristic length in the system. For example, in QED, the solution is to introduce a scale at which one set the effective *renormalised* charge, defined through the measured interaction at that scale.

Also in the 20th century the way to describe *interactions* changed radically through the concept of gauge theories. According to this, forces between particles arise from vector fields or, equivalently, from the associated force-carrier particles. The canonical example of an (Abelian) gauge theory is the quantisation of Maxwell's theory, QED. Almost 70 years ago, Chen Ning Yang and Robert Mills formulated the theory of *local isotopic spin rotations*, today known as Yang-Mills theory (YM), in their paper [2]. Their theory models the nuclear interaction by generalising QED to a non-Abelian gauge theory, called QCD, where the gluon vector field interacts with itself and with the quarks. Gauge theories have an underlying rich geometry, which resembles the mathematical fundaments of Einstein's gravity. However, within the frame of QFT and RG, there is much more to tell. YM theory should be able to reproduce the short-range nuclear forces, however, as a non-Abelian generalisation of the Maxwell equations, it describes massless waves, which propagate at the speed of light. Having massless propagating modes is precisely what we want when describing the electromagnetic field. However, if we intend to describe the nuclear forces, this theory seems to be wrong. Puzzling enough, QCD correctly described the bunch of strongly interacting massive particles (hadrons) discovered by the 1970s. From the point of view of RG, this is actually not that surprising. Quarks and gluons are the degrees of freedom at very small scales, where the interaction is vanishingly small. This is the so-called *asymptotic freedom*, discovered by David Gross, Frank Wilczek and David

Politzer in 1973. According to this, at very short distances the YM theory becomes a non-interacting (or Gaussian) fixed point. In other words, at high energies the interactions are Coulomb-like, as in electromagnetism, and the gluons are massless waves. When we start zooming-out with the RG, the large-scale behaviour is determined by the interaction, which becomes larger and larger. At large distances, the lightest particle in the spectrum of QCD has a mass $\Delta > 0$. In this spectrum the gluons and quarks are inexistent as free states and are *confined* inside the hadrons. Also, the vacuum is dominated by pairs of condensed quarks. These three phenomena are still very poorly understood. One of the Millennium Prize Problems of the Clay Mathematics Institute is to *"prove that for any compact simple gauge group G, a non-trivial quantum Yang-Mills theory exists on $\mathbb{R}^4$ and has a mass-gap $\Delta > 0$"*[3]. Thus, we don't really understand *how* hadrons arise from gluons and quarks. To understand that is necessary for our modern world-view, since these particles make almost all of the visible Universe and thus we experience them every day.

These two observations on emergence and gauge theories suggest that the quest for the ultimate description of Nature is very subtle. The problems that emergence poses are as fundamental as the question of what the most elementary degrees of freedom are. Both are indeed intertwined. To find a high energy description of Nature, we must assure that it reproduces the effective theories of the phenomena we have learnt to understand in the last decades. But our understanding of the low energy also depends on relevant properties of the high energy degrees of freedom. In that sense, it is believed that the global geometry of the gauge fields have an impact on the origin of their low energy properties. In recent years also new proposals of emergence have appeared in the context quantum gravity through an interplay of information theory and gauge-gravity dualities [4], namely that the bulk space-time geometry (in the holographic sense) emerges from entanglement entropy (and quantum complexity) of the quantum fields [5, 6].

Also related to string theory is the *concept* of *supersymmetry* (SUSY), which allows to transform bosonic and fermionic degrees of freedom into each other. Mathematically, SUSY is a graded extension of the isometry transformations of the space-time. It has been part of many attempts to complete the Standard Model of particle physics by assigning a *superpartner* to every known particle. That fermion-boson symmetry or degeneracy leads to the cancellation of additive quadratic corrections to the mass of the Higgs boson, which is often seen as *unnatural*. Although a large portion of the high energy physics community were confident about the Large Hadron Collider at CERN to discover super-symmetric particles [1], this has not been the case and the hope for SUSY to be discovered near the electroweak (TeV) scale has pretty much vanished. Independently from the fact

---

[1]From 2000 until 2016 there was even a very famous bet among the leading scientists within high energy physics. The mathematical beauty of SUSY led some of them to lose a bottle of expensive Cognac on the non-discovery of SUSY particles by 2016.

of whether SUSY is part of Nature or not, SUSY QFTs can be very useful in order to understand how YM behaves at low energies. The reason is, roughly said, that the cancellation between fermionic and bosonic quantum corrections leads to the fact that many features at large scales can be exactly computed from classical contributions. A especial SUSY model is the so-called Super Yang Mills (SYM) theory, whose field content is the YM field plus its superpartner, the gaugino. This model shares many of the interesting low-energy properties of QCD and thus may help us understand the origin of rather enigmatic phenomena like quark confinement, quark condensation and a possible hidden underlying relation between them.

It turns out that coupling more than one gaugino to the YM field yields very interesting non-SUSY theories, also known as *adjoint QCD*. Depending on the number of gauginos, these theories become fixed points of the RG at very large distances, or may well have a very weak scale dependence. This latter property is essential within a family of *technicolour* theories, which are, like SUSY, possible extensions of the Standard Model of particle physics. These theories would solve the *unnaturalness* of having a fundamental scalar Higgs boson by adding a strong interaction at high energies. Beyond that, studying the evolution of adjoint QCD at low energies and their fixed points is an exciting subject by itself, as understanding gauge theories in general may be a key part into a deeper understanding of our Universe. This mere theoretical understanding is important, because of a difficulty that derives itself from the RG: if many of the short distance properties of a system become irrelevant at large distances, then looking after the theory of everything at our accessible energies may be out of reach. Especially the lack of experimental evidence for new physics makes the progress of theoretical physics, where experiments have historically played an essential role, especially difficult.

Yet, how can we tackle the difficulties of exploring the long distance properties of YM? Also the RG, and Wilson, are key in this regard. With them we learn that QFT can describe both elementary particles and also the emergent large-scale physics of condensed matter systems. Hence, we can re-formulate the QFT we are interested in, in such a way that it resembles a *finite* (strongly coupled and fluctuating) many body system. Then we can use the tools of statistical mechanics to solve it. The reformulation or discretisation is made in such a way that in the continuum limit, in the RG sense, the high energy theory is recovered. The main ingredient behind this so-called *lattice field theory* is to replace the space-time by a lattice and solve the finite system on a computer by means of Monte Carlo methods.

In this work we use lattice field theory in order to explore the emergent behaviour of SYM and adjoint QCD at large scales (i.e. low energies). In chapter 2 we introduce the foundations of YM, Wilson lines and instantons. Then in chapter 3 we give an overview on the most important aspects of the RG, which are relevant for our investigations. Also in

chapter 3 we introduce the conformal window, which is the range of number of gauginos with a low-energy fixed point. The generalities of SUSY, its algebra and the Witten index are introduced in chapter 4. After that, in 5 we focus on the low-energy properties of SYM: confinement, gaugino condensation and the chiral anomaly. Lattice field theory and Monte Carlo simulations are handled in chapter 6. In chapter 7 we introduce the Gradient Flow (GF). This is a method we combine with the lattice techniques. In classical YM, the GF is a flow towards the minima of the classical action. We will see that in QFT the GF is very useful. It allows to set a scale, to compute a renormalised coupling and to compute expectation values of local composite operators, like currents and densities. Moreover, under some circumstances, the GF can be related to the RG and thus it can facilitate the computation of the scaling behaviour of operators. In chapter 8 we present results of the thermal phase diagram of $SU(2)$ and $SU(3)$ SYM. In chapter 9 we explore confinement and the Witten index in $SU(3)$ SYM on a cylinder $\mathbb{R}^3 \times \mathbb{S}^1$ and compare the results with the thermal case. Finally, in chapter 10 we use the relation between the GF and the RG to compute the scaling of the mass anomalous dimension in adjoint QCD and its critical value at the fixed point.

Chapter 2

Yang-Mills theory

In the last decades YM theory has led to a cross-fertilisation between mathematics and theoretical physics. While in physics classical YM describes the high-energy regime of strong interactions, in mathematics it has led to important results in the characterisation of the topology of four-manifolds [7]. In this chapter we review classical YM theory, Wilson lines and the instantons. As we will encounter as we progress in this work, global (topological) features of the fields are believed to play an important role in the low-energy behaviour of YM theory. In most of the chapter we follow closely Ref. [8]. In the section about instantons we additionally take as reference the nice lecture notes found in [9].

2.1   Classical Yang-Mills theory

YM is a theory of principal $SU(N)$-bundles with a locally defined connection A, also called the gauge field, whose transition functions on the base manifold are gauge transformations. Hence, both A and objects constructed out of it, are globally well-defined. The connection lives on the tangent bundle at the group identity. In other words, it is in the Lie algebra $su(N)$ and can thus be written in the basis of Lie algebra generators T_i as

$$A_\alpha = A_\alpha^a T_a, \quad [T_a, T_b] = f_{ab}^c T_c, \quad \text{Tr}(T_a T_b) = \delta_{ab}. \tag{2.1}$$

From the connection we can find the curvature form $F = dA + A \wedge A$, which in turn defines the gauge invariant action functional

$$S_{\text{YM}} = \int_M (F \wedge \star F) = \int_M |F|^2 \, dV. \tag{2.2}$$

S_{YM} determines the dynamics through the principle of stationary action.

We call A a Yang-Mills field if it is a critical point of the action, i.e. if $d_A F = d_A(\star F) = 0$. This condition is clearly a generalisation of the Maxwell equations for $su(N)$ covariant fields.

2.2 Wilson lines

We discuss now how to describe the movement of an external particle (field source) ϕ in the gauge bundle. We can describe particles as vectors in an associated bundle, which transforms in some representation of the gauge group, e.g. the fundamental ϕ_i, $i = 1, \cdots, N$, for some general field ϕ. Similar to general relativity, where the movement of matter is determined by the space-time geometry, a test particle would also be influenced by the geometry (and topology) of the gauge bundle. The analogy is clear: the YM connection A_μ describes the parallel transport of vectors, just as the Levi-Civita connection on curved manifolds. Accordingly, when ϕ_i is parallel transported, it gets rotated. This phenomenon is similar to the Aharonov-Bohm effect in $U(1)$ gauge theory, where a test particle would pick up a phase after having been transported along a closed path. It is moreover natural that the transport of the vector ϕ_i is given by a path ordered product of $SU(N)$ elements. As a consequence, if the curvature of the bundle is not trivial, transporting ϕ_i along a closed path C would transform it as

$$\phi' = W[C]\phi, \quad W[C] = \mathrm{tr}\left\{ \mathcal{P} \exp\left\{ i \oint A \right\} \right\}. \tag{2.3}$$

$W[C]$ is nothing but the holonomy, also known as the *Wilson loop* and it is a gauge invariant observable of the theory. Later we will see that Wilson loops can provide insightful information into the low-energy behaviour of YM theory.

It is worth to point out that the present analysis of the parallel transport by considering the particle as a vector is very simplistic. It should be understood to be valid only on the classical level. Of course, in a more realistic semi-classical theory we should consider the test particle to span a finite dimensional Hilbert space. Although it is a very nice exercise to see how to quantise the degrees of freedom of ϕ_i, it lies outside the scope of this work.

2.3 The theta term and instantons

Let us remember the YM action in local coordinates (cf. Eq. 2.2)

$$S_{YM} = -\frac{1}{2g^2} \int d^4x \ \mathrm{tr}(F^{\mu\nu}F_{\mu\nu}).$$

It is clear that we can also take into account another four-form, which is also gauge and Lorentz invariant, namely

$$S_\theta = \frac{\theta}{16\pi^2} \int d^4x \ \text{tr}(\star F^{\mu\nu} F_{\mu\nu}). \tag{2.4}$$

This extra term is known as the *theta-term*. The theta-term carries with itself information about the global topology of the gauge bundle. The reason for this is that $P = \text{tr}(\star F^{\mu\nu} F_{\mu\nu})$ is a characteristic class, more precisely the second Chern class, and thus its integral is a topological invariant number, the second Chern number. More specifically, P is given by the derivative of the Chern-Simons 3-form K:

$$S_\theta = \frac{\theta}{16\pi^2} \int d^4x \ \partial_\mu K^\mu$$

$$K^\mu = \epsilon^{\mu\nu\rho\sigma} \text{tr}\left(A_\nu \partial_\rho A_\sigma - \frac{2i}{3} A_\mu A_\rho A_\sigma \right)$$

and we notice that, since $dF = 0$, it must obviously hold that P is closed, i.e. $dP = 0$. This is how P defines a cohomology class, i.e. the second Chern class. If P is globally exact, i.e. if $P = dK$ with K globally defined, then one would expect S_θ to vanish. If we have no global K, then the theta-term does not vanish. To see this let us compactify $\mathbb{R}^4$ on the four-sphere S^4 by including a point in infinity. We can cover the sphere with two charts U_+, U_- in such a way that

$$U_+ \ \rightarrow \ S^4 - \{\infty\} \qquad , \qquad U_- \ \rightarrow \ \text{ball around } \infty.$$

Clearly $U_+ \cap U_- \simeq S^3$. Let us call the restrictions of K on the charts K_+ and K_-. Thus we can write

$$\int_{S^4} P = \int_{U_+} dK_+ + \int_{U_-} dK_- = \int_{S^3} (K_+ - K_-) = \int_{S^3} (K(A_+) - K(A_-))$$

where we make explicit de dependence of K on the connection. Since A change by a gauge transformation Ω in the intersection $U_+ \cap U_-$, the integral reads

$$\int_{S^4} P = \int_{S^3} (K(\Omega A_- \Omega^{-1} + i\Omega\partial\Omega^{-1}) - K(A_-)).$$

We note that the curvature F must vanish at infinity, i.e. on S^3, otherwise we would have infinite energy and the theory wouldn't make sense. Therefore, A must be a pure gauge. We can pick $A_- = 0$, and thus $A_+ = i\Omega\partial\Omega^{-1}$. It is thus straightforward to see that the value of the integral is determined by the gauge transformations Ω alone. These gauge transformations are indeed maps from the intersection manifold S^3 on to the group manifold, $\Omega : S^3 \mapsto SU(N)$. They are, in fact, separated into different homotopy classes

$\Pi_3(SU(N)) = Z$. This means that gauge transformations are characterised by the times S^3 wraps around the Lie group manifold, i.e. by the winding number $n \in Z$. For example, if $N = 2$, we have $SU(2) \simeq S^3$ and thus the homotopy classes are labelled by the winding number of the map $S^3 \mapsto S^3$. It can be shown that, with the proper normalisation, the winding number determines the value of S_θ

$$S_\theta = \frac{\theta}{16\pi^2} \int P = n\theta, \quad n \in Z. \tag{2.5}$$

In other words, homotopic Ω elements give the same theta term. Since the contribution of S_θ to the path integral is $e^{in\theta}$, then $\theta \in [0, 2\pi)$.

The theta term is tightly related to the vacuum structure of classic YM theory. If the vacuum is characterised by $S = 0$, then the curvature must vanish, i.e. $F = 0$. For this to happen, A doesn't have to vanish if it is a pure gauge, as stated above. But, since Ω is divided in homotopy classes, we get different vacua labelled by the winding number n, e.g. $|n\rangle$. One would be tempted to think that these vacua are isolated, since one cannot deform, say $\Omega(m) \to \Omega(n)$. This is however not true. In fact, we can have field configurations that minimise the action with $S \neq 0$, which then allow to go jump among the "different" vacua. To see which configurations are let us write the YM action, with the aid of equations 2.4 and 2.5, as

$$S_{YM} = \frac{1}{2g^2} \int d^4x \ \mathrm{tr} \ F^{\mu\nu} F_{\mu\nu} = \frac{1}{4g^2} \int d^4x \ \mathrm{tr}(F_{\mu\nu} \mp \star F_{\mu\nu})^2 \tag{2.6}$$

$$\pm \frac{1}{2g^2} \int d^4x \ \mathrm{tr} \ F_{\mu\nu} \star F^{\mu\nu} \geq \frac{8\pi^2}{g^2} |n|. \tag{2.7}$$

It is obvious that S_{YM} is minimised when the bound, also known as Bogomol'nyi bound, is saturated and that this happens when

$$F_{\mu\nu} = \pm \star F_{\mu\nu}, \tag{2.8}$$

i.e. when the curvature is self-dual or anti-self-dual. These special field configurations not only minimise the action but they also have a non-vanishing winding number n. They are called *instantons* and because of them the winding number is also known as *instanton number*, among other several names found in the literature. The instanton equations actually imply the equations of motion. It can be furthermore shown that an instanton with winding number k yields the tunnelling amplitude between two vacua $|m\rangle \to |m + k\rangle$.

The existence of instantons interpolating the topological vacua gives us a glance at

how the vacuum of YM theory may look like. In the semi-classical approximation of the path integral, instantons have the main contribution and one can describe the ground state of the theory as the overlap of all topological vacua

$$|\theta\rangle = \sum_n e^{i\theta n} |n\rangle.$$

Here the tunnelling between different $|\theta\rangle$-vacua is forbidden by a super-selection rule and thus θ is a parameter of the theory that cannot be changed. Moreover, different theta values describe physically inequivalent theories, since $\theta \neq 0$ breaks CP symmetry explicitly.

Instantons are very interesting objects. As we saw, they are gauge bundles with non-vanishing second Chern class and self-dual curvature. Therefore, they carry information about the global topological properties of the base manifold on which the theory is defined. This rises the question about the usefulness of instantons in order to describe the physics of YM theory. As we saw above, they seem to characterise pretty good the ground state of the theory through the semi-classical approximation. However, as we will shortly see, this is not necessarily true. Let us get a feeling of what is going on by looking at the SU(2) YM. An instanton with $n = 1$ can be easily constructed for this gauge group[1]:

$$A_\mu = \frac{1}{x^2 + \rho^2} \eta^i_{\mu\nu} x^\nu \sigma^i, \quad F_{\mu\nu} = -\frac{2\rho^2}{(x^2 + \rho^2)^2} \eta^i_{\mu\nu} \sigma^i$$

here $\eta^i_{\mu\nu}$ are three 4×4 self-dual matrices, which are an irreducible representation of su(2), also known as 't Hooft matrices. We don't give their explicit form here, as we don't really need it. Moreover σ are the Pauli matrices and ρ parametrises the size of the instanton. It can be shown that the contribution of one $n = 1$ instanton to the path integral in the semi-classical approximation is

$$Z = \int \mathcal{D}A e^{-S_{YM} + iS_\theta} \approx \int_0^\infty d\rho \, f(\rho) e^{-8\pi^2/g^2} e^{i\theta}.$$

Here $f(\rho)$ contains the Jacobian of the change of variables in the path integral and also the determinant of the expansion of the action up to quadratic order in the fluctuations around the instanton. Without going into the details, this integral diverges as ρ becomes large. This means that the main contribution is carried by large instantons. This is a big problem since, as we know, in the quantum theory the coupling of YM runs and

---

[1] This is not the only form the $n = 1$ instanton can take. In fact, there is the ADHM construction, which allows to find all the possible instantons for a given winding number n in $SU(N)$. There are, in total, $4Nn$ solutions to Eq. 2.8.

gets strong at low energies / long distances. At strong coupling the semi-classical approximation is however no longer valid. As a result, instanton calculations cannot describe the low energy behaviour of YM theory.

Nevertheless, the failure of the semi-classical approximation doesn't mean that studying instantons is useless at all. Later in this work we will see that instantons play an interesting role in the physics of YM when coupled to matter, specifically in the appearance of the chiral anomaly. Moreover we will learn how instanton contributions yield exact results in supersymmetric theories and that there is a very interesting relation between supersymmetry and instantons. Instantons have also been highly useful in mathematics and mathematical physics. A great example is the work of Donaldson, as he used instantons to find new topological invariants and develop new theorems for four-manifolds [7]. His results are in fact ultimately related to the later work of Witten and Seiberg on supersymmetric gauge theories [10].

Chapter 3

The renormalisation group and the conformal window

Throughout this chapter we will focus on the qualitative aspects of the RG, which are necessary for the introduction of the conformal window and for the understanding of the idea behind lattice field theory. We explore the Wilsonian RG from a rather conceptual point of view and hence don't include the machinery behind the functional RG. We take as a guide the references [11][12][13].

3.1   Short review of the RG

If we wish to describe the interactions of particles as seen in some given experiment, we usually write down the partition function Z of a QFT with an UV cut-off, as we don't really have information about what happens at infinitely large energies. There is some freedom in choosing the cut-off (or scheme). It can be sharp or smooth, in momentum or in real space. Let us consider a very general d dimensional theory with fields ϕ. The partition function is given by

$$Z(\Lambda_0, g_0^i) = \int_{\Lambda < \Lambda_0} \mathcal{D}\phi \, e^{-S[\phi_0, g_0]},$$

$$S_{\Lambda_0}[\phi_0, g_0] = \int d^d x \left(\frac{1}{2}(\partial^\mu \phi)^2 + \sum_i \Lambda_0^{d-d_i} g_0^i \mathcal{O}_i(x) \right),$$

where d_i is the dimension of the operators $\mathcal{O}_i$ and g^i are the couplings. For the illustrative purposes of this section, we choose a sharp UV cut-off Λ_0 in momentum space, which leads to a clear picture of what the RG is about. In practice, in the context of the functional RG, it is custom to work with soft cut-off functions (see for example [14]). If we are interested in energies $\mu \ll \Lambda_0$, we are free to change the cut-off down to some Λ_1, if $\mu \ll \Lambda_1 < \Lambda_0$, without altering the physics at μ. We explicitly decompose ϕ into its low and high energy parts, i.e. $\phi = \varphi + \psi$ respectively. The measure can thus be written simply

as $\mathcal{D}\phi = \mathcal{D}\varphi\mathcal{D}\psi$. We then integrate over all modes with momentum $\Lambda_1 < |p| < \Lambda_0$, i.e. over ψ, finding the effective action at Λ_1 to be given by

$$e^{-S^{\mathrm{eff}}_{\Lambda_1}[\phi]} = \int_{\Lambda_1 < |p| < \Lambda_0} \mathcal{D}\psi \, e^{-S[\phi_0, g_0]}. \tag{3.1}$$

This is the first step of a RG transformation, also known as *coarse graining*. Of course, this process of integrating over high momenta modes can be systematically repeated. In every step we can write the effective action from the original one by absorbing the information of the integrated modes in the renormalisation of the fields and couplings. The effective action can be written in general as:

$$S^{\mathrm{eff}}_\Lambda = \int d^d x \left(\frac{z_\Lambda}{2} (\partial^\mu \phi)^2 + \sum_i \Lambda^{d-d_i} z_\Lambda^{n_i/2} g_i(\Lambda) \mathcal{O}_i(x) \right), \tag{3.2}$$

where $g_i(\Lambda)$ are the effective couplings at Λ, and z_Λ are the wave-function renormalisation factors. Since we have just integrated over a finite momentum shell of our integral, the partition function Z should not change. The derivatives of Z, i.e. the correlation function $\langle \phi(x_1) \cdots \phi(x_n) \rangle \equiv G^n_\Lambda(x_1, \cdots, x_n; g(\Lambda))$, should remain the same up to renormalisation factors of the fields. It follows a so-called *Callan-Symanzik equation*

$$\Lambda \frac{dG^{(n)}_\Lambda}{d\Lambda} = \left(\Lambda \frac{\partial}{\partial \Lambda} + \beta_i \frac{\partial}{\partial g_i} + n\gamma_\phi \right) G^{(n)}_\Lambda(g) = 0. \tag{3.3}$$

From this we can see that the integration of the higher modes is compensated by a change in the couplings, which is described by the β-functions, and in the normalisation factor of the kinetic term, which is described by the *the anomalous dimension* γ_ϕ:

$$\beta_i = \Lambda \frac{\partial g_i}{\partial \Lambda}, \quad \gamma_\phi = -\frac{1}{2} \Lambda \frac{\partial \ln z_\Lambda}{\partial \Lambda}.$$

A consequence of the Callan-Symanzik equation is that, when integrating between $(s\Lambda_0, \Lambda_0)$ for some $s < 1$, the correlation functions would change as

$$G^{(n)}_{s\Lambda_0}(x_1, \cdots, x_n; g_i(s\Lambda_0)) = \left(\frac{z_{s\Lambda_0}}{z_{\Lambda_0}} \right)^{n/2} G^{(n)}_{\Lambda_0}(x_1 \cdots x_n; g_i(\Lambda_0)). \tag{3.4}$$

Here we encounter a problem. We have integrated out a momentum shell but the resulting theories explicitly depend on different cut-offs. To be able to compare the different effective theories, we have to rescale all momenta and distances, so that the cut-off Λ_0 is restored. Equivalently, if we are working in real space with a lattice cut-off a, coarse-graining would leave us with a coarser space-time a/s, and it would be necessary to

rescale the lattice, i.e. to "zoom out". This is then equivalent to look at the theory from larger distances. A scale transformation that leaves the action invariant is given by

$$\Lambda_0 \to \Lambda_0/s, \quad x_i \to s x_i \quad \phi(sx) = s^{(2-d)/2}\phi(x).$$

Inserting this into the lhs of Eq. 3.4 yields

$$G_{\Lambda_0}^{(n)}(x_1/s, \cdots, x_n/s; g_i(\Lambda_0)) = \left(s^{2-d} \frac{z_{\Lambda_0}}{z_{s\Lambda_0}} \right)^{n/2} G_{\Lambda_0}^{(n)}(x_1, \cdots, x_n; g_i(s\Lambda_0)), \qquad (3.5)$$

where we have changed all the original operator insertion points $x_i \to x_i/s$. We notice that, as this is a mere rescaling, the coupling constants don't change. We know that the correlators must depend on the distance between the insertion points, i.e. $|x_j - x_i|/s$. If we consider correlators within the original theory, i.e. $g_i(\Lambda_0)$, taking $s \to 0$ on the lhs means that the insertion points are very far away from each other or, in other words, that the correlators are probing the long-distance (IR) properties of the theory. The rhs then tells us that this long-distance behaviour is described by theory at $s\Lambda_0$, with the insertion points left constant. The factor $s^{n(2-d)/2}$ on the rhs of Eq. 3.5 accounts for the classical scaling of the correlation functions, as the field ϕ has mass dimension $(d-2)/2$. The non-trivial scaling part is given by $z_{\Lambda_0}/z_{s\Lambda_0}$. This ratio is, of course, related to γ_ϕ and it carries information about the quantum corrections to the classical scaling behaviour. Writing $s = 1 - \delta s$, with δs infinitesimally small, one finds for each ϕ insertion in $G^{(n)}$

$$\left(s^{2-d} \frac{z_\Lambda}{z_{s\Lambda}} \right)^{1/2} \approx 1 + \left(\frac{d-2}{2} + \gamma_\phi \right) \delta s$$

The rescaling is the second step of a RG transformation. For the effective action S_Λ^{eff} in Eq. 3.2 to look like the action at Λ_0, a third and final step is necessary, namely the redefinition of the fields $\phi \to \phi' = z_\Lambda^{1/2}\phi$, so that the kinetic term is canonically normalised. A RG transformation is thus a map

$$\mathcal{R}_s(S[\Lambda, g_i(\Lambda)]) \mapsto S'[g_i'(s\Lambda), z_{s\Lambda}],$$

consisting of the three steps mentioned above. Clearly, applying two consecutive RG transformations is equivalent to applying one transformation with a smaller step s. It thus holds that $\mathcal{R}_a\mathcal{R}_b \to \mathcal{R}_{ab}$. Historically, this property suggested the name of renormalisation *group*. However, since integrating out is a non-reversible process, there is no inverse element such that $\mathcal{R}_a^{-1}\mathcal{R}_a = \mathbb{1}$ and so it is actually a semigroup. We can imagine all possible couplings g_i to span an infinite dimensional configuration space $\mathcal{M}$, where each point correspond to a different theory and the RG transformations map

theories into each other. Then, starting at some given point, the application of successive $\mathcal{R}_i$ generates a flow on $\mathcal{M}$. We can parametrise this flow by the flow-time $t = -\log(s)$, so that $\Lambda(t) = \Lambda_0 e^{-t}$. As we saw, $\mathcal{R}$ continuously changes the coupling and then, for large flow-times t, we would either end up with a coupling running all the way up to infinity or hit a *fixed point* where $\beta_i(g_i^*) = 0$. These fixed points are invariant under RG transformations and thus are scale invariant. The irreversibility of the RG flow was formally proved in two dimensions in [15] through the *c-theorem*. Accordingly, a function $c(g)$ was proposed which monotonically decreases with the RG flow, i.e. $c_{IR} < c_{UV}$, and whose value at the fixed points is the central charge of the conformal field theory (CFT). In four dimensions a generalisation of the c-theorem, the so-called *a-theorem*, was proved in [16].

It is frequently said that the scale invariant fixed points correspond to CFTs[1]. However, the equivalence of scale and conformal invariance is not yet fully proven. A proof exists only in two-dimensions, and was given by Polchinski in [17]. In higher dimensions a proof of the conformal symmetry enhancement is still missing. However, it has been shown that if the trace of the energy-momentum tensor can be written as

$$T_\mu^\mu = \partial^\rho \partial^\sigma L_{\rho\sigma}, \tag{3.6}$$

for some local operator L, then there exists a conserved conformal current. With this observation, the authors [18] argued that in four dimensions unitarity and scale invariance imply Eq. 3.6 and, as a consequence, conformal invariance [2]. When we discuss the conformal window, we will assume that this argument hold and that the fixed point is conformal.

To gain information about the RG flow, it is interesting to look at the vicinity of a fixed point $S^*(g_i*)$, which would be parametrised by small perturbations of the couplings $g_i = g_i^* + \delta g_i$. The behaviour of these perturbations is then given by expanding β_i up to leading order in δg_i:

$$\beta_i(g_i^* + \delta g_i) = B_{ij}\delta g_j + \mathcal{O}(\delta g_j^2).$$

This makes explicit the fact that $\mathcal{R}$ can in general mix the couplings. If we diagonalise B_{ij} we can write in terms of the eigenvectors σ_i and eigenvalues λ_i

$$B\sigma_i \equiv \partial_t \sigma_i = \lambda_i \sigma_i \quad \Rightarrow \quad \sigma_i(t) = \sigma_i(0)e^{\lambda_i t}.$$

[1]In the CFT the correlation length either $\xi = 0$ or $\xi = \infty$ and thus the correlators follow a power law, which only depend on the separation of the insertion points and the scaling dimensions. This can be inferred from Eq. 3.3

[2]Additional discussions on this subject can be found in the review article [19]

We see that if $\lambda > 0$ then σ_i runs unbounded with t. This is a *relevant* deformation that takes us away from the fixed point. If $\lambda < 0$ the perturbation gets smaller with t and eventually brings the flow back to the fixed point. This is an *irrelevant* deformation. The case $\lambda = 0$ is a so-called *marginal* deformation. In general, the number of couplings defining a given theory is infinite. However, almost all of them are irrelevant. The set of irrelevant couplings span an infinite dimensional sub-manifold of the theory space called the *critical manifold C*. All theories lying exactly on C, i.e. with no relevant operators turned on, will, after some flow-time, reach S^*. This lies at the heart of universality, as theories that look very different at high energies, are described by the same theory in the IR. Notice that turning on a relevant coupling would shoot the flow away from S^*, unless we tune it properly.

Until now we have said nothing about removing the cut-off, i.e. taking the continuum limit. Being able to do this means that our theory is valid up to arbitrary short distances. Let us suppose we are interested in probing the theory at some low energy Λ_R. If we are sitting on the critical surface, sending $\Lambda_0 \to \infty$ means that we need increasingly longer flow-times to reach Λ_R by consecutive actions of $\mathcal{R}$, i.e. $t \to \infty$. As a consequence, we hit the fixed point. However, we know that theories used to describe Nature are not CFTs (with the exception of critical systems). If we want to describe a non-scale-invariant theory at Λ_R, which also makes sense in the continuum limit, we must fix the finite relevant coupling $g(\Lambda_R)$. This can be done, for example, by measuring some observable in an experiment. We the then tune the bare relevant coupling so that $\sigma \to 0$ as $\Lambda_0 \to \infty$, i.e. towards C. We call $g(\Lambda_R)$ the *renormalised coupling*, whose definition depends on the new scale Λ_R (or scheme). Consequently, the effective theory at Λ_R is originated from an UV fixed point, by turning on a relevant deformation. A nice example of such a theory is, indeed, YM theory where the relevant direction is given by the YM coupling. This can be seen from the sign of the β-function at one loop

$$\beta(g) = \mu \frac{dg}{d\mu} = \beta_0 g^3, \quad \beta_0 = -\frac{11}{3} \frac{N}{(4\pi)^2}. \tag{3.7}$$

The coupling grows as we flow down to the IR and vanishes towards the UV, i.e. we find a UV Gaussian fixed point. This is the asymptotic freedom we mentioned in chapter 2. It turns out that the contrary happens in QED, where the β function has a positive sign, so that the theory gets weaker in the IR, where the effective charge $e(\mu)$ of the electron diminishes. Such a phenomenon can be rather intuitively explained through the charge screening of one external electron by a cloud electron-positron pairs. But how can we picture the opposite effect in the YM case? We can certainly think of a kind of colour-electric anti-screening. In fact, anti-screening in the YM vacuum appears simultaneously with paramagnetism, which arises from the spin of the gauge field.

3.2 The Yang-Mills conformal window

Up to this point we have discussed the properties of classical and semi-classical YM, as well as the generalities of the RG flow. In last section we saw that YM theory has a non interacting UV fixed point and that, at least at one loop order, the coupling grows without bounds with increasing length scale. When we couple YM to N_f Dirac fermions in the R representation of $SU(N)$, the scheme-independent (universal) one-loop and two-loop coefficients of the β-function take the form [20]

$$\beta(g_0)^{2-\text{loops}} = \beta_0 g_0^3 + \beta_1 g_0^5, \quad \beta_0 = -\frac{1}{(4\pi)^2}\left(\frac{11}{3}C_2(\text{adj}) - \frac{4}{3}T_R N_f\right),$$

$$\beta_1 = -\frac{1}{(4\pi)^4}\left(\frac{34}{3}C_2(\text{adj})^2 - \frac{20}{3}T_R N_f C_2(\text{adj}) - 4T_R N_f C_2(\text{adj})\right)$$

where $C_2(\text{adj})$ is the quadratic Casimir of the adjoint representation and T_R the normalisation of the generators. Since we are interested in fermions transforming in the adjoint representation, we have $C_2(\text{adj}) = T_{\text{adj}} = N$. We thus reproduce Eq. 3.7 if $N_f = 0$. We notice that the two-loop beta-function has a non trivial fixed point at $g_*^2 = -\beta_0/\beta_1$. As we increase N_f, we find a zero at some N_f^u. For $N_f > N_f^u$ the β-function become positive and the coupling would hence grow with the energy, missing the UV fixed point, i.e. we lose asymptotic freedom. At the same time, the coupling goes to zero in the IR, i.e. it hits an IR free fixed point. These kind of theories have no well-defined continuum limit. As we lower the energy, we need to add higher loop corrections to the β-function. We thus change the zeroes of β and span an interval of possible N_f values that lead to IR fixed points with different critical g_*. We denote the lowest flavour number N_f^l. The interval $N_f^l < N_f < N_f^u$ is called the *conformal window*. In that region we have UV and IR fixed points. If the critical coupling is $g_* \ll 1$, we talk of a Banks-Zaks fixed point. This portion of the conformal window can be investigated perturbatively. Below N_f^l we miss the IR fixed point and the coupling grows at long distances, as in the pure YM case. We then expect to find confinement and chiral symmetry breaking. We will say more about these two phenomena when we discuss the supersymmetric version of YM theory, which is surely below the conformal window.

Since at the lower edge of the conformal window the critical coupling g_* is large, we cannot employ perturbation theory and thus the exact determination of N_f^l is a non-perturbative problem. Indeed, for general gauge theories this is still an open problem, with exact computations being only possible for some models with extended supersymmetry. In chapter 10 we will explore the conformal window of adjoint QCD, i.e. YM theory coupled to N_f adjoint fermions, on the lattice.

Chapter 4

Supersymmetry

In this chapter we learn how the dynamics of SUSY models are greatly constrained by the underlying supersymmetry. We will moreover briefly discuss on the intriguing relation between instantons and SUSY, which allows instanton computations to yield exact non-perturbative results. This relation is related to further advances made in mathematics, which were initiated by Witten [21] after the work by Donaldson we mentioned earlier. These advances ended up in the Witten-Seiberg theory of the electric-magnetic duality in $\mathcal{N} = 2$ SYM [22, 23].

4.1   Algebraic aspects of SUSY

In the 1960s Gell-Mann's *eightfold way* successfully organised all the experimentally known hadrons in $SU(3)$ multiplets. This triggered the attention of the particle physics community to look for more general multiplets, which could also include particles with different spins. One of the proposals back then (see Ref. [24]) was that this $SU(3)$ *flavour* symmetry of quarks could be extended to a $SU(6)$ group, where different spins and strangeness numbers would be part of a single *super-multiplet*. The three flavours of quarks (up, down and strange), and their two spin projections (up and down), would be part of a single multiplet. This kind of unification ideas got however greatly restricted in 1967, as Coleman and Mandula published their very famous no-go theorem [25]. This states that, in an interacting theory, the most general symmetry of the S-matrix is a direct product of the Poincaré group times internal symmetries. The reason behind this theorem is that the existence of any conserved tensorial charge different than the momentum P_μ, the Lorentz generators $J_{\mu\nu}$ and some Lorentz scalars B_k, would make the S-matrix trivial. However, a loop-hole in the Coleman-Mandula theorem allowed Golfand and Likhtman [26] to give birth to SUSY in the early 1970s. The loop-hole is that, although tensor charges are excluded, the theorem doesn't consider the case of having spinor charges. In [27] all possible supersymmetries of the S-Matrix were classified.

4.1.1 SUSY Algebra

The generators of the Poincaré algebra are B_k, P_μ and $J_{\mu\nu}$, which transform in the bosonic $(0,0)$, $(\frac{1}{2}, \frac{1}{2})$ and $(0,1) \oplus (1,0)$ representations of $SL(2, \mathbb{C})$. The space-time symmetries of a supersymmetric QFT include, in addition,[1] the spinor charges $\mathcal{Q}_\alpha$ and $\mathcal{Q}_{\dot\alpha}^\dagger$, which transform in the $(\frac{1}{2}, 0)$ and $(0, \frac{1}{2})$ representations, respectively. In general, we are not restricted to have a single supercharge. Thus, to keep the discussion as general as possible, let us consider $\mathcal{N}$ supercharges. These satisfy the relations

$$\{\mathcal{Q}_\alpha^i, \mathcal{Q}_{\dot\alpha}^{j\dagger}\} = 2\delta^{ij}\sigma_{\alpha\dot\alpha}^\mu P_\mu, \quad [\mathcal{Q}_\alpha^i, P_\mu] = 0, \quad [J_{\mu\nu}, \mathcal{Q}_\alpha^i] = \frac{1}{2i}(\sigma_{\mu\nu})_\alpha^\beta \mathcal{Q}_\beta^i, \tag{4.1}$$

where $i = 1, \cdots, \mathcal{N}$. These relations are, in turn, invariant under a so-called R-symmetry, which is generated by the elements T_r in some representation r

$$[T_r, \mathcal{Q}_\alpha^i] = (t_r)_j^i \mathcal{Q}_\alpha^j,$$

where $(t_r)_j^i$ are the structure constants. Clearly, in the case where $\mathcal{N} = 1$ this R-symmetry is only given by $U(1)$. By including $\mathcal{Q}$, we extend the Lie algebra of the Poincaré group to a so-called Lie superalgebra, whose underlying vector space is a $\mathbb{Z}_2$ graded vector space V. This graded vector space is the set-theoretical union of an even (bosonic) subspace V_0 and an odd (fermionic) one V_1 [28], i.e.

$$V = V_0 \cup V_1 \quad \text{with} \quad [V_0, V_0] \subset V_0, \quad [V_0, V_1\} \subset V_1, \quad \{V_1, V_1\} \subset V_0.$$

Eq. 4.1 yields moreover that the Hamiltonian of a supersymmetric QFT is a non-negative operator

$$H \equiv P_0 = \frac{1}{4}(\mathcal{Q}_1\mathcal{Q}_1^\dagger + \mathcal{Q}_1^\dagger\mathcal{Q}_1 + \mathcal{Q}_2\mathcal{Q}_2^\dagger + \mathcal{Q}_2^\dagger\mathcal{Q}_2), \tag{4.2}$$

which is manifestly non-negative, as it is given by the squares of supercharges. From this follows that the spectrum of the Hamiltonian has no negative eigenvalues. Thus, the lowest energy in the theory is zero, corresponding to the vacuum annihilated by the supercharges. It turns out that SUSY is not spontaneously broken only if the vacuum state has zero energy, what can be corroborated by noticing that

$$\text{if} \quad H|0\rangle \neq 0 \quad \Rightarrow \quad \mathcal{Q}_\alpha^i|0\rangle \neq 0 \text{ or } \mathcal{Q}_\alpha^{i\dagger}|0\rangle \neq 0$$

---

[1] In the case that conformal symmetry is not broken, we would have in addition dilations and special conformal transformations.

and the ground state wouldn't be invariant under SUSY transformations. As we will see below, each excited state has a corresponding superpartner with a spin increased or decreased by $\frac{1}{2}$. Moreover, the members of such a super-multiplet share the same mass, as a consequence of the commutation between $\mathcal{Q}$ and P_μ.

Let us briefly comment on the missing commutators in 4.1, namely $\{\mathcal{Q}, \mathcal{Q}\}$ (and h.c.). In some cases, like in SUSY QM, this commutator vanishes. However, this doesn't hold in general, as shown in Ref. [27]. Indeed, if $\mathcal{N} > 1$, the commutator must be a linear combination of operators in the irrep $(0, 0)$ and $(1, 0)$ of the Lorentz group. The only tensor satisfying this condition is the self-dual part of $J_{\mu\nu}$. However, this cannot be the case as the term doesn't commute with P_μ, contradicting the algebra relations. The commutator must thus be proportional to an element Z^{ij}, which commutes with all other elements of the superalgebra, i.e. an element of its centre

$$\{\mathcal{Q}^i_\alpha, \mathcal{Q}^j_\beta\} = 2\epsilon_{\alpha\beta}Z^{ij}, \quad \{\mathcal{Q}^{i\dagger}_{\dot\alpha}, \mathcal{Q}^{j\dagger}_{\dot\beta}\} = 2\epsilon_{\dot\alpha\dot\beta}Z^{ij\dagger}. \tag{4.3}$$

As Z^{ij} commutes with the space-time symmetries, it must be a linear combination of the R-symmetry generators, i.e. $Z^{ij} = \alpha^{ij}_r T_r$. These Z^{ij} are called central charges. Later, in the context of $\mathcal{N} = 1$ super Yang-Mills theory, we will see that also the theory with minimal SUSY admits a kind of central extension in the presence of topological defects.

4.1.2 Representations

Let us first consider massive states without central charges. Massive representations of the Lorentz group are characterised by their mass m, total spin s and one component of the spin, e.g. s_3. Accordingly, a given one-particle state in Fock space can be written as $|m, s, s_3\rangle$. In a rest frame the momentum operator would be given by $P_\mu = (m, \vec{0})$, and the SUSY algebra is just $\{\mathcal{Q}^i_\alpha, \mathcal{Q}^{j\dagger}_{\dot\alpha}\} = 2M\delta_{\alpha\dot\alpha}\delta^{ij}$. To construct the representations, we need to identify a vacuum state $|\Omega_s\rangle$, which is usually called the *Clifford vacuum*, together with creation and annihilation operators, which change the spin by $\pm\frac{1}{2}$. For the theory to be supersymmetric, $|\Omega_s\rangle$ must be annihilated by the supercharges. Following [29], one can write

$$|\Omega_s\rangle = \mathcal{Q}_1\mathcal{Q}_2|m, s', s'_3\rangle \quad \Rightarrow \quad \mathcal{Q}_1|\Omega_s\rangle = \mathcal{Q}_2|\Omega_s\rangle = 0,$$

which is a consequence of the supercharges being anti-commuting. With this observation, we can consider $\mathcal{Q}^i_\alpha$ as an annihilation operator and $\mathcal{Q}^{i\dagger}_{\dot\alpha}$ as a creation one. A general state is then just $\mathcal{Q}^{i_1\dagger}_{\alpha_1}\cdots\mathcal{Q}^{i_n\dagger}_{\alpha_n}|\Omega_s\rangle$. In general, there are $4^{\mathcal{N}}$ states which can be constructed by acting with the supercharges on a single $|\Omega_s\rangle$. The maximal possible spin is $s_{\max} = s + \frac{\mathcal{N}}{2}$.

Moreover, one gets different kind of super-multiplets, depending on the spin of the Clifford vacuum.

Massless states are labelled by their energy E and helicity λ. Here we can choose a frame $P_\mu = (E, 0, 0, E)$, yielding $\{\mathcal{Q}_\alpha^i, \mathcal{Q}_{\dot{\alpha}}^{j\dagger}\} = 2E\delta^{ij}(\sigma_0 + \sigma_3)_{\alpha\dot{\alpha}} \Rightarrow \quad \{\mathcal{Q}_2^i, \mathcal{Q}_{\dot{2}}^{j\dagger}\} = 0$. This means that $\mathcal{Q}_1^i$ ($\mathcal{Q}_1^{i\dagger}$) are the only annihilation (creation) operators. As a result, massless super-multiplets are shorter than the massive ones[2], since there are only $2^\mathcal{N}$ states.

In $\mathcal{N} = 1$, we usually call the super-multiplets *chiral* if the Clifford vacuum is $|\Omega_{s=0}\rangle$, and *vector* if one starts with $|\Omega_{s=1/2}\rangle$. The relevant SUSY model in this work is the $\mathcal{N} = 1$ massless vector super-multiplet. This is constructed starting with the vacua with helicities $\lambda = 1$ and $\lambda' = -1/2$, yielding a massless vector boson A, i.e. the gauge field, and a Weyl fermion λ, called the gaugino. This model is indeed the minimal supersymmetric YM theory, which will be extensively discussed throughout the next chapters. Because of SUSY, the fermion must transform, like A, in the adjoint representation of $SU(N)$. The on-shell action with $\theta_{YM} = 0$ is given by

$$S = \int dV \left[-\frac{1}{4} \operatorname{Tr} F_{\mu\mu} F^{\mu\nu} + \frac{i}{2} \operatorname{Tr}\left(\bar{\lambda}\slashed{D}\lambda\right) \right]$$

where $D_\mu \equiv \partial_\mu - ig[A_\mu, \cdot]$ is the gauge-covariant derivative and g the coupling constant. This action is invariant under the infinitesimal SUSY transformations δ_ϵ

$$\delta_\epsilon A_\mu = i\bar{\epsilon}\gamma_\mu\lambda, \quad \delta_\epsilon\lambda = iF^{\mu\nu}\Sigma_{\mu\nu}\epsilon \tag{4.4}$$

where ϵ is a Majorana spinor, which generates the transformations. In the upcoming chapters we will go deeper into the details of the low-energy dynamics of this theory.

4.2 The Witten index

Back in the 1980s, Witten proposed in Ref. [30] a constraint on the spontaneous breaking of SUSY, based on the index which now carries his name:

$$\Delta = \operatorname{Tr}(-1)^F = n_B^{E=0} - n_F^{E=0}, \quad (-1)^F = e^{2\pi i J_z}, \tag{4.5}$$

where F is the fermion number, i.e. $F = 0$ for bosons and $F = 1$ for fermions. The index 4.5 is only given by the zero-energy modes, since the excited ones cancel each other, thanks to the Fermi-Bose degeneracy of SUSY. If $\Delta \neq 0$, then SUSY can't be spontaneously

---

[2]The construction of the multiplets goes analogously to the massive case. However, CPT symmetry requires the helicities $-\lambda$ to be included.

broken. The reason behind this is that a zero index reflects an unbalance between the number of bosonic and fermionic ground states. This unbalance rules out the possibility for the ground state to form a super-multiplet, which could have a non-zero energy and then break SUSY. Witten's idea was to identify a topological-invariant-like quantity of the SUSY QFT[3], as perturbation theory is not reliable to determine whether the vacuum energy is zero or not. Having a topological invariant moreover allows the theory to be deformed in convenient ways. Witten considered a SUSY QFT on a torus, as having a finite volume discretises the spectrum of the Hamiltonian, making the pairing of the excited states evident. Moreover, if the ground-energy is zero at finite volume, it will remain to be zero at infinite volume. An important observation is that the zero modes are not paired and n_F and n_B can take arbitrary values. Moreover, smoothly deforming the theory, i.e. changing the volume of the torus and the coupling constants, would modify the spectrum as follows. Some Bose-Fermi pairs with zero-energy could get a positive energy and thus n_F and n_B would decrease by one. As a result, the difference $n_B - n_F$ would not change. Since this difference is insensitive with respect to how we deform the theory, one can take convenient limits, where it is easiest to compute. If the result is different from zero, then we can be sure that SUSY is not broken, although having $\Delta = 0$ doesn't necessarily imply that SUSY is broken[4].

A final remark is necessary. The trace in Eq. 4.5 runs over the all states of the Hilbert space, and it must be regulated in order to be well-defined. The following regulation

$$\Delta = \text{Tr}\big((-1)^F \text{e}^{-\beta H}\big) \tag{4.6}$$

will be for us, in fact, the definition of the Witten index. We will compute the derivative of this quantity for $SU(3)$ $\mathcal{N} = 1$ SYM in chapter 9.

---

[3]It is important to notice that the topological invariant concerns the whole theory and not single field configurations.

[4]At this point it is necessary to comment on the subtleties of the previous discussion. Firstly, although one could be concerned with regard to how Witten's argument would change in the presence of ultraviolet divergences, one should take into account that the index is sensitive with respect to the zero-modes alone. The second subtlety deserves important attention and concerns the potential energy for large field strengths. Although it seems that we are free to deform the theory as we like, there could be a discontinuity in $\Delta = \text{Tr}(-1)^F$ if a deformation changes the asymptotic behaviour of the potential in field space. This would allow for new zero-modes to move from or out to infinity. In other words, large theory deformations could drastically change the original Hilbert space and the whole argument would be invalid. This subtlety is more deeply addressed in the original paper by Witten.

4.3   Instantons and non-perturbative SUSY

Non-perturbative physics in SUSY models is particularly accessible to analytical methods. The reason is the Fermi-Bose degeneracy and the special underlying relation between instantons and SUSY. Recalling the transformations 4.4, it turns out that the self-dual instanton equation $F = \star F$ implies $F^{\mu\nu}\Sigma_{\mu\nu}\epsilon = 0$, i.e. the SUSY transformations ϵ are preserved in the presence of an instanton, while the other half ($\bar{\epsilon}$) are broken, as it generates fermion zero modes $\bar{\lambda} = F^{\mu\nu}\bar{\Sigma}_{\mu\nu}\bar{\epsilon}$ [9]. This is a rather intriguing observation, since general background fields do break SUSY completely. Because the instantons preserve SUSY, this property still holds for the fluctuations around them. This is extremely useful. In double expansion, i.e. semi-classical plus perturbative

$$\mathrm{e}^{-\frac{8\pi^2}{g^2}}\left(c_0 + c_2 g^2 + c_4 g^4 + \cdots\right)$$

the Fermi-Bose degeneracy ensures that the loop expansion vanishes to all orders. In this case instanton computations yield exact results [31]. In some cases, multi-instanton calculus is necessary. However, in many practical problems already one-instanton computations are exact [32]. For example, since all perturbative corrections to the vacuum energy vanish, a non-zero vacuum energy, i.e. spontaneous breaking of SUSY, can only arise non-perturbatively through instantons. This also applies for low-energy phenomena in SUSY YM like confinement and gaugino condensation, which we will discuss in upcoming chapters.

Chapter 5

Low energy $\mathcal{N} = 1$ super Yang-Mills theory

In this chapter we focus on the low-energy features of $\mathcal{N} = 1$ SYM, especially on confinement and the spontaneous breaking of chiral symmetry. The IR of YM, and QCD-like theories in general, is highly non-trivial and can't be tracked analytically. Especially confinement is one of the most prominent puzzles in theoretical physics [33]. In the IR QCD-like theories are strongly coupled and thus both perturbative and semi-classical analysis of instantons fail. An ideal toy model to study how QCD-like theories behave in the IR is $\mathcal{N} = 1$ SYM. The reason for this is two-fold. First, as mentioned earlier, the interplay between SUSY and instantons makes instanton computations exact, and thus the properties of the SUSY ground state are analytically accessible. Secondly, $\mathcal{N} = 1$ SYM is the only QCD-like theory with SUSY. With QCD-like we mean four-dimensional asymptotically free and confining gauge theories without elementary scalars. Indeed, some models with extended SUSY are under analytical control and exact results have been found. For example, the work by Seiberg and Witten in $\mathcal{N} = 2$ SYM showed that in that theory confinement arises from monopole condensation [22]. However, these theories always have scalars, which can't be really removed from the theory, without changing the physics [34].

As we will see, SUSY allows for the exact computation of the beta-function in $\mathcal{N} = 1$ SYM. It moreover leads to the proof of gaugino condensation at zero temperature, where the theory is furthermore confining. The theory has a mass-gap and its low-energy spectrum was analytically predicted by Veneziano and Yankielowicz (see Ref. [35]) to consist of a chiral super-multiplet of mesons and a gaugino-glue state. Later, this picture was extended to include glue-balls in Refs. [36, 37]. The formation of the spectrum has been studied on the lattice for $SU(2)$ and $SU(3)$ gauge groups in [38–40].

5.1   Symmetries and anomalies of SYM

In this section we would like to discuss the symmetries of SYM in the IR. Regarding gauge invariance, contrary to extended SUSY models, there are no scalars that can trigger a Higgs mechanism and thus the $SU(N)$ redundancy prevails[1]. In general, the symmetries of the classical action can be *anomalous*, i.e. they may not be a symmetry of the path integral. Moreover, quantum symmetries may be *spontaneously broken*, i.e. they may not be a symmetry of the ground state. Anomalies are stable with respect to the renormalisation group, meaning that they are reproduced at all energies [41]. Spontaneously broken symmetries can however be restored, and this is often related to phase transitions.

When we discuss confinement, we will mostly rely on Ref. [33]. We will moreover notice that confinement is naturally discussed in the terms of lattice field theory. Indeed, this phenomenon is thought to arise from the non-triviality of the vacuum, through the global properties of the gauge bundles. As we discuss in chapter 6, the gauge fields on the lattice are described by group (instead of algebra) elements. This feature makes the lattice formulation more sensitive to the global properties of the theory.

5.1.1   Scale invariance

Without a soft-breaking gaugino mass term, the classical action of SYM is scale invariant. This is can immediately be seen from the fact that the couplings of the Lagrangian are dimensionless. However, the quantum theory is not scale invariant, as the coupling is scale dependent and this dependency is encoded in the beta-function. More specifically, in order to have scale invariance on the quantum level, we must have a conserved dilation current[2] $\partial^\mu J_\mu^d = 0$. It is also a well-known fact that $\partial^\mu J_\mu^d = T_\mu^\mu$ [42] and thus the theory is scale invariant if the energy-momentum tensor is traceless. It is however not the case, as it holds the trace anomaly [43][3]

$$T_\mu^\mu \quad \sim \quad \beta(g)(F^{a\mu\nu}F_{\mu\nu}^a).$$

Scale invariance is thus explicitly broken once we turn on deformations that push the theory away from the fixed point. In other words, it amounts to add operators to the CFT, which explicitly break the conformal symmetry.

---

[1]Later in chapter 9 we will see that the symmetry can be Higgsed through compactification.

[2]On the quantum level, these equations are understood as operator equations, i.e. to be valid inside correlation functions with arbitrary operator insertions.

[3]This trace anomaly has a slightly different nature than the trace anomaly in CFTs. A conformal theory on flat space can get a trace anomaly when a background curvature is turned on $T_\mu^\mu \sim cR$, where R is the Ricci scalar and c the central charge.

5.1.2   Centre symmetry and confinement

A sidenote on what we mean by confinement

It is worth to devote a couple of words to explain what we actually mean when we talk about *confinement*. Although this concept is widely used in the literature, it is often not clear what physicists actually mean by it (see Ref. [33] for a thorough discussion on the subject). We would like to distinguish among confinement as

- A mass gap Δ, i.e. that the Hamiltonian H has no eigenvalues in $(0,\Delta)$.

- The existence of only colour-singlets in the spectrum.

- A linear-growing inter-quark potential, up to string breaking.

All these properties lead to a spectrum where quarks are "trapped" inside hadrons and, especially the last two, are often labelled as confinement. A colour-singlet spectrum is, however, also seen in gauge-Higgs-theories with fundamental Higgs [44][45]. Indeed, in some limit the Higgs condensate screens the colour-electric field. Moreover, there is no phase transition associated to this. Although in QCD there is actually no deconfinement phase transition but a crossover, one hopes to understand the mechanism behind confinement by exploring QCD-like theories like SYM, which actually has a phase transition. Therefore, in this work we consider confinement as the linear potential between a quark and an anti-quark and, very importantly, its connection with a phase of "magnetic disorder" and centre symmetry.

Confinement and Wilson lines

It can be shown that a linearly growing quark potential arises when the expectation value of a Wilson loop (cf. Eq. 2.3)

$$W[C] = \mathcal{P}\left\{ \exp\left[\oint_C A_\mu dx^\mu \right] \right\} \tag{5.1}$$

falls exponentially with its area

$$\langle W(R,T) \rangle \sim \mathrm{e}^{-cR\dot{T}} \sim \mathrm{e}^{-V(R)T},$$

where R is the space and T the time separation, respectively, and $V(R) \sim cR$ a linear potential. Without a rigorous proof, this fact can be easily seen on a lattice. Indeed, we can create a pair quark-antiquark at time $t = 0$, separated from each other by a distance R. We then let the pair propagate up to some time $t = T$. If the pair is created by an

operator Q_0 and annihilated by $Q_T^\dagger$, then the propagation is given by $\langle Q_T^\dagger Q_0 \rangle$. We know that for $T \to \infty$ the correlator should have the form

$$\langle Q_T^\dagger Q_0 \rangle = \mathrm{e}^{-\Delta E_{\min} T}.$$

Moreover, it should depend on the expectation value of the product of links around the path $R \times T$, i.e. the Wilson loop. Since in the presence of the two particles the energy difference ΔE is just the static potential, if the potential is linear, then the Wilson loop must exponentially fall with the area. It turns out that this area-law exists when the magnetic fluxes running through the loops are uncorrelated. In the jargon of statistical mechanics, this situation represents a vacuum in a phase of "magnetic disorder". Moreover, similar to the Ising model, we can think of a transition to a "magnetised" or deconfined phase. As in the Ising model, we can also think of an underlying symmetry that is spontaneously broken. This is a nice picture, as it suggests that, as we may suspect, confinement is a consequence of the highly non-trivial vacuum structure.

Centre symmetry and confinement

Let us consider Euclidean YM with the time-direction x_4 compactified on a circle with radius β. It turns out that, for the gauge field A_μ to be periodic, i.e. for $A(\vec{x}, x_4 + \beta) = A(\vec{x}, x_4)$, it must hold for the gauge transformations that

$$g(\vec{x}, x_4 + \beta) = z \, g(\vec{x}, x_4),$$

where z is an element of the centre of $SU(N)$, which is isomorphic to the cyclic group Z_N, and is made up of the N roots of the unity times the unity matrix:

$$z_n \mathbb{1}_N = \exp\left(\frac{2\pi i n}{N}\right) \mathbb{1}_N, \quad n = 0, 1, 2, \ldots, N - 1.$$

If the condition is satisfied, the theory is invariant under Z_N. Although the gauge symmetry $SU(N)$ cannot be broken, this Abelian global subgroup can break spontaneously. It is worth to notice that this symmetry is physical and it's not a mere redundancy, as $SU(N)$ is. This can be immediately understood from the fact that gauge invariant Wilson loops are not invariant under this transformations [4]. A possible order parameter to probe the breaking of Z_N is the Wilson loop winding around the compact time-direction, i.e. the

---

[4]In the modern jargon of high energy physics Z_N is a so-called 1-form symmetry, since it acts on line operators. In recent years, the development of higher form symmetries [46], combined with 't Hooft anomaly matching, has shown itself to be a very useful non-perturbative tool.

Polyakov loop

$$P_L = \exp\left\{ \oint dx^4 A_4 \right\},, \quad P_L \neq z\, P_L. \tag{5.2}$$

As P_L is not invariant under the centre, its expectation value can signal the breaking of the symmetry, just as the average spin serves as order parameter in the Ising model. The expectation value of P_L is related to the exponential of the free energy F_q of an isolated quark

$$\langle P_L \rangle = e^{-\beta F_q},$$

and thus a vanishing expectation value of the Polyakov loop implies that the free energy of the static quark is infinite and that the centre symmetry is unbroken. Conversely, if at some β one has $\langle P_L \rangle \neq 0$, then there is a phase transition to broken centre symmetry, i.e. to a deconfined phase. It is important to notice that the quark is not dynamical, otherwise, its presence would break the centre symmetry explicitly and there would be no phase transition but a crossover. This is indeed the case of QCD. There, in the confined phase, the quark-antiquark potential grows linearly until the energy of the confining field is high enough for a quark-antiquark pair to arise from the vacuum[5].

The story is different when we add adjoint matter to the theory, as is the case of SYM and adjoint QCD. Adjoint fermions have the same (zero) N-ality as the gauge fields and thus transform on the same way, leaving the theory still invariant under Z_N. At this point it is important to notice that the confinement of gluons and gauginos inside bound states *is not* the confinement we relate to centre symmetry and "magnetic disorder". The absence of asymptotic coloured in the spectrum is, in fact, due to colour screening. Indeed, since the string-tension for zero N-ality is zero, as sources start to separate, they get rapidly screened. Hence, the confining properties of these theories is just as the YM case, even though they include fermionic matter. The vacuum thus acts as a confining medium for external static quarks.

5.1.3 Chiral symmetry and the anomaly

$\mathcal{N} = 1$ supersymmetric Yang-Mills theory is chiral when no soft-SUSY-breaking mass term is included in the action. Unsurprisingly, the chiral symmetry coincides with the $U(1)$ R-symmetry on the classical level. Under chiral rotation the gaugino transforms as

$$\lambda \to \lambda' = \exp(-i\omega\gamma_5)\lambda, \tag{5.3}$$

---

[5]As a remark, confinement shouldn't be confused with the fact that a single-quark state is not gauge-invariant. Indeed, when one talks about a single quark, one should think about it as a quark with a Wilson line attached. As we see, the configuration quark plus Polyakov loop is gauge-invariant but has infinite energy in the confined phase.

where ω parametrises the transformation. We notice that if we choose ω to depend on the position, the fermionic part of the SYM action transforms as

$$S = \frac{1}{2} \int d^4x \, \left(\bar{\lambda} \slashed{D} \lambda \right) \quad \rightarrow \quad S' = \frac{1}{2} \int d^4x \, \left[\bar{\lambda} \slashed{D} \lambda - i(\partial_\mu \omega(x)) \bar{\lambda} \gamma^\mu \gamma_5 \lambda \right]. \tag{5.4}$$

If we let ω to be a constant, we immediatly see that the action is invariant. It is easy to see that the corresponding Noether current is just

$$J_\mu^A = \bar{\lambda} \gamma_\mu \gamma_5 \lambda, \quad \text{with} \quad \partial^\mu J_\mu^A = 0.$$

On the quantum level, this symmetry is anomalous because of instanton configurations [47]. A nice way to derive the anomaly is the very illustrative Fujikawa's procedure [48], which we review in Appendix B. Accordingly, the anomaly function $\mathcal{A}(x)$ is related to both the instantons and the fermion zero modes as

$$\int d^4x \, \mathcal{A}(x) = n_+ - n_-, \quad \frac{1}{8\pi^2} \int d^4x \, \text{Tr} \left(\tilde{F}^{\mu\nu} F_{\mu\nu} \right) = n_+ - n_- \equiv n, \tag{5.5}$$

where n_+ and n_- are the number of zero modes for each chirality. This equation relates solutions of the Dirac operator to the topology of the gauge bundles. Indeed, the rhs equals the algebraic index of the Dirac operator

$$\text{index}(\slashed{D}) = \dim(\ker \slashed{D}) - \dim(\ker \bar{\slashed{D}}) = n_+ - n_-,$$

while the lhs is the instanton winding number $n \in \pi_3(\text{SU}(N)) = \mathbb{Z}$ and hence a topological invariant, the topological index. This relation represents the celebrated Atiyah-Singer index theorem. What underlies the theorem, and the chiral anomaly itself, is that the dimension of the kernel of an elliptic differential operator on a compact manifold is determined by the topology of the manifold itself[6]. The relation between the anomaly and the index theorem was first discussed in [49]. If we look closely at the anomaly $\mathcal{A}(x)$, we immediately recognise that it is, indeed, the same as the theta term of the YM action. This means that we can compensate a chiral rotation by a change in the theta term $\theta_{\text{YM}} \rightarrow \theta_{\text{YM}} - 2N\omega$. Since the theta term is periodic, including it in the SYM action makes the breaking of the chiral symmetry explicit, as only chiral rotations with $\omega = \frac{n\pi}{N}$, $n = 0, \cdots, 2N - 1$ leave the action invariant. This means that the chiral symmetry is no longer $U(1)_R$ but Z_{2N}. The relation between the theta angle and chiral rotations has an even more deep and subtle physical meaning. In chapter 2 we saw that the theta term is physical in pure YM theory,

---

[6]Thus, the analysis given for the chiral anomaly only holds in Euclidean space, as there the Dirac operator is elliptic and instantons exist.

because it labels the different vacua of the theory, and these vacua are interpolated by the instantons. If we include fermions, however, the theta term is not physical anymore, precisely because a change in theta can be compensated by a chiral rotation.

5.1.4 Spontaneous chiral symmetry breaking and the gaugino condensate

We have seen that the non-anomalous chiral symmetry of SYM is the discrete group Z_{2N}. It turns out that, at strong coupling, the vacuum is populated by pairs of gauginos, also known as the gaugino or chiral condensate. In other words, one has the non-vanishing correlator $\langle \lambda(x)\lambda(x) \rangle \neq 0$. Semi-classically, the condensation can be understood from an observation made by 't Hooft in Ref. [50]. He saw that in the presence of an $n = 1$ instanton background, the vacuum-to-vacuum amplitude vanishes unless operators with fermion zero modes are inserted in the correlator:

$$\langle 0||0\rangle = 0, \quad \langle 0|\bar\lambda\lambda|0\rangle \neq 0.$$

Thus, the vacuum in this background is populated condensed fermion pairs. Because of arguments given before on SUSY and instantons, we expect this observation to be accurate for SYM [7]. The condensate breaks the non-anomalous chiral symmetry down to some subgroup. In SYM theory, the chiral symmetry is spontaneously broken down to a sign flip, i.e one has the symmetry breaking pattern $Z_{2N} \to Z_2$. The spontaneous breaking of this discrete symmetry has a deep physical meaning. It was conjectured by Witten [30] that the N different vacua, labelled by the different values of the condensate, are supersymmetric and that N is precisely the Witten index. This means that SUSY in SYM can't break spontaneously. The gaugino condensate was computed for the first time in [51]. In the last decades, several other authors have computed the "exact" condensate. Some of the procedures to achieve this involve instanton calculus, others Seiberg-Witten theory in softly broken $\mathcal{N} = 2$ gauge theory. We use quotes when referring to the exact condensate because there has been some disagreement in the literature regarding its exact value[8]. Currently, however, the issue seems to be settled and the following result is widely accepted, as different methods agree on it:

$$\langle \lambda\lambda \rangle = cN\Lambda^3 \mathrm{e}^{2n\pi i/N},$$

---

[7]For a non-SUSY theory, however, the existence of a chiral condensate is very difficult to prove analytically. In QCD we know that a chiral condensate exists because it is an essential parameter in the effective chiral Lagrangian, which describes very well the low energy hadron spectrum seen in experiments. In some cases one can use anomaly matching conditions in order to infer that, if the theory confines, then there must exist a non-vanishing condensate

[8]A thorough review on this issue can be found in Sec. VII of Ref. [32].

where the term $e^{2n\pi i/N}$ shows the existence of the N degenerated vacua. One approach to this result is the so-called *weak coupling instanton* (WCI). Accordingly, one adds matter superfields, i.e. quarks and squarks, to the SYM and study the theory in the Higgs phase, where the theory is in the weakly-coupled regime and semi-classical analysis with instantons is valid. The end result for the condensate is found when the matter fields are decoupled. This is precisely the method used in [51]. A non-instanton-approach is for example the semi-classical study of the non-thermally compactified theory on $\mathbb{R}^3 \times S^1$, where condensation of magnetically charged objects contribute to the value of the condensate (see Ref. [52]).

An important last remark is that, since in SYM the original quantum chiral symmetry is discrete, there are no Goldstone-bosons. This is very different from QCD, where the pions are a consequence of the formation of the chiral condensate. In SYM we rather get domain walls, which interpolate the N different vacua. From the point of view of the softly-broken SUSY theory, the spontaneous breaking of the symmetry means that, at $m_g = 0$, there is a first order phase transition, where we find the coexistence of the N vacua, separated by the domain walls.

5.2   The domain wall in $\mathcal{N} = 1$ SYM

In Refs. [53, 54] Dvali and Shifman showed that, because of the domain walls, $\mathcal{N} = 1$ SYM in four dimensions has tensor central charges. They moreover argued that the domain walls are BPS-saturated states, meaning that the QFT on the wall has half of the bulk supersymmetries. Let's briefly show how central charges can arise in $\mathcal{N} = 1$ SYM. In four dimensions, the general form of the anti-commutator of supercharges reads

$$\{\mathcal{Q}_\alpha, \mathcal{Q}_{\dot{\alpha}}^\dagger\} = 2\sigma^\mu_{\alpha\dot{\alpha}}P_\mu + 2(\gamma_5\sigma^{\mu\nu}|J^{\mu\nu}|)_{\alpha\dot{\alpha}}.$$

The operator $J^{\mu\nu}$ in the second term is normally not taken into account, since it vanishes when translational symmetry is not spontaneously broken [54]. This is actually a consequence of the Coleman-Mandula theorem, which forbids conserved tensorial charges. However, translational symmetry does break due to the domain wall, and then $J^{\mu\nu}$ is a conserved current. It turns out that the tensor is given by $J^{\mu\nu\alpha} = \epsilon^{\mu\nu\alpha\beta}\partial_\beta(\lambda\lambda)$ [53].

Chapter 6

Lattice quantum field theory for SUSY and adjoint QCD

In chapter 3 we motivated the non-perturbative study of the conformal window of adjoint QCD. Then, in chapter 5, we saw that we need non-perturbative methods in order to investigate confinement and the spontaneous breaking of the discrete chiral symmetry through the gaugino condensate. These are formidable problems to be tackled by means of the best established non-perturbative method: lattice Monte-Carlo simulations. In this chapter we first review how these simulations can yield an approximate solution of the Euclidean path integral. We then discuss how to discretise gauge theories with adjoint fermions, and the complications arising from chiral symmetry and SUSY. After that, we focus on the technical part of the simulations, i.e. how to generate configurations and measure observables. Much of the general aspects of lattice field theory are discussed following Ref. [55].

6.1   The idea of lattice field theory

Lattice field theory is a method to compute full correlators of quantum fields by solving the Euclidean path integral numerically, i.e. non-perturbatively and exact up to numerical uncertainties. Its birth dates back to the 1970s and is due to the work of Kenneth Wilson on the RG in strong coupling [56, 57]. He observed that the anomalous dimensions in QFT are related to critical exponents in statistical mechanics and that, in this sense, the Ising model can be regarded as a QFT living on a space-time lattice. These observations led him to study QCD in a novel form, namely by regularising the theory on an Euclidean four-dimensional lattice with the gauge fields located on the links and the quarks on the sites.

Let us elaborate more on how this works. In QFT, we are interested in computing correlation functions of fields. The canonical way to do that is through the Feynman path

integral formulation. For a given QFT with classical action $S[\phi]$, the expectation value of a functional $\mathcal{F}[\phi]$ can be written in Minkowski space as

$$\langle \mathcal{F} \rangle = \frac{\int \mathcal{D}\phi \, \mathcal{F}[\phi] \, \mathrm{e}^{iS[\phi]}}{\int \mathcal{D}\phi \, \mathrm{e}^{iS[\phi]}},$$

where the measure $\mathcal{D}\phi$ samples over the whole field space and thus $\langle F \rangle$ is not only determined by the fields that minimise the action $S[\phi]$, but also by in general arbitrary large fluctuations around these minima. This becomes clear from the fact that the term $\mathrm{e}^{iS[\phi]}$ greatly oscillates for field configurations with large action. Solving such an integral is in general impossible. However, if we give up on studying time dependent phenomena, we can perform a Wick rotation and rewrite the path integral in Euclidean signature as

$$\langle \mathcal{F} \rangle = \frac{\int \mathcal{D}\phi \, \mathcal{F}[\phi] \, \mathrm{e}^{-S_E[\phi]}}{\int \mathcal{D}\phi \, \mathrm{e}^{-S_E[\phi]}}. \tag{6.1}$$

It is clear now that configurations with large Euclidean action are exponentially suppressed. More interestingly, the Euclidean formulation makes explicit the tight relation between QFT and statistical mechanics. Indeed, the denominator in equation 6.1 looks just like the partition function Z of, let's say, a spin system with Hamiltonian $H[s]$ in a heat bath at temperature T

$$Z = \sum_s \mathrm{e}^{-\frac{H[s]}{T}} \quad \Leftrightarrow \quad \int \mathcal{D}\phi \, \mathrm{e}^{-S_E[\phi]}.$$

Both structures are evidently similar: in the spin system the number of states is given by a sum over spin configurations with Boltzmann factor $\mathrm{e}^{-H[s]}$ and, in the QFT, it is given by the integral over field configurations with action $S_E[\phi]$. We can thus regard the denominator in Eq. 6.1 as a partition function. This observation allows us to employ methods from statistical mechanics in order to study QFT on an Euclidean manifold. It is further useful to make the space-time finite, in order to make the similarity to statistical mechanics explicit, what also makes the numerical work possible. We thus reformulate the QFT on a finite Euclidean space-time lattice[1] with spacing a and length L, so that a space-time point x is given by

$$\Gamma = \left\{ x \mid x = \sum_{\mu=1}^{4} a n_\mu \hat{\mu}, \ n_\mu \in \mathbb{Z} \right\},$$

---

[1] Along this work we will only consider hypercubic lattices. Other geometries are however possible and to some extent studied in the literature.

where $\hat{\mu}$ are unit vectors pointing in every space-time direction, and n_μ are the coordinates. The lattice volume L^4 puts an IR cut-off in the system, while the lattice spacing a has the effect of introducing a UV cut-off. The cut-off a renders the measure of the integrals in 6.1 finite, as only momenta in the Brillouin zone $p \in [-\pi/a, \pi, a)$ are allowed

$$\int \mathcal{D}\phi \quad \Rightarrow \quad \int \prod_{x_i=[a,\cdots,L]} d\phi(x_1, x_2, x_3, x_4).$$

Thus, we have in total $(\frac{L}{a})^4$ integrals. Later we'll see how to solve them by means of Markov chain Monte Carlo (MC) methods. It is interesting to mention that Lorentz symmetry is, unsurprisingly, explicitly broken by the lattice down to the subgroup of hypercube isometries. Fortunately, $SO(4)$ invariance is restored in the continuum limit.

6.2 Gauge theories on the lattice

To solve YM with adjoint fermions on the lattice, we have to properly discretise the action

$$S = \int d^4x \left[\frac{1}{2g_0^2} \text{tr}(F^{\mu\nu} F_{\mu\nu}) + \frac{1}{2} \sum_i^{N_f} \bar{\lambda}^i \left(\slashed{D} + m_0 \right) \lambda^i \right] \tag{6.2}$$

Here λ_i are N_f Majorana fermions. The subscripts in g_0 and m_0 denote that they are bare parameters. We will shortly see why we have to add a mass term and why we simulate Majorana instead of the original Weyl fermions. Naturally equation 6.2 represents SYM for the case $N_f = 1$. The first discretisation step is to change the space-time integral by a sum over the lattice points $\int d^4x \rightarrow a^4 \sum_x$. We would like to define a bare action at cut-off $\Lambda_0 \sim 1/a$ and coupling $\beta \sim 1/g_0^2$, so that the continuum limit reproduces the original quantum continuum theory. In the context of the RG flow, this means that we have to design our lattice action to lie on the critical manifold whose fixed point is the theory we want to study. One has to be careful, as the RG transformations can give rise to all the terms compatible with the symmetries of the theory (and of the lattice). Thus, we have to ensure that only irrelevant operators, i.e. those that die off as $a \rightarrow 0$, are produced[2]. It turns out not to be a major problem for gauge fields and, to some extent, fermions, unless they are massless. Further, we have to tune the relevant couplings, e.g. g and m, so that they vanish with a. This is thus similar to the continuum limit of YM discussed in chapter 2. As we will shortly see, we will encounter subtleties arising from the fermions and SUSY.

---

[2]This can be problematic for scalar fields as the quantum corrections to the mass grow with the momentum cut-off. This is analogous to the mass corrections to the Higgs mass in the SM.

6.2.1 Gauge fields

Let us start with the discretisation of the gauge action. Since we are not on a continuum manifold anymore, we cannot demand the gauge fields to live on the Lie algebra of $SU(N)$. Instead we work with group elements $U \in \mathrm{SU}(N)$, defined through the exponential map of A_μ, i.e. $A_\mu \to e^{iaA_\mu(x)} \equiv U_\mu(x)$, with A_μ in the fundamental representation. These are just the parallel transporters, or Wilson lines, connecting the site x with the site $x + \mu$ and hence live naturally on the links of the lattice (see Fig. 6.1). As group elements they transform naturally as

$$U_\mu(x) \to \Omega(x)U_\mu(x)\Omega(x + \hat{\mu}).$$

This already gives us a hint about how to construct gauge invariant operators, namely by closed paths of Wilson lines, as the Wilson loops introduced in section 2.2. The simplest Wilson loop is given by the plaquette

$$U_{\mu\nu}(x) = U_\mu(x)U_\nu(x + \hat{\mu})U_\mu^\dagger(x + \hat{\nu})U_\nu^\dagger(x),$$

where $U_\mu(x)$ goes from x to $x + \hat{\mu}$, while $U_\mu^\dagger(x)$ from $x + \mu$ to x. This yields an orientation of the paths. Since a closed path of the connection yields a curvature term, we can already guess that we can use the plaquette to define the gauge lattice action. Indeed, we can find the continuum version of the plaquette by expanding $U_{\mu\nu}$ in terms of the gauge connection by using the Baker-Campbell-Hausdorff relation $\exp(A)\exp(B) = \exp\left(A + B + 1/2[A, B] + \cdots\right)$ and the Taylor expansion $A_\nu(x + \hat{\mu}) = A_\nu(x) + a\partial_\mu A_\nu(x) + \mathcal{O}(a^2)$. The explicit computation yields

$$
\begin{aligned}
U_{\mu\nu}(x) &= \exp\left\{ia^2\left(\partial_\mu A_\nu(x) - \partial_\nu A_\mu(x) + i[A_\mu(x), A_\nu(x)] + \mathcal{O}(a^3)\right)\right\} \\
&= \exp\left(ia^2 F_{\mu\nu}(x) + \mathcal{O}(a^3)\right) \\
&= 1 + a^2 F_{\mu\nu}(x) - \frac{1}{2}a^4 F_{\mu\nu}F^{\mu\nu} + \cdots.
\end{aligned}
$$

We are of course interested in the term quadratic in F. We can cancel the identity and the term $\mathcal{O}(a^2)$ by writing the action as

$$S_G[U] = \frac{2}{g^2}\sum_{x\in\Gamma}\sum_{\mu<\nu}\mathrm{Re}\ \mathrm{tr}\left[1 - U_{\mu\nu}(x)\right] = \frac{a^4}{2g^2}\sum_{x\in\Gamma}\sum_{\mu<\nu}\mathrm{tr}[F_{\mu\nu}F^{\mu\nu}(x)] + \mathcal{O}(a^2), \qquad (6.3)$$

where $a^4\sum$ is just the discretisation of the space-time integral. This means that the plaquette corresponds to the continuum action up to $\mathcal{O}(a^2)$ operators. Fortunately those operators are irrelevant. Moreover, the derivation of the gauge lattice action suggests that we have some freedom on constructing it. Indeed, we can for example sum over
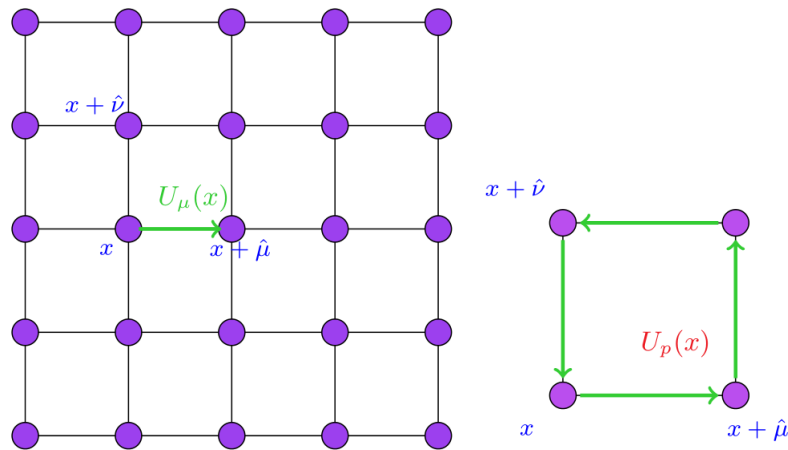
FIGURE 6.1: *Parallel transporters and the plaquette*

bigger plaquettes, in such a way that some higher order terms in F cancel, as long as we reproduce the main F^2 term. This kind of actions are said to be *Symanzik improved* [58]. A common choice is to add rectangles made out of double-plaquettes $\Box\Box \equiv R_{\mu\nu}$

$$S_G^{\text{symanzik}}[U] = \frac{2}{g^2} \sum_{x\in\Gamma} \left[c_0 \sum_{\text{plaquettes}} \text{Re tr}(1 - U_{\mu\nu}) + c_1 \sum_{\text{rect}} \text{Re tr}(1 - R_{\mu\nu}) \right], \qquad (6.4)$$

$$c_1 = -\frac{1}{12}, \; c_0 = \frac{5}{3}.$$

This action agrees with the continuum one, up to $\mathcal{O}(a^4)$.

After having discretised the action, we can now take care of the measure $\mathcal{D}A$ in the continuum path integral. However, as we already mentioned, on the lattice the gauge fields live in the Lie group instead of in the Lie algebra, and the relevant measure is thus $\mathcal{D}[U]$. This simplifies the analysis. Indeed, in the continuum we have to sum over all the orbits of A and we end up fixing the gauge through the Faddeev-Popov method. On the lattice, we integrate over the $SU(N)$ manifold, which is compact, and whose measure is just the Haar measure.

6.2.2 Fermions

We now focus on the more subtle part of the discretisation: the fermion action. We already saw that chiral symmetry is anomalous in the presence of gauge fields, as the the conservation of the axial current is broken by instantons. So let us for a moment ignore the gauge field. In the continuum we know that free fermions conserve their chiralities. But what would happen if we try to put free chiral fermions on a lattice? This was addressed long ago by Susskind in Ref. [59]. Let's consider a single free right Weyl fermion ψ_- living on a 3d spatial lattice, so that the time remains continuous. The Hamiltonian

reads

$$H = i \int d^3x \, \psi_-^\dagger \sigma^i \partial_i \psi_-,$$

and discretising with a symmetric derivative:

$$H = -ia^3 \sum_{x \in \Gamma} \psi_-(x) \sum_i \sigma^i \left[\frac{\psi_-(x + a\hat{i}) - \psi_-(x - a\hat{i})}{2a} \right] \tag{6.5}$$

Expanding the spinor in Fourier modes yields

$$\psi_-(x) = \int \frac{d^3k}{(2\pi)^3} e^{ikx} c_k.$$

Since we are in a lattice only the momenta in the Brillouin zone $k_i \in [-\pi/a, \pi/a)$ contribute. This brings us to the Hamiltonian

$$H = \frac{1}{2a} \int_{BZ} \frac{d^3k}{(2\pi)^3} \sum_i 2\sin(k_i a) c_k^\dagger \sigma^i c_k$$

Denoting the vacuum as the Dirac sea $|\Omega\rangle$, the energy of a state $|k\rangle = c_k^\dagger |\Omega\rangle$ is given by

$$E(k) = \frac{1}{a} \sum_i \sin(k_i a) \sigma^i.$$

This dispersion relation shows that the energy has zeroes at $k_i = 0$ and π/a. The latter corresponds to a left-handed fermion. This is called *fermion doubling*. Since $i = 1, \cdots, 3$, we have $2^3 = 8$ zeroes in total. The half of them are left and the other half are right handed. As a consequence, we cannot have a single Weyl fermion, as second one with opposite chirality would be produced alone by the presence of the lattice. Therefore, the lattice breaks the chiral symmetry explicitly even without gauge fields. Unfortunately, this problem doesn't go away if we discretise time. On the contrary, it gets worse, as 2^4 *doublers* appear as poles in the fermion propagator at the corners of the Brillouin zone. Indeed, if we discretise the free Dirac operator $\bar{\lambda}\slashed{\partial}\lambda$ as above in equation 6.5, we find that its inverse in momentum space is given by

$$D(p)^{-1} = \frac{-ia^{-1} \sum_\mu \gamma_\mu \sin(p_\mu a)}{a^{-2} \sum_\mu \sin(p_\mu a)^2},$$

where we see that there are 15 poles more than the one we would get in the continuum at $p_\mu = 0$. One has to better get rid off these doublers, as they are not physical degrees of freedom in the continuum theory. As we will see, there are ways to remove them but, in

most cases, the solutions require that we give up on chiral symmetry.

A widely used way to remove the doublers is due to Kenneth Wilson and the so discretised fermions are called Wilson fermions. This is the type of discretisation we used in all the simulations presented in this work. Wilson proposed to add a new term to the naive fermion action, equivalent to the continuum operator $-(a/2)\partial^2$:

$$-\frac{a}{2}\bar{\lambda}\partial^2\lambda \;\rightarrow\; -\frac{a}{2}\bar{\lambda}\left(\frac{\lambda(x+a\hat{\mu}) - 2\lambda(x) + \lambda(x-a\hat{\mu})}{a^2}\right). \tag{6.6}$$

The effect of this term is to give a mass $m \sim 1/a$ to the doublers, forcing them to decouple in the limit $a \to 0$. Another effect is that this term is a mass, even though we started with a massless fermion. Hence, the Wilson term breaks chiral symmetry explicitly. Moreover, although the term is irrelevant, we can always get a residual mass $m_s \sim 1/a$. As a consequence the gaugino mass renormalises additively. This is similar to the quantum corrections the Higgs field becomes in the SM. To get a zero renormalised mass m_g, we have to tune the bare mass $m_0 \to m_s$. This justifies the necessity for a bare mass parameter in the action.

6.2.3 The lattice action

We are now ready to write down the lattice action of YM coupled to adjoint Majorana fermions. On the way we have seen that we can't put single Weyl fermions on the lattice and that we need a mass term, in order to tune towards the continuum limit. The only missing step is to include the parallel transporters in the Dirac operator. For this purpose we have to transform the link variables U_μ, which are in the fundamental representation, into the adjoint one through [38]

$$V_\mu^{ab}(x) = 2\operatorname{tr}\bigl(U_\mu^\dagger(x)T^a U_\mu(x)T^b\bigr). \tag{6.7}$$

Collecting this expression with the discretisations in equations 6.3 and 6.6, the lattice action reads

$$S_L = \beta \sum_p \left(1 - \frac{1}{N}\operatorname{Re}\operatorname{tr} U_p\right) + \frac{1}{2}\sum_{xy}\sum_i^{N_f} \bar{\lambda}_x^i (D_{\mathrm{w}})_{xy}\lambda_y^i, \tag{6.8}$$

$$(D_{\mathrm{w}})_{x,a,\alpha;y,b,\beta} = \delta_{xy}\delta_{a,b}\delta_{\alpha,\beta} - \kappa \sum_{\mu=1}^{4}\bigl[(1-\gamma_\mu)_{\alpha,\beta}(V_\mu(x))_{ab}\delta_{x+\mu,y}$$

$$+ (1+\gamma_\mu)_{\alpha,\beta}(V_\mu^\dagger(x-\mu))\bigr],$$

where the bare lattice coupling is $\beta = 2N/g_0^2$, and p is an index labelling the plaquettes. Moreover, the Dirac-Wilson operator D_{w} is written with the aid of equation 6.7, with (a, b) and (α, β) being the $SU(N)$ and spinor indices respectively. The bare mass and the Wilson term coefficient are summarised in the hopping parameter $\kappa = 1/(2am_0 + 8)$. As already mentioned, the gauge action in 6.8 equals the continuum one up to $\mathcal{O}(a^2)$ terms, while the discretisation effects of the Wilson-Dirac operator are $\mathcal{O}(a)$. In the simulations carried out in this thesis we usually employ a Symanzik improved gauge action (see eq. 6.4). We also frequently use an improved Wilson fermion action along the lines of the Symanzik improvement program [60], which reduces the errors to $\mathcal{O}(a^2)$. This consists in adding an irrelevant operator, the so-called *clover term* to the action

$$\frac{-c_{sw}(g)}{4}\bar{\lambda}(x)\sigma_{\mu\nu}F^{\mu\nu}\lambda(x), \quad c_{sw} = c_{sw}^0 + c_{sw}^1 g^2 + c_{sw}^2 g^4 + \cdots$$

where c_{sw} is the Sheikholeslami-Wohlert coefficient. We use the one-loop value of c_{sw} found in [61]. The clover discretisation of $F_{\mu\nu}$ is given by

$$F_{\mu\nu} - i\frac{1}{4}\sum_p (U_p - U_p^\dagger). \tag{6.9}$$

6.2.4 SUSY

As previously said, the Lorentz symmetry is broken on the lattice down to a discrete subgroup. This subgroup is enhanced to the full Lorentz symmetry as $a \to 0$. If we are interested in studying properties of supersymmetric theories, we would like to keep SUSY unbroken, at least in the continuum limit. However the SUSY algebra

$$\{\mathcal{Q}_\alpha, \mathcal{Q}_\beta^\dagger\} = 2\sigma_{\alpha\beta}^\mu P_\mu$$

is completely broken on the lattice, as we don't have a generator of infinitesimal translations on a discrete space-time. What is more, the Wilson term and the bare mass break the Fermi-Boson degeneracy. There are ways to overcome this as reviewed in Refs.[62–64], so that SUSY models can be formulated on the lattice. A natural way is to tune the relevant couplings so that the supersymmetric critical point is achieved in the continuum limit [65]. For extended SUSY this procedure can become quickly too complex from the technical point of view, as one would have to take control on many parameters. Because of this reason, in the last years some proposals to discretise SUSY have arisen [66–70], according to which the subalgebra $\{\mathcal{Q}^\dagger, \mathcal{Q}\} \sim P = 0$, i.e. nilpotent supercharges, is conserved at $a \neq 0$ and the full algebra is recovered in the continuum. Although these approaches are very interesting, we don't make use of them in the present work and won't have too much to say in this regard. We will rather work within the proposal of Curci and Veneziano to

study $\mathcal{N} = 1$ SYM on the lattice [71]. They suggested the lattice action in equation 6.8 (for $N_f = 1$) and investigated the tuning to the SUSY point. They showed that, although the lattice and the Wilson discretisation explicitly break chiral symmetry and SUSY, both are simultaneously restored in the continuum limit. Especially, the chiral limit implies SUSY. Therefore, to restore SUSY we only need to tune the bare gaugino mass, as mentioned above, so that the renormalised mass vanishes. There are several ways to achieve that and some methods are more expensive from the computational point of view than others. One method is to measure the residual mass from the Ward identities on the lattice [72]. Also, since at the chiral point the gaugino condensate has a 1$^{\text{st}}$ order phase transition, one can determine the critical hopping parameter value $\kappa_c \sim 1/m_g$ where this happens.

A cheaper way to tune the mass is through the square of the unphysical "adjoint-pion" state, as it holds that $m_{\text{a}-\pi}^2 \sim m_g$, as shown in Ref. [73] [3]. The mass $m_{\text{a}-\pi}$ can be obtained from the connected part of the propagator of $\bar{\lambda}(x)\gamma_5\lambda(x)$ (see below). The chiral and supersymmetric point is then found by taking the limit $m_{\text{a}-\pi}^2 \to 0$.

6.3 Simulating Yang-Mills with adjoint Majorana fermions

After having discretised the action, we now show how to actually compute the path integral in equation 6.1. We saw that the lattice cut-off renders the path integral finite. However, the remaining integral is in general still very large and difficult to compute by direct numerical integration. This problem can be overcome by means of importance sampling [74]. Indeed, the Boltzmann factor e^{-S_E} in the path integral tells us that not all regions of field space contribute equally to the integral. We can create a Markov-Chain of randomly generated field configurations $\{U,\lambda\}^{(0)} \to \{U,\lambda\}^{(1)} \to \cdots$, whose distribution asymptotically converges to

$$dP = \frac{1}{Z}[dU][d\lambda]\mathrm{e}^{-S_L}.$$

Once some number N_{conf} of configurations has been generated, the expectation value of some observable $\mathcal{F}$ is computed as the average (cf. 6.1)

$$\langle\mathcal{F}\rangle = \lim_{N_{\text{conf}}\to\infty} \frac{1}{N_{\text{conf}}} \sum_{n=1}^{N_{\text{conf}}} \mathcal{F}[U_n,\lambda],$$

---

[3]Such a relation is widely used in chiral perturbation theory, since the pions are Goldstone bosons and thus physical states of the theory. There one has $F_\pi^2 M_\pi^2 = -m^{(r)}N_f\Sigma^{(r)}$. Where F_π is the pion decay constant, M_π the pion mass and Σ the renormalised chiral condensate.

and the statistical error goes as $1/\sqrt{N_{\text{conf}}}$. The algorithm we have used to originate the Markov Chain of field configurations is the so-called *Rational Hybrid Monte Carlo* RHMC. The Hybrid Monte Carlo method [75] (without the R) is a combination of the well-known Metropolis algorithm and molecular dynamics. The latter describes an evolution along a trajectory in phase space, parametrised by a spurious time τ. Let us denote with $\phi(x,\tau)$ a general bosonic field. In the field chain, the first configuration $\phi^{(0)}$ is chosen randomly. A configuration $\phi^{(k+1)}$ in the chain is obtained from $\phi^{(k)}$ as follows

1. Generate random Gaussian distributed conjugate momenta $P_i(x,0)^{(k)}$ to $\phi_i(x,0)^{(k)}$

2. Compute the initial energy: $H(0) = S[\phi^{(k)}] + \frac{1}{2}\sum_i (P_i^{(k)})^2$

3. Integrate the equations of motion $\frac{d\phi_i}{d\tau} = P_i\phi_i$, $\frac{dP_i}{d\tau} = -\frac{\partial S[\phi]}{\partial \phi_i}$ up to time τ to obain $P_i(x,\tau)^{(k)}$, $\phi_i(x,\tau)^{(k)}$

4. Compute the energy of the new fields and momenta $H(\tau)$

5. Generate a random number $0 < r < 1$. Accept the new field configuration, i.e. $\phi^{(k+1)} = \phi(x,\tau)$ if $r < e^{H(0)-H(\tau)}$. Otherwise reject it, i.e. $\phi^{(k+1)} = \phi^{(k)}$.

Originating configurations with Majorana fermions requires special care. We note that the fermion integral is a Gaussian integral over Grassmann numbers and thus we can easily integrate out the fermions. When having a "full" Dirac fermion, the integration yields $\det(D_W)$. However, since a Majorana fermion has the half of degrees of freedom, we get the Pfaffian of the Wilson-Dirac operator $\text{Pf}(D_W)$, which is not positive definite

$$\int [d\lambda]\, e^{-\frac{1}{2}\bar{\lambda}D_W\lambda} = \text{Pf}(CD_W) = \text{sign}(\text{Pf}(CD_W))\sqrt{|\det(CD_W)|}.$$

In our sampling algorithm we use the square root of the determinant. The reason for this is that we want to use the fermion Pfaffian as a probability weight factor for the gauge fields, but a negative value would lead to a sign problem, as it couldn't be interpreted as a probability. A negative sign is expected to appear more often at smaller masses and larger lattice spacings [38, 40, 76]. This sign problem can thus be avoided by controlling the lattice parameters, while a sporadic sign can be introduced through reweighting. Furthermore we write $\sqrt{|\det(D_W)|} = \sqrt[4]{\det((\gamma_5 D_W)^2)}$. This rewriting is useful, since the matrix $(\gamma_5 D_W)^2$ is Hermitian, and it thus has real non-negative eigenvalues. We now write the determinant as a Gaussian integral over complex bosonic fields F, the so-called *pseudofermions*

$$(\det((\gamma_5 D_W)^2))^{1/4} = \int [dF][dF^\dagger] \exp\{-F^\dagger((\gamma_5 D_W)^2)^{-1/4}F\}.$$

Note that we can write the action in terms of the Gaussian distributed χ, with $F = ((\gamma_5 D_W)^2)^{1/8}\chi$. To compute F we use the rational approximation of the matrix [77]

$$M^{1/8} = \sum_k \frac{a_k}{M + b_k},$$

and F is obtained by solving the Dirac equation

$$((\gamma_5 D_W)^2 + b_k)\eta_k = \chi \quad \rightarrow \quad F = \sum_k c_k \eta_k$$

This rational approximation gives the name to the RHMC algorithm. We generate the chain of fields analogue to the standard HMC discussed above

1. Generate random Gaussian distributed vector χ and momenta P. Then compute F as shown above

2. Compute the initial energy as before, plus the fermion contribution $\chi^\dagger \chi$

3. Fix F and integrate the equations of motion to find the new field $\phi(x, \tau)$ and momenta $P(x, \tau)$

4. Compute $H(\tau)$ and do the last accept/reject step.

6.4 Extracting physics from the lattice

6.4.1 Measuring correlators

On the lattice one often wants to measure propagators of composite operators made of gauge fields and fermions. Although in this thesis we are mostly interested in observables like the gaugino condensate, the Polyakov loop and the plaquette, in chapter 10 we will need to measure the correlators of meson-like operators. To achieve that one constructs field-interpolators $O, \overline{O}$, which are the lattice equivalents to the creation and annihilation operators in the Hilbert space. One choose the interpolators in such a way that it has the same quantum numbers as the continuum state we want to measure. Once we have identified the correct interpolator, we just use Wick's theorem to express the propagator as a sum over fermion contractions. Let's briefly see how this works taking as example

the propagator of the pseudo-scalar operator $O_{PS} = \bar{\lambda}\gamma_5\lambda$:

$$
\begin{aligned}
\langle O_{PS}(y)\overline{O}_{PS}(x)\rangle &= (\gamma_5)_{\alpha'\beta'}(\gamma_5)_{\alpha\beta}\langle \bar{\lambda}(y)_\alpha \lambda(y)_\beta \bar{\lambda}(x)_{\alpha'} \lambda_{\beta'}(x)\rangle \\
&= (\gamma_5)_{\alpha'\beta'}(\gamma_5)_{\alpha\beta}\left\{ -2(S_W)^{-1}_{\alpha'\beta}(x,y)(S_W)^{-1}_{\alpha\beta'}(y,x) \right. \\
&\quad \left. +(S_W)^{-1}_{\alpha\beta}(y,y)(S_W^{-1})_{\alpha'\beta'}(x,x)\right\} \\
&= -2\,\mathrm{tr}\left[\gamma_5 (S_W)^{-1}(x,y)\gamma_5(S_W)^{-1}(y,x)\right] \\
&\quad + \mathrm{tr}\left[(S_W)^{-1}(y,y)\right]\mathrm{tr}\left[(S_W^{-1})(x,x)\right]
\end{aligned}
\tag{6.10}
$$

The first part is called the *connected part* and the second one the *disconnected part*. The latter arises because of the Majorana condition $\bar{\lambda} = \lambda^T C$. To obtain the full correlator we measure the quantity 6.10 on every configuration and then take the Monte Carlo average. The inverse of the Wilson-Dirac operator is computed by means of a point source and the conjugate gradient. Finally the propagator is extracted by means of a zero momentum projection, placing the source in the origin (see Fig. 6.2)

$$
\langle O_{PS}(p=0,t)\overline{O}_{PS}(0,0)\rangle = \frac{1}{V_3}\sum_{\vec{x}}\langle O_{PS}(\vec{x},t)\overline{O}_{PS}(0,0)\rangle
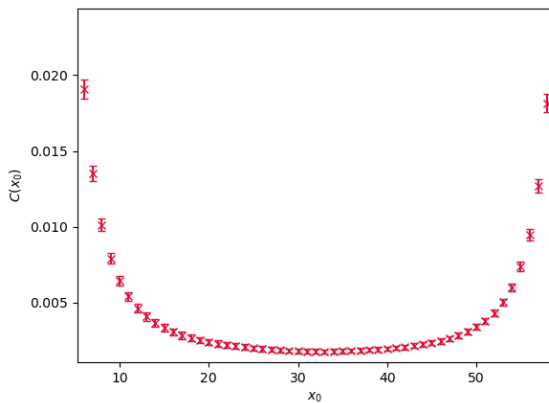\tag{6.11}
$$

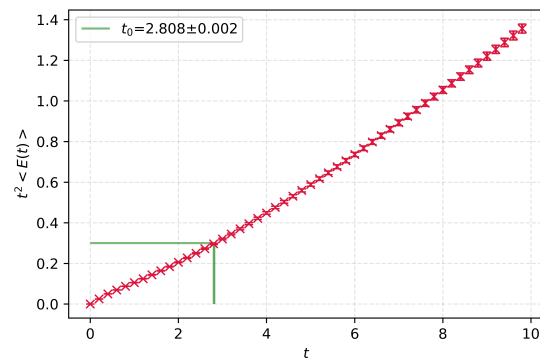FIGURE 6.2: *Correlator of $\mathcal{O} = \bar{\lambda}\gamma_5\lambda$ in $SU(2)$ $N_f = 2$ adjoint QCD*

FIGURE 6.3: *Determination of t_0 on a $32^3 \times 64$ lattice at $\beta = 1.65$ and $\kappa = 0.175$ in SU(2) SYM.*

6.4.2 Setting the scale

We have seen how to approximate path integrals by means of Monte Carlo methods and how to measure quantities on the thereby generated configurations. There is however a last point to discuss. The output of our measurements is always a dataset of dimension-less numbers, given in terms of the lattice spacing a, which is the only physical scale in

the simulation. For example, if we extract the mass of O_{PS} by taking the logarithm of the correlator 6.10, we would get a number aM, where M is the physical mass. If we want to extract physical information from our lattice data, for example in order to relate our results to experimental results or to other lattice studies, we have to set the scale, i.e. to determine the lattice spacing in physical units. In theories like QCD, this can be done by measuring an experimentally well-known quantity like the Sommer scale or the hadron masses. This procedure is of course analogue to our discussion in chapter 3, where we reviewed the RG flow. We fix a finite value of the renormalised coupling at some scale Λ_L, and we then tune the bare coupling to zero as we remove the cut-off. On the lattice, the observables also obey a Callan-Symanzik equation, which describes the flow of the coupling as function of a. To one-loop one has that a in general depends on the coupling as

$$a(g) = \frac{1}{\Lambda_L}(\beta_0 g^2)^{-\beta_1/2\beta_0^2} \exp\left(-\frac{1}{2\beta_0 g^2}\right)(1 + \mathcal{O}(g^2)),$$

and the scale Λ_L depends on the regularisation scheme. In the case of SYM, we make use of the NSZV beta function, whose two first coefficients are universal [78, 79]

$$\frac{\partial g}{\partial \log(a)} = -\frac{g^3}{16\pi^2}\frac{3N}{1 - \frac{Ng^2}{8\pi^2}} \quad \Rightarrow \quad a(g) = \frac{1}{\Lambda_L}\exp\left(-\frac{8\pi^2}{3Ng^2}\right). \tag{6.12}$$

Throughout this thesis we fix the scale by using the Wilson flow [80] (see chapter 7). We compute the flowed energy density

$$E(t) = \frac{1}{4}G_{\mu\nu}^a G_{\mu\nu}^a(t), \tag{6.13}$$

where $G_{\mu\nu}^a$ is the clover discretisation of the field strength tensor as in Eq. (6.9), with the links flowed through the integration of the flow equation 7.2. The scale t_0 parameter is then defined as

$$t^2\langle E(t)\rangle\big|_{t=t_0} = 0.3, \tag{6.14}$$

and has dimension length squared, so that $\sqrt{t_0}/a$ is dimensionless. An example of a typical determination of t_0 can be seen in Fig. 6.3. This measurement is computationally very inexpensive and the value of $t^2 E(t)$ is rather stable over the Markov Chain, as can be noticed from the tiny error bars in the figure. From some intermediate t on, the flow-time dependence of the observable is moreover almost lineal. This behaviour is related to the scaling (running) of the coupling, and it will be discussed in the next chapter (cf. Eq 7.7). In chapter 10 we will see that, in the case of near conformal theories, plotting $t^2 E(t)$ against t already gives us hints on scale invariance.

Chapter 7

The gradient flow

In the last decade, the gradient flow (GF) method [80–84] has caught a lot of attention especially within the lattice field theory community [85, 86]. It has not only found several important applications in the simulation of QFTs, but also motivated theoretical work related to its likely relation to the renormalisation group [87–91]. In this chapter we will introduce the GF, starting with its original formulation as given in [80, 82]. Considering the flow-time as an additional dimension, we will discuss how it doesn't introduce any UV singularities and thus flowed local composite operators are finite. We moreover show how the GF can be used to define a renormalised coupling constant, which may be used to compute a numerical non-perturbative beta-function. At the end of the chapter we will discuss how the GF can be related, in some situations, to the RG. We anticipate that this relation will allow us to extract the anomalous dimension of scaling operators, what we employ in chapter 10 in the context of adjoint QCD.

One of the main contributions of the author to the investigations of SYM and adjoint QCD within our collaboration has been to include the GF into the measurements carried out through the C++ code of the Monte Carlo simulations. As we will see, the fermion flow plays a central role in most of the results shown in this work. Its implementation has made possible the first observation of gaugino condensation, and thus of chiral symmetry breaking, made with Wilson fermions in SYM at zero temperature. Before, this had only been achieved by means of Ginsparg-Wilson fermions. Being able to compute the fermion flow (and thus flowed interpolators) has moreover made possible the very first investigations of the conformal window of adjoint QCD using the GF.

7.1   Flow equations

$$\partial_t B_\mu = D_\nu G_{\nu\mu}, \qquad\qquad B_\mu|_{t=0} = A_\mu, \qquad (7.1)$$
$$G_{\mu\nu} = \partial_\mu B_\nu - \partial_\nu B_\mu + [B_\mu, B_\nu], \qquad\qquad D_\mu = \partial_\mu + [B_\mu, \cdot]$$

This diffusion equation defines the gradient flow of the gauge field A_μ on field space, where we call t the *flow-time*. Moreover B and G are the flowed gauge field and curvature, respectively. The flow equation in terms of the lattice link variables $U_{x,\mu}$ is given by the flow of the Wilson action S_W:

$$\dot{V}_t(x, \mu) = -g_0^2 \left\{ \partial_{x,\mu} S_{\mathrm{w}}(V_t) \right\} V_t(x, \mu), \quad V_t(x, \mu)|_{t=0} = U(x, \mu). \tag{7.2}$$

Equation 7.1 is clearly highly non-linear, as several interaction terms appear because of the non-Abelian nature of the fields. To see how the flow acts on the fields, we can consider a perturbative ansatz $B_\mu = \sum g_0^k B_{\mu,k}$. At leading-order, the flowed field is

$$B_{\mu,1}(t, x) = \int d^D y \, K_t(x - y) A_\mu(y), \quad K_t(z) = \int \frac{d^D p}{(2\pi)^D} e^{ipz} e^{-tp^2} = \frac{e^{-z^2/4t}}{(4\pi t)^{D/2}}, \tag{7.3}$$

where $K_t(z)$ is the kernel of the diffusion equation. We see that the kernel has a smoothing effect on the fields. Indeed, the kernel manifestly smears the field over a space-time region, which can be easily determined to be $\sqrt{8t}$. Moreover, the term e^{-tp^2} is an evident momentum cut-off. It turns out that no UV divergences appear at higher order in perturbation theory. Further, it is also possible to write a flow equation for fermion fields. A simple choice is to consider a heat equation

$$\partial_t \chi = \Delta \chi, \quad \partial_t \bar{\chi} = \bar{\chi} \overleftarrow{\Delta}, \quad \chi|_{t=0} = \psi, \quad \bar{\chi}|_{t=0} = \bar{\psi}, \tag{7.4}$$
$$\Delta = D_\mu D^\mu, \quad D_\mu = \partial_\mu + B_\mu \cdot,$$

where the gauge fields in the covariant Laplacian are at the same flow-time as the fermions. This form of the fermion flow is not unique and other formulations have been given, e.g. the supersymmetric gradient flow [92–94][1]. Although it is fairly easy to see that the smoothening of gauge fields leads to the finiteness of correlators of composite gauge operators, the treatment of correlators involving flowed fermion fields requires some caution. As we will see, the fermion fields require an extra multiplicative renormalisation constant at $t > 0$. The full perturbation theory of the gradient flow was developed in [83], which we now briefly review.

---

[1]Although this approach explicitly preserves SUSY, it still remains a formal construction, since its practical implementation would demand a high computational cost.

7.2 D+1 dimensional theory

The flow-time can be lifted to be the extra dimension of a $D+1$ dimensional (non-Abelian gauge) field theory. From that point of view, the theory lives in the D dimensional boundary, while the smeared fields are local operators living in the bulk[2]. The new space-time manifold is simply $\mathbb{R}^4 \times (0, \infty]$. In the $D + 1$ theory the flow equations are imposed through Lie-algebra-valued Lagrange-multiplier-fields $L_\mu(t, x)$, $\lambda(t, x)$. Accordingly, the action can be written as

$$S_{\text{tot}} = S_D + S_{\text{gauge},t} + S_{\text{fermion},t} + S_{\text{ghost},t},$$

$$S_{\text{gauge},t} = -2 \int_0^\infty dt \int d^D x \, \text{tr} \left\{ L_\mu(t, x) \left(\partial_t B_\mu - D_\nu G_{\nu\mu} - D_\mu \partial_\nu B_\nu \right) (t, x) \right\}$$

$$S_{\text{fermion},t} = \int_0^\infty \left\{ dt \int d^D x \, \bar{\lambda}(t, x) \left(\partial_t - \Delta + \partial_\nu B_\nu \right) \chi(t, x) + \bar{\chi} \left(\overleftarrow{\partial}_t - \overleftarrow{\Delta} - \partial_\nu B_\nu \right) \lambda(t, x) \right\}$$

$$S_{\text{ghost},t} = -2 \int_0^\infty dt \int d^D x \, \text{tr} \left\{ \bar{d}(t, x) \left(\partial_t - D_\mu \partial_\mu \right) d(t, x) \right\}$$

where S_D is the usual YM action with matter. For simplicity it is possible to focus first on the gauge fields, provided they are flowed independently from the fermions. The theory on the boundary, as custom in the continuum, is gauge-fixed through the Faddeev-Popov mechanism. We moreover express the boundary theory through renormalised quantities. We have the renormalisation constants $Z, Z_3, \tilde{Z}_3$ corresponding to $A_{\mu,\text{R}}$, c_R, and $\bar{c}_\text{R}$, respectively. A natural question to ask is whether additional divergences arise in the bulk. To answer this question we begin by writing the gauge action as

$$S_{\text{gauge}} = \Delta S + S_{\text{bare}} + \Delta S_{\text{bc}},$$

where ΔS_{bc} are extra terms needed if one rewrites the boundary condition as

$$B_\mu|_{t=0} = A_{\mu,R}, \quad d|_{t=0} = c_R.$$

These new terms merely set the bulk fields on the boundary to be equal to the renormalised unflowed ones. As usual in perturbation theory, we expect infinities to appear in loop diagrams. Moreover, the required counter-terms should involve either only boundary fields or only bulk ones (see Ref. [83] for a thorough discussion on this). To see which divergent loop-diagrams contribute to the correlation functions of bulk fields, one should take a look at the general form of the diffusion kernel. The importance of the kernel is obvious, since this object drives the flow like a sort of flow-propagator, connecting fields

---

[2]There have been investigations where this picture is used in the context of gauge/gravity dualities, see Ref. [95, 96]

at different flow-times. The general form of the kernel to all orders in the coupling can be derived by solving equation (7.1). This can be split into the linear partial derivative term plus an interaction R_μ

$$\partial_t B_\mu = \partial_\nu \partial_\nu B_\mu + \partial_\mu \partial_\nu B_\nu + R_\mu, \quad R_\mu = 2[B_\nu, \partial_\nu B_\mu] - [B_\nu, \partial_\mu B_\nu] + [B_\mu, \partial_\nu B_\nu] + [B_\nu, [B_\nu, B_\mu]].$$

With this, the kernel is given by

$$K_t(z)_{\mu\nu} = \int \frac{d^D p}{(2\pi)^D} \frac{e^{ipz}}{p^2} \left\{ (\delta_{\mu\nu} p^2 - p_\mu p_\nu) e^{-tp^2} + p_\mu p_\nu e^{-tp^2} \right\}$$

and the bulk gauge field can be written as

$$B_\mu(t, x) = \int d^D y \left\{ K_t(x - y)_{\mu\nu} A_\nu(y) + \int_0^t ds \, K_{t-s}(x - y)_{\mu\nu} R_\nu(s, y) \right\}. \qquad (7.5)$$

The Feynman graphs would be built from interaction vertices, boundary operators and directed lines of increasing flow-time. From this we see, however, that the kernel is a retarded propagator and thus all flow-loops have to vanish. As a consequence, there are no divergences arising in the bulk. Any possible extra counter-term must arise from the value of the bulk fields on the boundary. This possibility is actually very restricted, as the only allowed counter-term in the action is

$$\text{c.t.} \sim \int d^D x \, \text{tr} \left\{ z_1 L_\mu(0, x) A_{\mu, \text{R}}(x) + z_2 \bar{d}(0, x) c_\text{R}(x) \right\}.$$

It turns out that BRS symmetry requires this counter-term to vanish. A similar analysis follows for the fermions. Since the fermion integral is Gaussian[3], we can use Wick's theorem and express the n-point functions through the contractions

$$\overbrace{\psi(x)\bar{\psi}}(y) = S(x, y), \quad \overbrace{\lambda(t, x)\bar{\lambda}}(s, y) = 0, \qquad (7.6)$$

$$\overbrace{\chi(t, x)\bar{\lambda}}(s, y) = \theta(t - s) K(t, x; s, y),$$

$$\overbrace{\lambda(t, x)\bar{\chi}}(s, y) = \theta(s - t) K(s, y; t, x)^\dagger,$$

$$\overbrace{\chi(t, x)\bar{\chi}}(s, y) = \int d^D v \, d^D w \, K(t, x; 0, v) S(v, w) K(s, y; 0, w)^\dagger$$

---

[3]Although $S_{f,t}$ is linear on the fields, integrating over the Lagrange-multiplier λ yields the flow equations through a delta-distribution. Therefore, the action is still quadratic in the fermion fields.

Hence, any counter-term must be proportional to either of these fields and, because of the discussion given above, it must live on the boundary. The only possible counter-term is

$$\text{c.t.} \sim \int d^D x \; \{\bar{\lambda}(0, x)\psi(x) + \bar{\psi}(x)\lambda(0, x)\},$$

which is related to a multiplicative wave-function renormalisation constant Z_χ

$$\chi = Z_\chi^{-1/2}\chi_{\mathrm{R}}, \quad \lambda = Z_\chi^{1/2}\lambda_{\mathrm{R}}.$$

Contrary the gauge fields case, this counter-term does not vanish and therefore the flowed fermionic fields require an extra renormalisation constant. It may seem that the GF would bring extra difficulties to actual computations. This is however not true. What the GF tells us is that for $t > 0$, all correlators we compute are automatically renormalised, up to a multiplicative renormalisation constant for the fermions. Since the flowed fields are smeared, this means that complicated local composite operators renormalise according to its field content, i.e. all we need is Z_χ. Moreover, the GF is defined in the continuum and is independent of the regularisation. This means that we can use these results and especially the advantages they bring for renormalisation, in lattice computations. On the lattice, the GF makes computations of currents and densities easier. As an especial case, we will see that the additive renormalisation constant, which is necessary for the computation of the gaugino condensate with Wilson fermions, is not necessary if these are flowed up to some finite flow-time.

7.3   Gradient flow and the renormalised coupling

The fact that correlators of flowed gauge fields are renormalised, allows us to use these kind of observables to define a renormalised coupling. As suggested in [80], a especially easy observable to measure with the GF is the energy density in Eq. 6.13. In terms of the $\overline{\mathrm{MS}}$ scheme of dimensional regularisation, its expansion in perturbation theory is

$$\langle E(t)\rangle = \frac{3(N^2 - 1)}{16t^2\pi^2}g_{\overline{\mathrm{MS}}}^2(\mu)\left(1 + c_1 g_{\overline{\mathrm{MS}}}^2(\mu) + \mathcal{O}(g_{\overline{\mathrm{MS}}}^4)\right).$$

One then defines the GF renormalised coupling as

$$g_{\mathrm{GF}}^2(\mu) = \frac{16\pi^2}{3(N^2 - 1)}t^2\langle E(t)\rangle\bigg|_{t=1/8\mu^2} \tag{7.7}$$

7.4 Relation between the gradient flow and RG transformations

The soft UV cut-off the GF puts on the fields (see Eq. 7.3), resembles the coarse graining step of a RG transformation. The similitude is evident if instead of the hard cut-off used in Eq. 3.1, one introduces a soft one like in the Polchinski equation. However, the GF is not a coarse graining in the RG sense. The issue is that the GF is a deterministic flow, which tends to bring the system to the classical minima of the bare action at large flow-times. This fact can already be seen from the flow equations. The RG flow, on the contrary, would lead the system to minima of the *effective action*. This means that the GF would correspond to a RG transformation if we would solve the flow equations for the effective action at each step of the RG. In the context of scalar field theory, it has been noted in Refs. [87, 90] that a RG transformation can be seen as originating from a stochastic process given by a Langevin equation

$$\partial_t \phi_t(x) = -\Delta \phi_t(x) + \eta_t(x), \quad \phi_0(x) = \varphi(x)$$

with solution

$$\phi_t(x) \equiv \phi_t[\varphi; \eta] = (K_t \varphi)(x) + \int_0^t ds (K_{t-s} \eta_s)(x),$$

where φ, ϕ are scalar fields, $\eta(x)$ is Gaussian distributed noise, and K_t is the GF or heat kernel. In this sense the flowed field is only the mean with respect to the noise η. As shown in [90], the Langevin equation generates a distribution $P_t(\phi, \varphi)$, i.e. the probability distribution of $\phi(t)$, given the initial condition φ at $t = 0$. It is moreover noted that the distribution is equivalent to a *constraint functional* in the context of functional RG. With such a distribution, the effective action is written as (cf. Eq. 3.1)

$$e^{-S_t[\phi]} = \int \mathcal{D}\varphi \, P_t(\phi, \varphi) e^{-S_0[\varphi]}, \quad P_0(\phi, \varphi) = \delta(\phi - \varphi) \tag{7.8}$$

where $S_0[\varphi]$ is the bare action. Moreover ϕ and φ are the lower and higher modes, respectively. Let us consider the correlator of some observable $\mathcal{O}$ in the effective theory:

$$\langle \mathcal{O}(\phi) \rangle_{S_t} = \frac{1}{Z} \int \mathcal{D}\phi \, \mathcal{O}(\phi) e^{-S_t[\phi]}.$$

By replacing Eq. 7.8 into the integrand, we notice that the integration over ϕ yields a stochastic mean value with respect to P_t:

$$\int \mathcal{D}\phi \, \mathcal{O}(\phi) P_t(\phi, \varphi) = \langle \mathcal{O}(\phi_t[\varphi, \eta]) \rangle_\eta$$

and this leads to the double expectation value

$$\langle \mathcal{O}(\phi) \rangle_{S_t} = \langle \langle \mathcal{O}(\phi_t[\varphi, \eta]) \rangle_\eta \rangle_{S_0}. \tag{7.9}$$

This remarkable result tells us that correlators in the low-energy effective theories are equivalent to the correlators of bare fields evolved by the Langevin equation. In other words, up to the expectation value over the noise η, we can compute the low energy expectation values from the GF of the bare theory. In the given references it was shown that the contribution from the stochastic noise becomes irrelevant when the insertion points of the correlators are well separated. As a result, at least in the context of scalar field theory, the GF may be related to the coarse graining step of a RG transformation and can be used to explore the long-length properties of a theory. Of course, only if the large separation condition is satisfied. In chapter 10 we will be interested in computing the flow of the mass anomalous dimension γ_m of adjoint QCD, in order to see if we find hints for the existence of an IR fixed point. At the fixed point, γ_m stops to run and reaches its critical value γ_*. In that chapter we will show how this value can be extracted from the GF, given the discussion presented in this section.

Chapter 8

The phase diagram of $\mathcal{N} = 1$ super Yang-Mills theory on the lattice

We saw in chapter 5 that, at zero temperature, massless SYM has a one-form Z_N symmetry which acts on Polyakov loops and which is related to the confinement of static external quarks. We have moreover seen that, also at zero temperature, the non-anomalous Z_{2N} symmetry is spontaneously broken down to Z_2 by the non-vanishing gaugino condensate. With that information, in this chapter we pursue the following two tasks.

First, we check if this zero temperature scenario is in fact dynamically realised by the theory. For this purpose, we will measure the expectation value of the Polyakov loop and the flowed gaugino condensate on different lattices at zero temperature. Despite the fact that the condensate has been computed analytically from instanton calculus, it is important to be able to compute its value from the full theory, without deformations and without breaking the gauge symmetry. This study is moreover a further step towards a determination of the exact normalisation constant of the condensate in the continuum and chiral limits, which could be compared to other renormalisation schemes.

The second task is to turn on a temperature and use the Polyakov loop and the condensate as order parameters to test the realisation of the centre and chiral symmetries. To achieve finite temperatures, we impose antiperiodic boundary conditions in the Euclidean time direction for the fermions and vary the length of the time compactification radius. The expectation is that at some critical temperature T_c^d we find a deconfinement phase transition signalled by a non-vanishing Polyakov loop expectation value. Moreover, we expect to see a phase transition at T_c^χ where the non-anomalous chiral symmetry Z_{2N} is recovered, i.e. where the gaugino condensate vanishes. It is natural to ask what kind of phases the theory has at different temperatures. Anomaly matching conditions give us the hint that confinement implies the spontaneous breaking of the chiral symmetry. From this follows that the following relation must hold [97–99]

$$T_c^\chi \geq T_c^d. \tag{8.1}$$

In other words, at T_c^d, we may find a phase transition to a mixed phase where the ground state is not confining but where chiral symmetry is still broken. The matching of the anomalies doesn't give us any further information and there is no other analytic way to confirm or rule out the existence of this mixed phase. At the end of this chapter we will have shown that, within the uncertainties of the numerical lattice computations, this phase is not realised by the $SU(2)$ gauge theory. Moreover, we will see that there are evidences, which suggest that it is also the case for $SU(3)$. Hence, the bound in equation 8.1 must be saturated. The $SU(2)$ results have been published in [100]. Our findings for $SU(3)$ are expected to be published soon. However, some preliminary observations have been presented in Ref. [101].

Let us now briefly comment on the technical difficulties we encounter when computing the order parameters. Although the computation of the Polyakov loop through the lattice version of equation 5.2

$$P_L = \frac{1}{V_3} \sum_{\vec{x}} \mathrm{Tr} \left\{ \prod_{t=1}^{N_t} U_4(\vec{x}, t) \right\} , \quad P_L \neq z\, P_L \tag{8.2}$$

is pretty straightforward, measuring the condensate is a more subtle and difficult task on the lattice. The reason is, of course, that the condensate is a true order parameter of the spontaneous breaking of the chiral symmetry when the gaugino is massless. We already saw that chiral symmetry is explicitly broken on the lattice and that we can only restore it either by tuning the renormalised gaugino mass to zero or by implementing Ginsparg-Wilson fermions. Since we use Wilson fermions, there is, besides the multiplicative renormalisation factor ($Z_{\bar{\lambda}\lambda}$), an additive renormalisation (b_0) in the condensate:

$$\langle \bar{\lambda}\lambda \rangle_{\mathrm{R}}^{\mathrm{W}} = Z_{\bar{\lambda}\lambda}(\beta)(\langle \bar{\lambda}\lambda \rangle_{\mathrm{B}}^{\mathrm{W}} - b_0(\beta)),$$

where the superscript "W" denotes that the condensate is computed with Wilson fermions. In the literature the additive constant b_0 is often removed by subtracting the value of the bare condensate at zero temperature [102]

$$\langle \bar{\lambda}\lambda \rangle_{\mathrm{S}}^{\mathrm{W}} = \langle \bar{\lambda}\lambda \rangle_{\mathrm{B}}^{\mathrm{W}}(T) - \langle \bar{\lambda}\lambda \rangle_{\mathrm{B}}^{\mathrm{W}}(T = 0).$$

This is however an incomplete solution, since the so "renormalised" condensate is forced to vanish at $T = 0$. Although this subtraction shouldn't have any effect in the determination of the critical temperature, with this ansatz it is not possible to determine whether the renormalised condensate vanishes at zero temperature or not.

8.1   The gaugino condensate from the gradient flow

In chapter 7 we saw that, in the flowed theory, the gauge fields don't renormalise and the fermions renormalise multiplicatively. Moreover, we found that composite operators renormalise just according to its field content. For the condensate, this means that

$$\langle \bar{\lambda}\lambda \rangle_{\mathrm{R}}(t) = Z_{\bar{\lambda}\lambda} \langle \bar{\lambda}\lambda \rangle_{\mathrm{B}}(t) = (Z_{\lambda}^{1/2})^2 \langle \bar{\lambda}\lambda \rangle_{\mathrm{B}}(t).$$

Since the GF is regularisation scheme independent, the flowed condensates should agree up to a multiplicative constant, both in the continuum and on the lattice, regardless of the explicit lattice discretisation. Thus, it must hold that

$$\langle \bar{\lambda}\lambda \rangle_{\mathrm{R}}(t)^{\mathrm{W}} = \langle \bar{\lambda}\lambda \rangle_{\mathrm{B}}(t) \sim \langle \bar{\lambda}\lambda \rangle_{\mathrm{R}}(t)$$

This means that there is no additive renormalisation constant in the flowed condensate, even with Wilson fermions. As a consequence, it is possible to determine from the flowed condensate whether the renormalised condensate is non-vanishing at zero temperature. Moreover, the both values would differ only by a constant factor. This computation would suffice to confirm the spontaneous breaking of chiral symmetry at zero temperature and in the chiral limit. The question about the flowed gaugino condensate being an adequate order parameter for chiral symmetry was already addressed by Lüscher in Ref. [82]. Since the GF equations preserve chiral symmetry, one expects the flowed chiral condensate to show the same critical behaviour as the unflowed one. As a consequence, measuring the temperature dependence of the former should be sufficient in order to explore the phase diagram of SYM. The issue of finding Z_λ can be avoided if the scale, i.e. β, is fixed.

The flowed gaugino condensate can be determined by means of Wick's theorem, together with the contractions in Eq. 7.6:

$$\langle \bar{\lambda}(x,t)\lambda(x,t) \rangle_{\mathrm{B}} = -\int d^D v d^D w \, K(t,x;0,v) S(v,w) K(t,x;0,w)^{\dagger}. \tag{8.3}$$

Thus, the flowed condensate is given by the action of the heat-kernel on the fermion propagator $S \equiv D^{-1}$. This is natural, since the (unflowed) condensate is proportional to the expectation value of the propagator: in the partition function $Z(m)$, the gaugino mass acts as a source for the fermion bilinear $\bar{\lambda}\lambda$, and thus the condensate can be computed as

the derivative of $\ln(Z(m))$ with respect to m:

$$\langle\bar{\lambda}\lambda\rangle_{\mathrm{B}} = -\frac{T}{V}\frac{\partial}{\partial m}\ln(Z(m)) \tag{8.4}$$

$$= -\frac{1}{Z(m)}\frac{T}{V}\frac{\partial}{\partial m}\left\langle\exp\left\{\left(\frac{1}{2}\mathrm{tr}\ln\left(D(m)\right)\right)\right\}\right\rangle_{S_g} = -\frac{T}{V}\left\langle\frac{1}{2}\mathrm{tr}D^{-1}\right\rangle$$

$$= -\frac{T}{V}\left\langle\frac{1}{2}\,\mathrm{tr}\,S\right\rangle.$$

It is worth to note how this derivation of the condensate allows for a comparison of the spontaneous breaking of chiral symmetry with the Z_N Ising model. In the Ising model the symmetry is broken by an external magnetic field and the order parameter is the spontaneous magnetisation. In SYM the mass act as the external field and the condensate as the magnetisation.

We stress again that the flowed condensate in equation 8.3 is proportional to any other renormalised condensate. The multiplicative factor in comparison to the $\overline{\mathrm{MS}}$ scheme can be determined from a small flow-time expansion [103].

8.2   The gaugino condensate on the lattice

The chiral condensate can be measured on each lattice configuration by means of the discrete version of equation (8.3)

$$\langle\bar{\lambda}(x,t)\lambda(x,t)\rangle_{\mathrm{B}} = -\sum_{v,w}\langle\mathrm{tr}\{K(t,x;0,v)(D_{\mathrm{W}}(v,w))^{-1}K(t,x;0,w)^{\dagger}\}\rangle,$$

where the trace runs over spinor and gauge group indices. For the numerical computation, it is helpful to insert a complete set of random complex noisy vector fields $\eta(x)$ with $\langle\eta(x)\rangle = 0$ and $\langle\eta(x)\eta(y)^{\dagger}\rangle = \delta_{x,y}$:

$$\langle\bar{\lambda}\lambda(t)\rangle = \frac{1}{N_{\Gamma}}\sum_{x\in\Gamma}\langle\bar{\lambda}\lambda(x,t)\rangle = -\frac{1}{N_{\Gamma}}\sum_{v,w}\langle\xi(t;0,v)^{\dagger}D_{\mathrm{W}}^{-1}\xi(t;0,w)\rangle, \tag{8.5}$$

$$\xi(t;s,w) = \sum_{x}K(t,x;s,w)^{\dagger}\eta(x).$$

This expression is evidently a lattice version of Eq. (8.4), where N_{Γ} represents the four-volume in lattice units. To compute the new vectors ξ, the following *adjoint* flow equation

$$\partial_s\xi(t;s,w) = -\Delta(V_s)\xi(t;s,w), \quad \xi(t;t,w) = \eta(w), \tag{8.6}$$

must be integrated from $s = t$ to $s = 0$, i.e. backwards in the flow-time. Here is where the computation turns out to be computationally expensive. We notice that the Laplacian $\Delta(V_s)$ is a covariant one. Thus, for every integration step, we need the value of the links V at flow-time s. Then, to integrate the noise fields from $s = t$ down to $s = t - \epsilon$, one first has to integrate the gauge field up to t. The algorithm to numerically compute the flowed condensate starts with the integration of the gauge fields:

1. Take an initial (unflowed) gauge configuration $V_{t=0}$

2. Integrate (7.2) up to some t by means of the following Runge-Kutta integrator with step-size ϵ

$$
\begin{aligned}
W_0 &= V_t, \\
W_1 &= \exp\{(1/4)Z_0\}W_0, \\
W_2 &= \exp\{(8/9)Z_1 - (17/36)Z_0\}W_1, \\
V_{t+\epsilon} &= \exp\{(3/4)Z_2 - (8/9)Z_1 + (17/36)Z_0\}W_2, \text{ with } Z_i = -\epsilon\partial_{x,\mu}S_{\mathrm{w}}(W_i),
\end{aligned}
$$

where S_w is the Wilson plaquette action. Equation 8.6 tells us that, to compute the flowed fermion for a given flow-time $s = t$, we need all the gauge fields from $t = 0$ up to $t = s$. The next steps in the algorithm are

3. Generate one random source vector $\xi_{s=t} = \eta$ on the lattice, for a given spinor-gauge-group index, and then integrate it by means of the following Runge-Kutta integrator down to $s = 0$

$$
\begin{aligned}
\lambda_3 &= \xi^\epsilon_{s+\epsilon}, \\
\lambda_2 &= \frac{3}{4}\Delta_2\lambda_3, \\
\lambda_1 &= \lambda_3 + \frac{8}{9}\Delta_1\lambda_2, \\
\lambda_0 &= \lambda_1 + \lambda_2 + \frac{1}{4}\Delta_0\left(\lambda_1 - \frac{8}{9}\lambda_2\right), \quad \text{with } \xi^\epsilon_s = \lambda_0
\end{aligned}
$$

4. Compute the vector $W(v) = \sum_w D(v, w)^{-1}\xi(t; 0, w)$ through the conjugate gradient method

5. Contract $W(v)$ with $\xi(t; 0, v)^\dagger$ and average over the lattice sites, i.e.

$$
-\frac{1}{N_\Gamma}\sum_v \xi_k(t; 0, v)^\dagger W(v)
$$

6. In order to have the full estimate of the condensate, the whole process must be repeated for sufficiently many source fields and covering all spinor-gauge-field-index combinations ($4 \times (N^2 - 1)$ for adjoint $SU(N)$).

At the end of the algorithm and from equation 8.5, we are left with an estimation of the flowed condensate $\langle \bar{\lambda}\lambda(t) \rangle$ for a given lattice configuration.

In the simulation code we have created a measurement sweep, where unflowed gauge configurations are read and then flowed according to points 1 and 2 of the algorithm. Afterwards they are converted into the adjoint representation and passed to the Laplacian operator Δ. Then points 2 through 6 are performed. A critical part is however the relation between memory usage and computing time. A direct implementation of the algorithm, i.e. computing the flowed gauge fields for every step of the adjoint fermion flow equation, yields a very slow performance. Computing speed can be improved by carrying out first the gauge integration for all flow-times, i.e. points 1 and 2, and keeping the flowed gauge fields in the memory, e.g. in a container of gauge configurations. This solution is ideal if one has access to large amounts of memory. It requires for example the usage of *fat* nodes on computer clusters. In our simulations we allow for a tuning of the ratio between memory usage and speed, depending on the available machines, the lattice parameters employed and the wished maximal flow-time. For example, for very large lattices and large flow-times, where huge amounts of memory are required, one can choose to save only some intermediate gauge configurations. Another important factor regarding the computation of the flowed condensate are both the integration step ϵ and the number of stochastic estimators $\eta(x)$. We will comment more on this later.

In the following sections we measure the flowed condensate at the scale t_0 and at different temperatures. An important step of the analysis is to check the flow-time dependence of the condensate. From the properties of the GF, one expects the condensate to take always larger values in the limit $t \to 0$, since there an additive renormalisation is required. At larger intermediate flow-times, the regularisation scheme independence of the GF should be evident and the condensate should vary very weakly with the flow-time, as it approximates the value of the renormalised condensate up to the multiplicative renormalisation constant. At very large flow-times, where the effective smearing radius $\sqrt{8t}$ is bigger than the lattice size, one expects oversmearing and thus non-physical results. In Fig.8.1 we show the flow-time dependence of the condensate. An example of how oversmearing affects the condensate can be seen in Fig. 8.4.
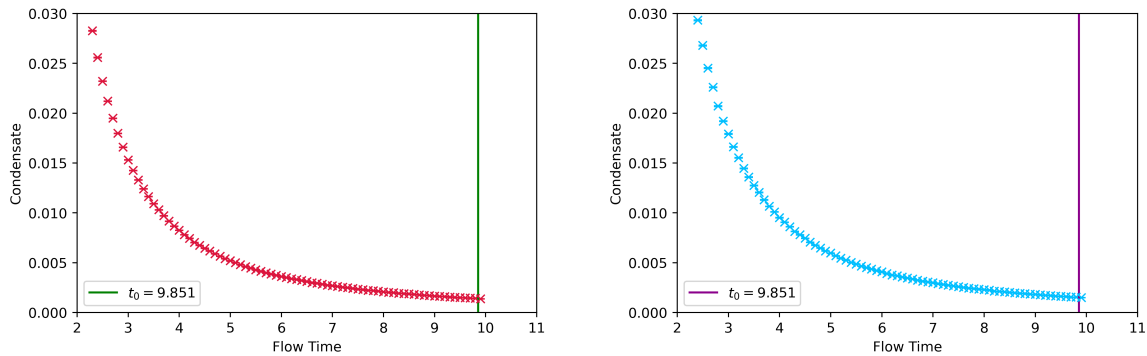
FIGURE 8.1: *flow-time dependence of the condensate in $SU(2)$ SYM at $\beta = 1.75$ and $\kappa = 0.1490$ with spatial volume 24^3. $N_t = 8$ (left) and $N_t = 10$ (right).*

8.3 The SU(2) SYM phase diagram

8.3.1 The gaugino condensate at zero temperature

We begin our investigations of the phase diagram of SU(2) SYM by measuring the gaugino condensate at zero temperature. Our lattice action is Symanzik improved (see Eq. 6.4). The links in the Dirac-Wilson operator have one-level stout smearing with $\rho = 0.15$. We choose a lattice coupling $\beta = 1.75$, volume $32^3 \times 64$ and four different bare gaugino masses with parameters $\kappa = 0.1490, 0.1492, 0.1494$ and 0.1495. The four different masses are used to extrapolate to the chiral/supersymmetric point, where the renormalised gaugino mass vanishes. All the results of the flowed condensate shown from this section on are expressed in units of t_0:

$$\langle \bar{\lambda} \lambda \rangle \ \equiv \ t_0^{3/2} \langle \bar{\lambda} \lambda(t) \rangle \ |_{t=t_0} \ .$$

For every κ value we have considered $\mathcal{O}(1000)$ configurations, starting at the 1000th in the Markov Chain to ensure thermalisation. We have moreover measured every fourth configuration, in order to reduce autocorrelation. Thus, we have analysed $\mathcal{O}(100)$ configurations for every κ value. We use t_0 to set the scale. We determined t_0 for each κ from Eq. 6.14 and found the chiral extrapolated value $t_0^{\text{chiral}} = 12.81(35)$. The flowed gaugino condensate was computed at the same flow-time t_0^{chiral} by employing the algorithm explained above. The results are summarised in table 8.1. Here is important to notice that the smearing radius at t_0 is smaller than the dimensions of the lattice box and then we shouldn't have any oversmearing troubles. The parameters of the computation are the integration step size ϵ and the number of stochastic estimators $\eta(x)$. In the case at hand, these parameters had to be chosen carefully. Regarding ϵ, one can be tempted to use a very small value, in order to gain precision in the Runge-Kutta integration. One

has however to take into account that the whole procedure of computing the flowed condensate is computationally very expensive. Not only the relation speed/memory explained above plays a role but also the inversion (cf. point 4 of the algorithm) of the Dirac operator at every integration step. After evaluating the influence of ϵ on the results, by analysing a small number of configurations, we have chosen $\epsilon = 0.01$. We have also chosen a rather conservative number of stochastic estimators, namely 10. The underlying reason is, again the computational cost. At the beginning of our analysis we have varied this number up to 100 on some test configurations and we observed no very significative deviations. In our simulations, after setting $n_\eta = 10$, we have controlled the error of the flowed condensate with respect to the stochastic estimators on every configuration and have seen that this error is in general $\sim \mathcal{O}(1e - 6)$. Moreover, the estimators on two different configurations are independent from each other. Thus, it suffices to only take into account the statistical uncertainty, which is quoted in the results of table 8.1. The statistical uncertainties are computed by means of jackknife resampling. It may be remarkable for the reader that the uncertainties are rather small. The stability of the value of the flowed condensate can be understood as arising from the following two factors. The first is the smoothening effect of the GF and the second is the fact that the renormalised gaugino masses we are considering are rather large (see 8.1). This means that we are still away from the chiral point and thus from the first order phase transition where both phases $(+, -)$ of the condensate coexist. If we were at smaller masses, we would see more fluctuations on the value of the flowed condensate and eventually tunnelling to the negative phase. We complement this discussion with the Monte Carlo histories of the flowed condensate in Fig. 8.2
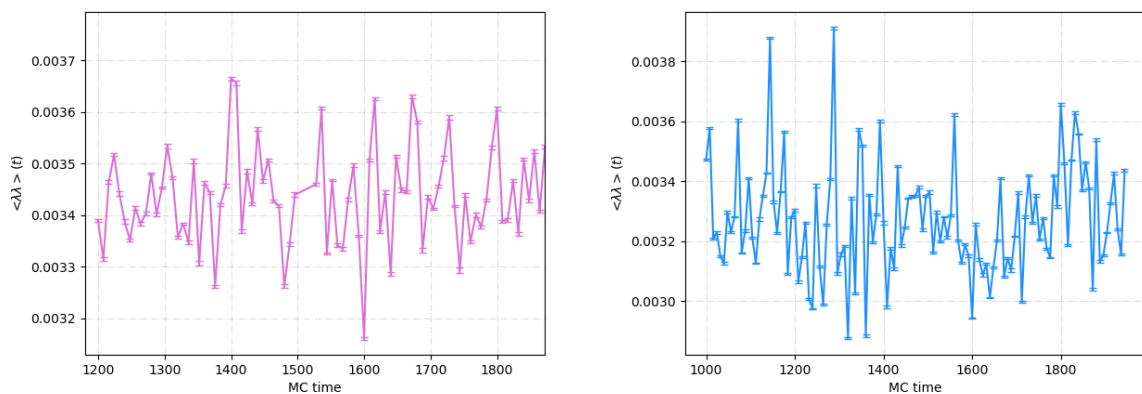
FIGURE 8.2: *Monte Carlo histories of the flowed condensate at $32^3 \times 64$, $\beta = 1.75$ and t_0^{chiral}. On the right $\kappa = 0.1492$, on the left $\kappa = 0.1495$.*

κ	am_π	t_0	$\langle \bar{\lambda}\lambda \rangle$
0.1490	0.23847(41)	9.851(32)	0.003520(23)
0.1492	0.20346(54)	10.545(69)	0.003441(10)
0.1494	0.1604(15)	11.262(72)	0.003353(9)
0.1495	0.1294(24)	12.49(18)	0.003269(21)

TABLE 8.1: *The GF scale t_0 for each κ and the values of the gaugino condensate for each ensemble.*

Linear	0.003185(14)
Quadratic	0.003160(30)

TABLE 8.2: *Extrapolations of the condensate to the chiral point.*

With the results of table 8.1, we have performed an extrapolation to the chiral/supersymmetric point, which can be seen in Fig. 8.3 and is summarised in table 8.2. The errors of the extrapolation result from the statistical uncertainties at every point. We can clearly see that the gaugino condensate doesn't vanish in the chiral limit. This result is actually the first clear numerical evidence, obtained with Wilson fermions, of the spontaneous breaking of the Z_{2N} chiral symmetry at zero temperature and zero gaugino mass. In previous non-gradient-flow studies found in the literature [38, 104], the formation of the condensate was inferred from a double peak observed in the Monte Carlo histogram. These simulations seem to have been however unstable, performed in small volumes close to the chiral point.

Because of the great advantages of the GF method, our results are as significant as those performed with Domain-Wall and overlap fermions in [64, 105–108]. Especially, there is a remarkable compatibility with the most recent results from overlap fermions (see Ref.[109]). As in our simulations, the authors of those works didn't determine the renormalisation factor $Z_{\bar{\lambda}\lambda}$ of the condensate and, therefore, their results are, as in our case, proportional to the renormalised condensate in the $\overline{\text{MS}}$ renormalisation scheme. These first GF investigations show that it is, in principle, possible to study the SYM vacua with Wilson fermions, which are computationally less expensive than the Ginsparg-Wilson fermions. This study can furthermore be seen as a first step towards more ambitious goals. As mentioned before, there have been discrepancies and puzzles regarding the output of analytical computations of the condensate by means of weak and strong coupling instanton calculations. One way to settle this issue would be to make more rigorous measurements of the condensate, so that one can get an exact value, which can be compared to the analytical predictions. For this purpose it would be necessary to

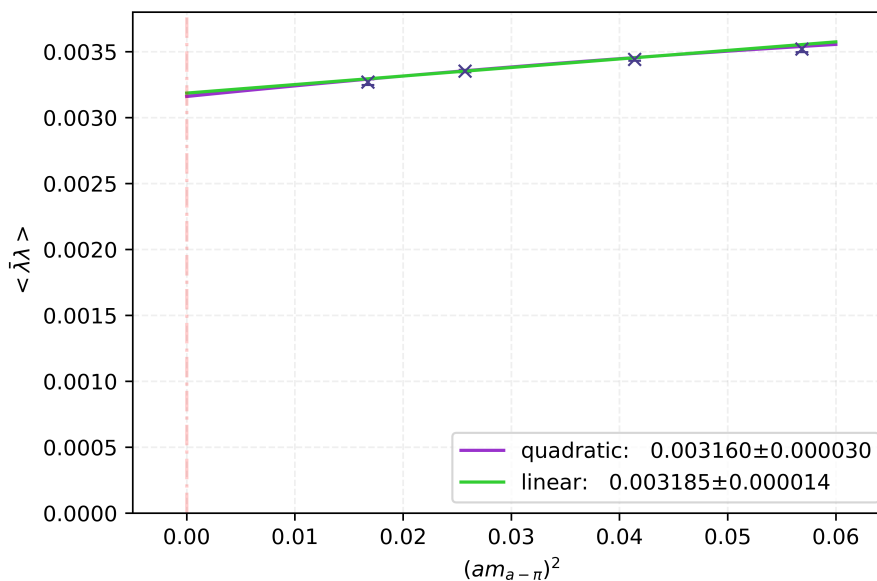1. Match our renormalisation scheme with, for example, $\overline{\text{MS}}$.

FIGURE 8.3: *Extrapolation of the condensate to the chiral point. It seems to scale linearly with the gaugino mass, while a weak quadratic dependence seems to appear as the mass grows.*

2. Determine the exact value of the renormalisation constant $Z_{\bar{\lambda}}$

3. Match the analytical, semi-classical predictions to $\overline{\text{MS}}$.

8.3.2 Chiral symmetry restoration and centre symmetry breaking

After having confirmed that chiral symmetry is broken at zero temperature, let us now see how the system behaves as the temperature rises. We analysed three different ensembles with coupling $\beta = 1.75$ and hopping parameters $\kappa = 0.1480, 0.1490, 0.14925$. We used the same lattice action as before. However, in order to check the lattice spacing effects in our results, we included an additional lattice with $\beta = 1.65$, $\kappa = 0.175$ and tree-level clover improved fermion action with unsmeared links. As mentioned above, non-zero temperatures are achieved by imposing anti-periodic boundary conditions for the fermions in the Euclidean time dimension. To achieve different temperatures we fix the lattice parameters and vary the length of the thermal circle N_t. The lattice volumes are thus $24^3 \times N_t$ for $N_t = 4, 5, 6, \cdots, 48$, with the upper bound labelling the zero-temperature limit. The number of configurations and the fermion flow integration parameters are analogous to the zero-temperature case. A difference is , however, that for these finite-temperature measurements we set a mass-dependent scale setting. This means that the flow-time t_0 where the gaugino condensate is measured, is different for each κ value. There are two reasons for this choice, which are related to the fact that t_0 becomes large in the chiral limit. The first one is that the numerical integration of the adjoint

flow equation 8.6 becomes very expensive as the flow-time grows. The second reason is that at large t and small N_t oversmearing takes over, leading to meaningless results. Luckily, all t_0 values allowed us to resolve inverse temperatures up to $N_t = 9$, which lie beyond the critical temperature. For the smallest gaugino mass, oversmearing can be seen already at $N_t = 8$, and is signalised by a growth in the value of the condensate. This can be seen in Fig. 8.4, where we have included the over-flowed value for illustrative purposes. To be sure that the mass-dependent scale doesn't introduce significant errors to the results, we measured the condensate at flow-times around t_0. For $t_0 \pm 0.1$, the value of the flowed condensate changes by about 1%. Therefore, we don't expect our results to significantly differ from those obtained with the chiral extrapolated fixed scale. This observation moreover means that the uncertainty in the value of t_0 at every κ doesn't greatly influence the determination of the critical temperature in physical units.
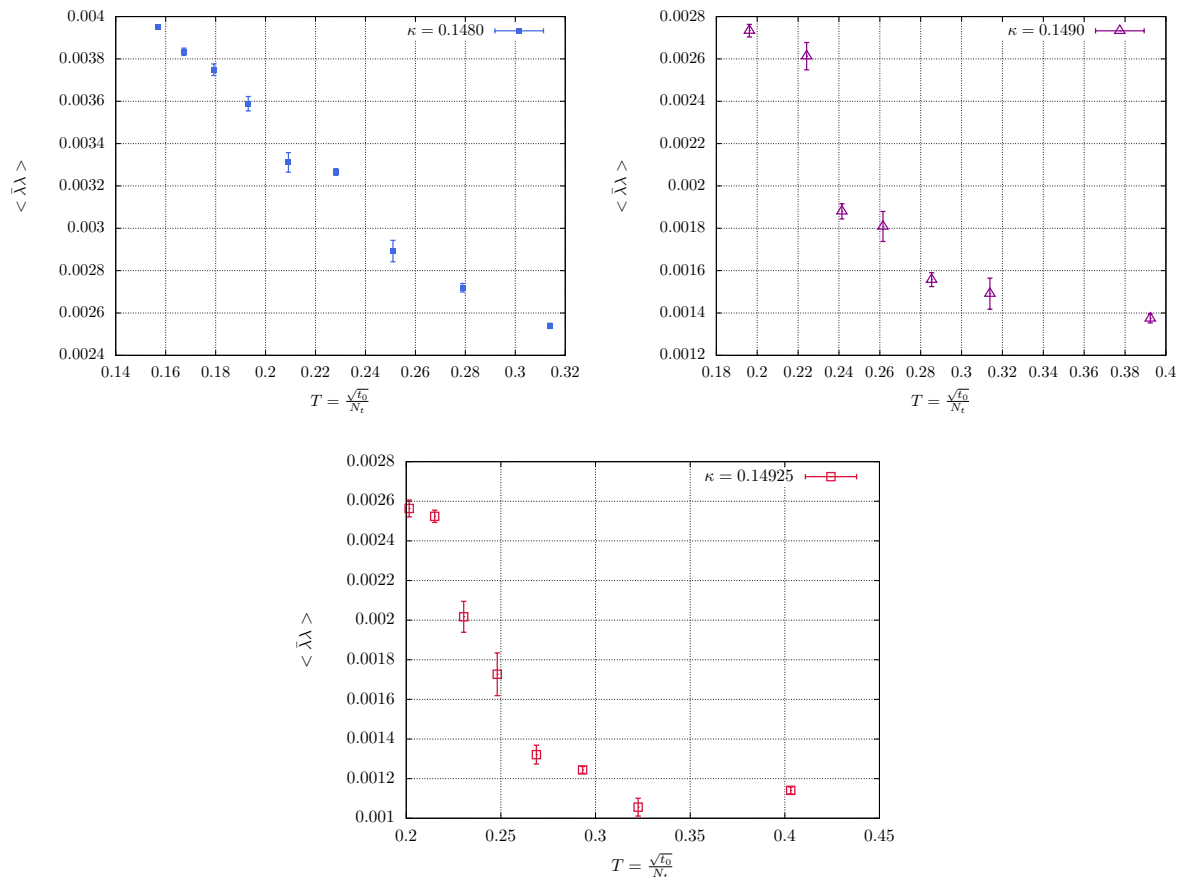
FIGURE 8.4: *Temperature dependence of the flowed gaugino condensate for $\kappa = 0.1480, 0.1490$ and 0.14925. On the lowermost graphic, the point corresponding to the highest temperature appears to show a growth in the condensate. This is however a non-physical over-smoothing artefact due to the fact that $\sqrt{8t_0} > N_t$ in that region.*
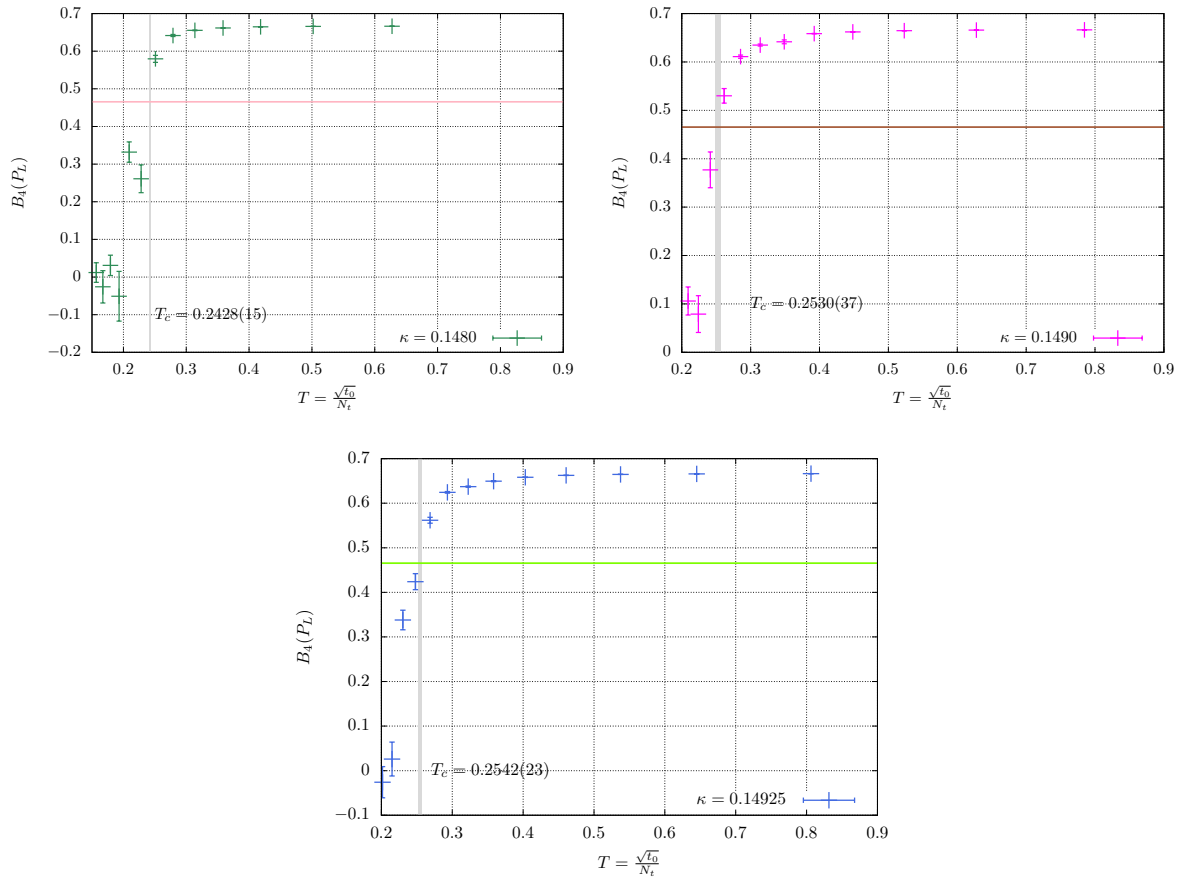
FIGURE 8.5: *Binder cumulant of the Polyakov loop at the same κ values of Fig. 8.4.*
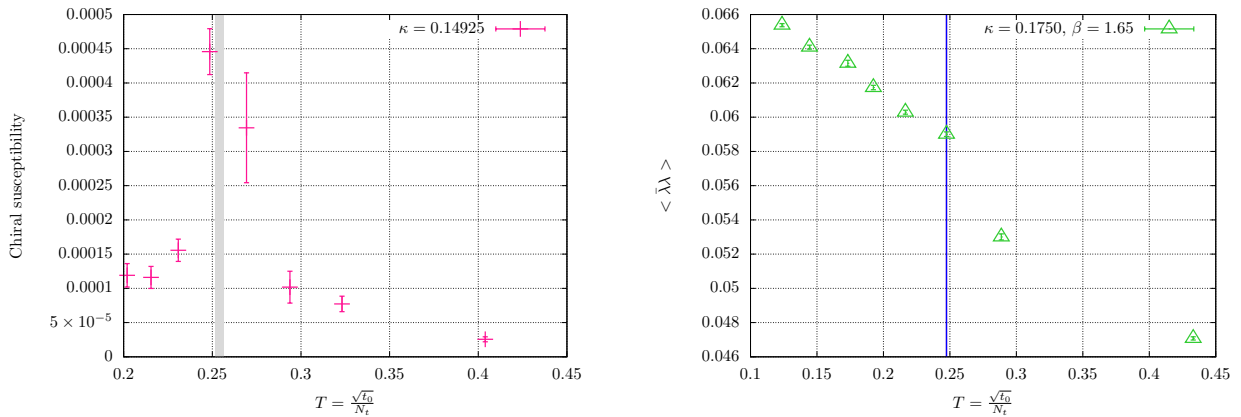
FIGURE 8.6: *Left: Chiral susceptibility at $\kappa = 0.14925$. The grey band denotes the critical temperature of the Polyakov loop. Right: gaugino condensate at $\beta = 1.65$ and $\kappa = 0.175$. The phase transition occurs at $N_t^c = 7$, which roughly agrees in dimensionless units with the critical temperature for $\beta = 1.75$.*

The results of the flowed condensate and the Polyakov loop are summarised in Figs. 8.4, 8.5, 8.6 and table A.1. In figure 8.4 we see that, at some temperature T_*^χ, the value of the condensate starts to quickly decrease. For the largest gaugino mass, this decreasing is almost monotonic. However, as the gaugino mass becomes smaller, we
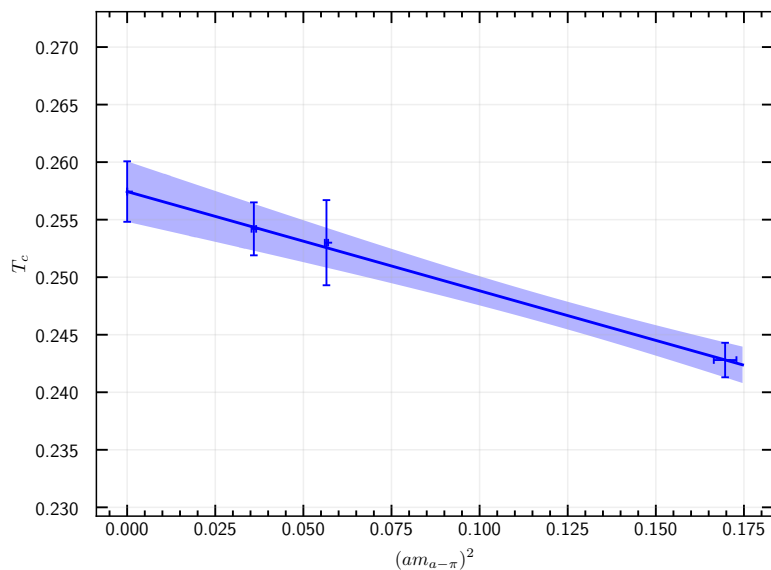
FIGURE 8.7: *Chiral extrapolation of the deconfinement phase transition. The deconfinement temperature extrapolated to the chiral limit is $T_c|_{m_{a-\pi}=0} = 0.2574(26)$.*

start to see a jump-like behaviour in the condensate value around T_*^χ. This is a pseudo phase transition, which we expect to become a true phase transition at zero gaugino mass, characterised by a jump to a vanishing condensate. Since T_*^χ doesn't change with the mass, we can say that this temperature is, in fact, the critical temperature, i.e. $T_*^\chi = T_c^\chi$. The existence of the phase transition can be more clearly seen from the disconnected chiral susceptibility in Figure 8.6.[1] From the peak of the susceptibility we see that the critical temperature is $T_c^\chi = \sqrt{t_0}/N_t \sim 0.25$. Remarkably, the same critical temperature is observed for $\beta = 1.65$ with the clover improved lattice action (see also Fig. 8.6). Although for most of the N_t values we analysed $\mathcal{O}(100)$ configurations, we have increased (doubled) the statistics at and around the critical temperature, e.g. $N_t \sim 13$ for $\kappa = 0.14925$. The reason is that, at these temperatures, the value of the flowed condensate shows significative fluctuations. This can be seen in the histories of Fig.8.8 and in the larger error bars in Fig. 8.4. Remarkably, as shown in the figure, it seems that we have spotted a negative condensate at one of the configurations.

We can now turn our attention to the deconfinement phase transition, which is a true phase transition even at non-zero fermion mass. In Ref.[102] it was found that the deconfinement phase transition is second order and that it shows the critical behaviour of the

---

[1]As noted in [102], it is expected that the largest contribution to the phase transition's peak comes from the disconnected part of the susceptibility.
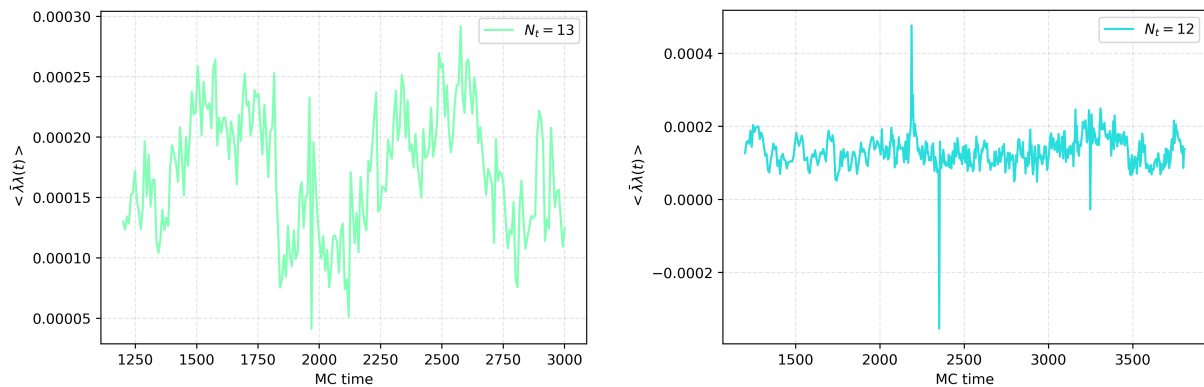
FIGURE 8.8: *Histories of the flowed condensate near the critical temperature at* $\kappa = 0.14925$.

Z_2 Ising model. Hence, one can use the Binder cumulant of the Polyakov loop

$$B_4(P_L) = 1 - \frac{1}{3}\frac{\langle P_L^4 \rangle}{\langle P_L^2 \rangle^2}$$

to determine the critical temperature. The transition occurs when $B_4(P_L)$ reaches the critical value $B_4^c = 0.46548(5)$ (for details see [110]). We measured B_4 at the given ensembles. The critical value B_4^c is shown as horizontal lines in the plots of Figure 8.5, for the different κ values. Here we would like to mention one drawback of the fixed scale approach, namely that we can only change the temperature by discrete steps. In order to precisely estimate at which temperature the critical point is achieved, we performed a linear interpolation of the Binder cumulant between the two points approaching the critical value B_4^c both from the left and from the right. The critical temperatures at finite gaugino mass were then extrapolated to the chiral/supersymmetric point through a linear fit. This extrapolation can be seen in figure 8.7. The extrapolated value is $T_c^d = 0.2574(26)$, which happens to coincide, up to numerical uncertainties, with T_c^χ. At this point it is worth to comment on the systematic uncertainties arising from SUSY breaking lattice artefacts. The authors of Ref. [40] investigated the low-energy particle spectrum and SUSY Ward identities on the same zero-temperature ensembles studied here. According to their results, the role of these lattice artefacts is expected to be small. Moreover, our findings are in agreement with the results of Ref.[102], obtained without GF, where a coincidence of the critical temperatures was also observed. The present work has however important differences, as we use an improved lattice action and smaller lattice spacing, combined with the advantages of the GF method. Our results are very remarkable. They suggest that the bound in equation 8.1, predicted from the matching of the anomalies, must be saturated. In this way lattice simulations allow us to get a deep insight into the physics of SYM, which is not possible from any known analytical tools. Indeed, the saturation of the bound is far

from trivial and some simulations of adjoint QCD have previously supported the existence of mixed deconfined-chirally-broken phases. In Ref. [111], for example, the authors found $T_c^\chi \simeq 8 T_c^d$ in $SU(3)$ two-flavour adjoint QCD with staggered fermions. Although non-perturbative analytical studies of SYM cannot predict our results, semi-classical analysis on $\mathbb{R}^3 \times \mathbb{S}^1$ have, in fact, predicted the coincidence of the phase transitions in SYM and adjoint QCD on that manifold (see Refs. [112–115]). Moreover, shortly we will see how the coincidence of the critical temperatures can be understood from the point of view of string-theory by means of a model which is equivalent to SYM at criticality.

To conclude the results for $SU(2)$ SYM, we compare the deconfinement critical temperatures of SYM and pure YM theory. The latter critical temperature is taken from Ref. [116]. We obtain the ratio

$$\frac{T_c(\text{SYM})}{T_c(\text{YM})} = \frac{0.2574(26)}{0.3082(2)} = 0.8352(90). \tag{8.7}$$

The temperatures are given through the GF scale as $\sqrt{t_0}/N_t^c$. The value of t_0 in $SU(2)$ YM was computed in Ref. [117]. Interestingly, the ratio is in rough agreement with the analytical prediction of Ref. [118], where the authors propose the value $\frac{T_c(\text{SYM})}{T_c(\text{YM})} = \sqrt{\frac{2}{3}} \sim 0.82$.

8.4 Prediction from string theory and anomaly matching

The coincidence of the critical temperatures not only means that confinement implies chiral symmetry breaking, as predicted from the consistency of the anomalies. Our results suggest, in fact, that both phenomena are non-trivially intertwined and that there should be an underlying mechanism that relates them. Such a result can't be inferred from non-perturbative analytical methods and thus the lattice shows itself as a very powerful tool. Unfortunately, the lattice is not able to provide us with the answer about *what* exactly causes the intertwining of these symmetries. Nevertheless, as often happens in physics, it is sometimes useful to take a look at dual formulations of a model. With dual formulation we mean that, in certain limits, a single phenomenon can be described by two different mathematical formulations. Thus, if one would find a dual framework describing the physics of SYM near criticality, and if we could have control on the topological aspects of this dual system, then it would be possible to predict the mentioned intertwining.

As it was shown by Witten, string theory formulations can, although not solve our problem, at least give some prediction in a model similar to our SYM. In Ref. [119] Witten considered a certain brane configuration consisting of two differently oriented NS five-branes and N D-four-branes stretching between them in weakly coupled IIA

superstring theory[2]. On the world-volume of the four-brane lives a 3+1 dimensional $SU(N)$ gauge theory with $\mathcal{N} = 1$ SUSY. This theory has N vacua, which can be regarded as the N vacua we get in SYM through spontaneous breaking of the chiral symmetry. Witten showed how the confining string emanating from a colour-electric source is topologically equivalent to the IIA fundamental string. Furthermore he found that the BPS-domain wall is a D-brane, and thus the confining strings can end on it. This fact directly relates confinement and chiral symmetry breaking. The domain wall, which is a kind of four-dimensional kink, has unbroken chiral symmetry in its core. Moreover a colour-electric source sufficiently near the wall behaves as a free quark, since the flux ends on the wall, charging it. Since the wall is colour-charged, the Polyakov loop expectation value doesn't vanish. This picture was further studied in Ref. [120] through an effective field theory for the condensate and the Polyakov loop. In the $SU(3)$ case, Z_3^χ restoration implies Z_3^c breaking. The authors of the study moreover argued that the results of Witten, i.e. that the confining strings end on the domain wall, can only be realised if both phase transitions agree.

Our results are in agreement with these observations. This is however not the end of the story. The string theory explanation is not fully satisfactory, since the model is just dual to SYM in some given limit. Therefore we don't learn much about how confinement and chiral symmetry breaking exactly arise in the first place. There is also no information about what happens after the phase transition, i.e. what the fate of the Z_N domain wall is.

8.5 The phase diagram of SU(3) SYM

After having explored the phase diagram of $SU(2)$ SYM, we focus now in the $SU(3)$, which is more similar to the real-world QCD. We measure again the Polyakov loop and the gaugino condensate. It is however important to notice that the vacuum structure is more complex and difficult to explore. In $SU(2)$ we had two degenerated vacua labelled by the two (real) values of the condensate $\langle \lambda\lambda \rangle = \pm 2c\Lambda^3$. In $SU(3)$ we have 3 degenerated vacua

$$\langle \lambda\lambda \rangle = 3c\Lambda^3 \begin{cases} \mathrm{e}^{2\pi i 0/3} \\ \mathrm{e}^{2\pi i 1/3} \\ \mathrm{e}^{2\pi i 2/3} \end{cases},$$

---

[2]The framework is actually M-theory. The brane model is not equivalent to SYM but is in the same universality class. SYM is obtained when taking the IIA, i.e. ten dimensional limit.

and only in one of them the condensate is real. As we see, the other 2 values of the condensate are complex. The extra imaginary part is given by a non-vanishing pseudoscalar condensate $\langle \bar{\lambda} \gamma_5 \lambda \rangle$. Non-vanishing values of the pseudoscalar condensate signal that the vacuum has broken CP symmetry. This is not surprising, as these vacua correspond to theta values different from 0 and π, and we know that only these two theta values yield CP symmetric vacua. It turns out that the observation of the first order phase transition at $m_g = 0$, i.e. the coexistence of the three degenerated vacua signalled by the corresponding peaks in the condensate histories, is as today an open problem. In fact, it seems that the exploration of the vacuum in the $SU(3)$ theory demands the use of Ginsparg-Wilson fermions. For this reason, we limit ourselves to the study of the thermal phase transitions, using the absolute value of the gaugino (scalar) condensate as the order parameter of chiral symmetry realisation. It is important to mention that this $SU(3)$ project is still a work in progress.

We choose a tree-level Symanzik improved gauge action and one-loop clover-improved Wilson-fermions with $c_{sw} = 1.598$. The lattice parameters are $\beta = 5.5$ and $V = 16^3 \times N_t$, with N_t between 4 and 12. The κ values are $0.165, 0.1667$ and 0.1673. The first part of our investigations consisted in the determination of the flowed condensate, analogous to the $SU(2)$ case. As expected, for $SU(3)$ the computational cost is much higher. Already the generation of $\mathcal{O}(2000)$ lattice configurations per κ and per N_t took quite a long time. The first results are shown in Fig. 8.9, where we show both the Polyakov loop and chiral susceptibilities for our two smallest gaugino masses. Remarkably both phase transitions appear to happen at the same critical temperature $T_c = 0.16$, which correspond to $N_t = 9$ in the case of $\kappa = 0.1673$ and $N_t = 8$ for $\kappa = 0.1667$. Hence, the critical temperature in physical units doesn't change considerably with the mass in the considered parameter range, and therefore the peaks of the susceptibilities signal a true phase transition. As a consequence, we also observe the intertwining of chiral and centre symmetries when the gauge group is $SU(3)$.

To observe the coincidence of critical temperatures at $N = 3$ is, in fact, not quite unexpected. There is actually no reason to think that the intertwining would disappear by increasing N. In fact, the string theory picture described above holds for general N. However, we cannot rush to assume that the phase transition is second order, like for $SU(2)$. Therefore, we have to look more carefully what is going on at and near the critical temperature. For this purpose we focused on the behaviour of the order parameter around $N_t = 9$ at the largest κ. The plot on the left of Fig. 8.10 shows the value of the unflowed gaugino condensate and the absolute value of the Polyakov loop for every analysed configuration. The plot on the right corresponds to the flowed gaugino
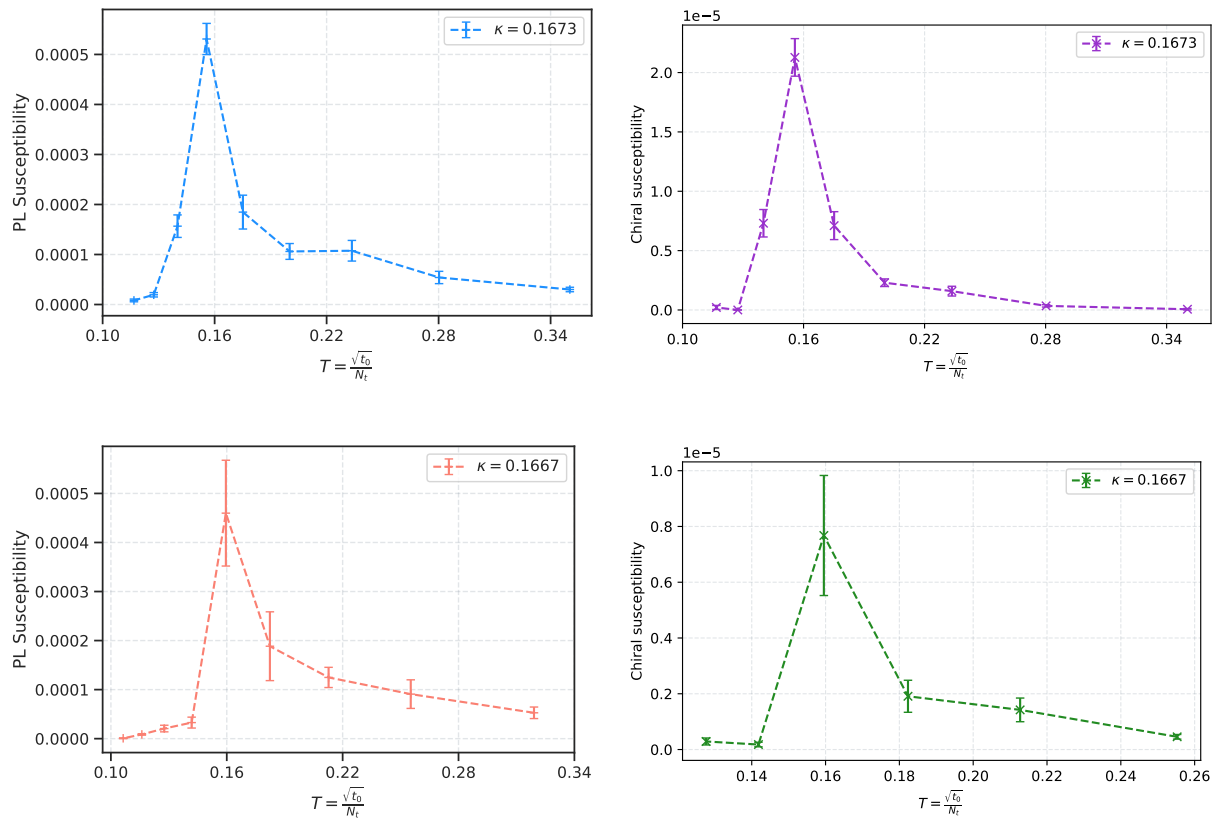
FIGURE 8.9: *Polyakov loop and chiral susceptibilities (left and right resp.) for different temperatures. The critical temperature for both phase transitions seem to be $T_c \sim 0.16$, which corresponds to $N_t = 9$.*
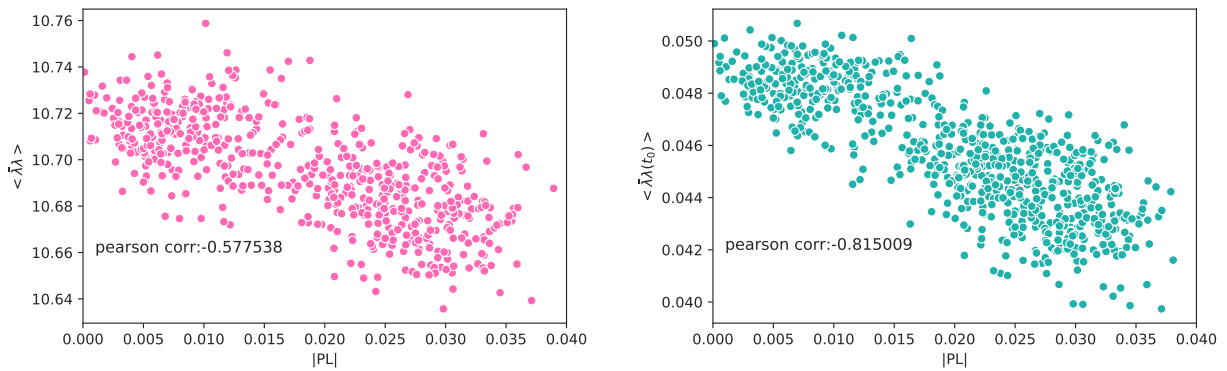

FIGURE 8.10: *Absolut value of the Polyakov loop against the unflowed (left) and flowed (right) gaugino condensate at $N_t = 9$, $\kappa = 0.1673$.*

condensate. Both plots provide us with two insightful pieces of information. We see that the order parameters seem to be correlated: configurations with a large Polyakov loop have a small gaugino condensate and vice versa. To confirm the correlation we considered the Pearson coefficient ρ in both cases. As shown in Fig. 8.10, the correlation number is significantly larger ($\rho = -0.815$) when employing the flowed condensate. This is a clear signal of the (anti)-correlation of both order parameters. The fact that the correlation is stronger when the condensate is flowed can be understood as a consequence of the gradient flow smoothing out the fluctuations. This observation further supports the coincidence of the phase transitions. The second piece of information is that there appear to form two domains, which correspond to the vacua at the phase transition. In both figures, the patch on the left corresponds to the confining/chiral-broken vacuum, while the patch on the right corresponds to the deconfined/chiral-restored one. This fact suggests the coexistence of the two kind of vacua and provide evidence for a possible first order phase transition.

In a similar way, the Monte Carlo histories (Fig. 8.11) and the 2d histograms (Fig. 8.12) of the Polyakov loop at different temperatures seem to support this picture. We see that, at high temperatures, the Polyakov loop is far away from zero. This corresponds to the deconfined phase. As we approach $N_t = 9$, the histogram starts to shift towards vanishing Polyakov loop expectation value. At $N_t = 9$, one starts to recognise high density regions, with one of them being near to zero. This is more visible when looking at the real part alone. At $N_t = 10$, the two peaks are more pronounced and one of them is centred around the origin. This can be interpreted as a hint for the coexistence of both the confined and deconfined phases at the critical temperature. Moreover, according to the data, the critical temperature should be somewhere between $N_t = 9$ and 10. As the temperature is further lowered, we see a unique peak around zero, which signals that the theory is confined, as expected. This is seen already at $N_t = 11$. To confirm the hypothesis of the phase transition being first order, further investigations are however required. For example, if it is first order, repeating the measurements on different volumes should yield that the positions of the peaks are stable with respect to the change in the volume and that the peaks become sharper. Also a larger statistics would be necessary. The completion of this study is currently work in progress.
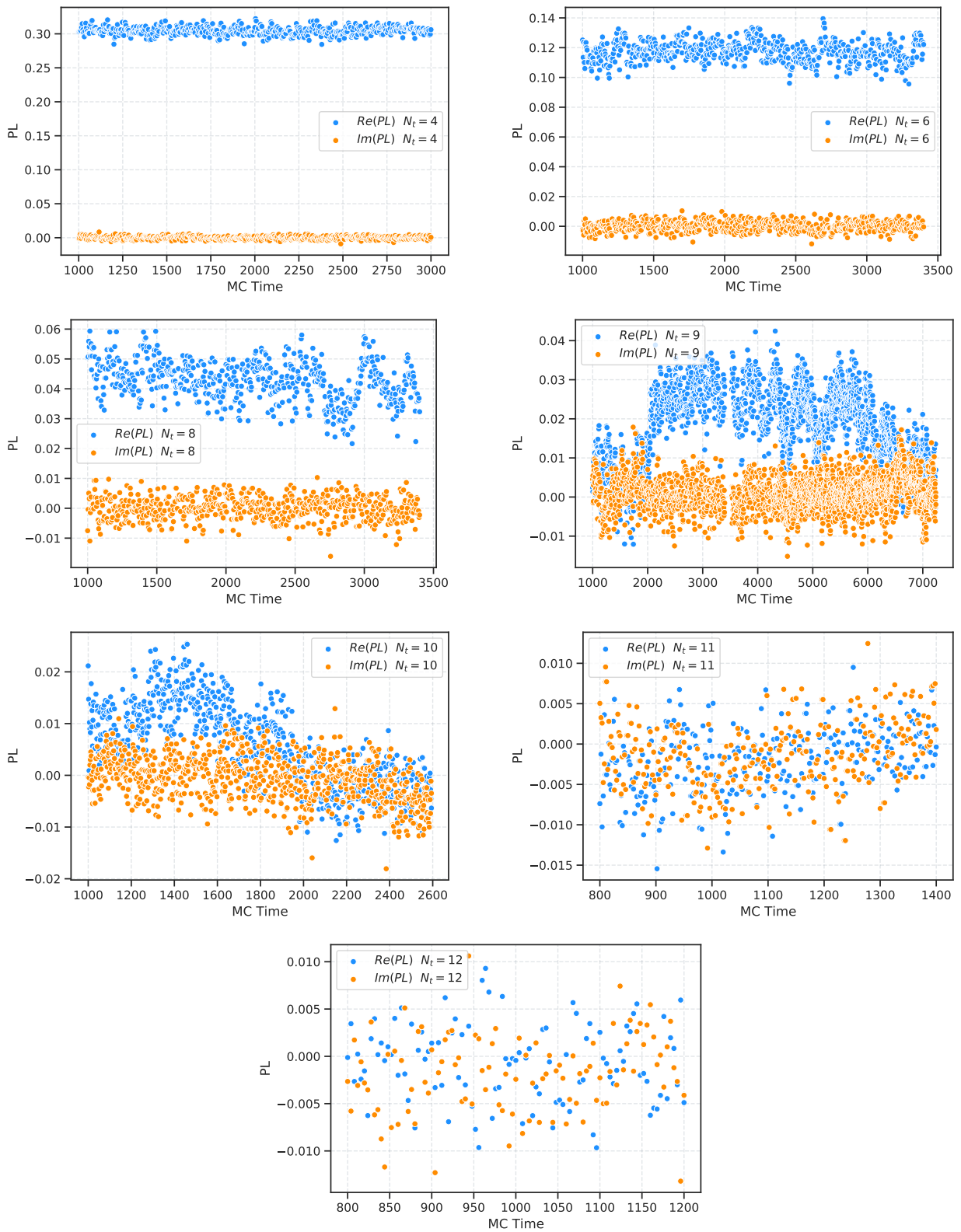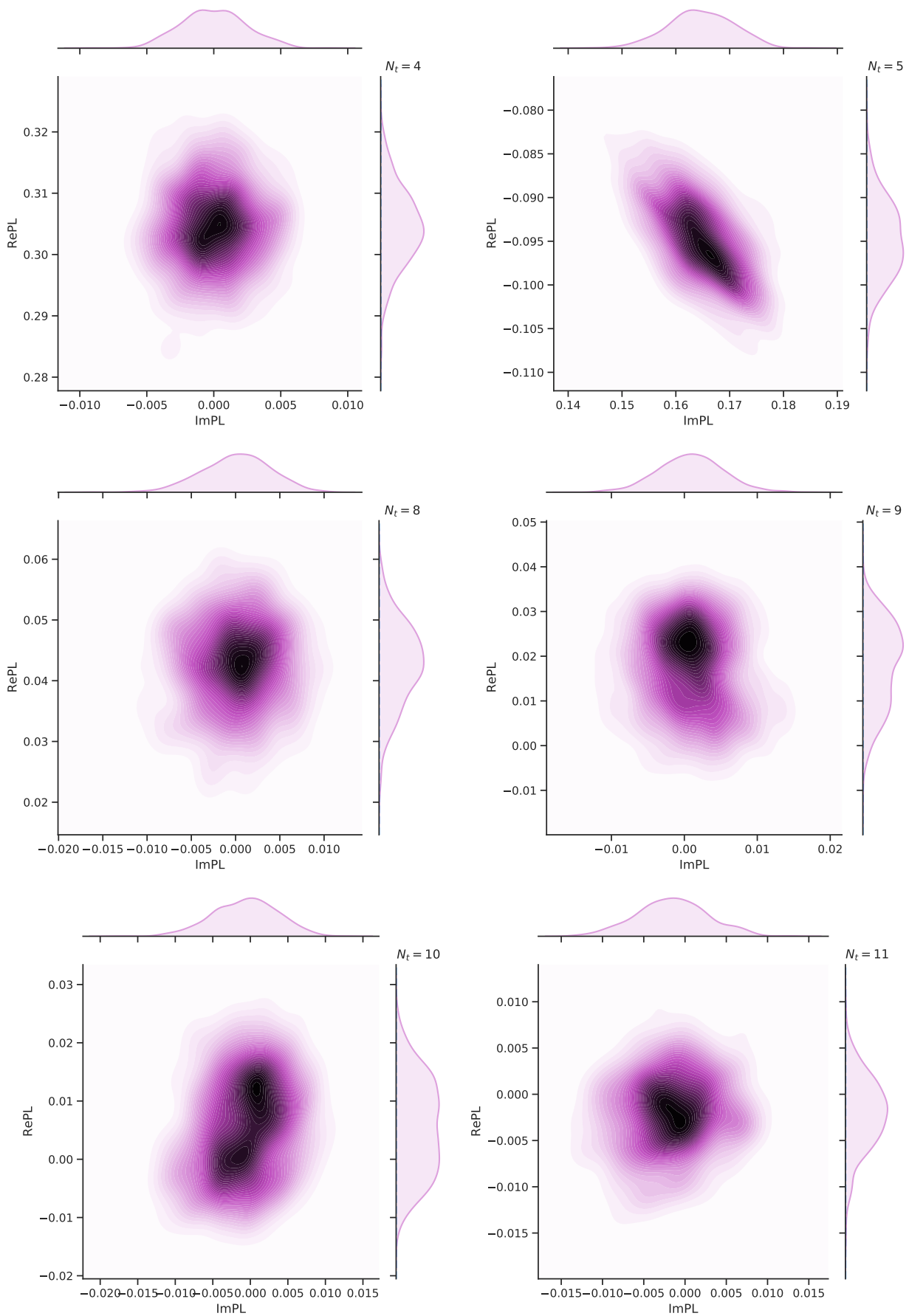
FIGURE 8.11: *Polyakov loop histories.*

FIGURE 8.12: *Polyakov loop density at $\beta = 5.5$, $\kappa = 0.1673$.*

Chapter 9

SU(3) super Yang-Mills theory on $\mathbb{R}^3 \times \mathbb{S}^1$

In this chapter we discuss the physics of adjoint QCD on $\mathbb{R}^3 \times \mathbb{S}^1$, with periodic boundary conditions for the fermions, and show results for the $n_f = 1$ supersymmetric case. In the large circle limit $L_4 \to \infty$ the theory naturally corresponds to the four-dimensional $\mathcal{N} = 1$ SYM theory, while the dimensional reduction $L_4 \to 0$ is $\mathcal{N} = 2$ SYM in three dimensions. In this chapter n_f denotes the number of Weyl fermions.

9.1 Semi-classics and confinement in adjoint QCD on the cylinder

The study of QCD-like theories defined on the cylinder $\mathbb{R}^3 \times \mathbb{S}^1$ has been a very active research topic in the last years (see for example Refs. [113–115, 121–128]). A clear motivation for this is the qualitative *understanding* of confinement. Although this phenomenon is well understood in some SUSY models with scalars, the same cannot be said for QCD-like theories on $\mathbb{R}^4$ and $\mathbb{R}^{(3,1)}$, where it is still an open problem. The reason behind this difficulty was already mentioned before. If we want to understand confinement from the non-perturbative contributions of gauge bundles with non-trivial topology, like instantons, we encounter the obstacle that semi-classical expansions are not valid at large distances. An insightful way to overcome this is to work with the theory on the cylinder. Because of asymptotic freedom, at small radii $L_4\Lambda \ll 1$, QCD-like theories are weakly coupled and thus we can trust semi-classical analysis. Using this technique with the hope of learning about confinement in $\mathbb{R}^4$, is however only realisable as long as there is no deconfinement at some critical radius L_c. If the small circle and infinite circle regimes are smoothly connected, i.e. if there are no phase transitions, we speak of *adiabatic continuity*. This requirement already fails for pure YM, where the theory on the cylinder is thermal and we have the familiar deconfinement transition at weak coupling[1]. It has been proposed that centre symmetry can be preserved at all L_4 if we include adjoint fermions

---

[1]A way out is to deform the theory by a double trace operator which stabilises the centre symmetry at small radii. This was proposed in [128]

[125]. We say then that the fermions dynamically stabilise the bosonic effective potential responsible for the breaking of the symmetry. Thus, the origin of confinement in adjoint QCD may be analytically studied through the semi-classical approximation on the cylinder. Also in Ref. [125], the authors have found that topological molecules called *bions* are responsible for confinement in the small radius regime. Let's briefly comment on the main results.

At the small radius regime, adjoint QCD is similar to the 3d Georgi-Glashow model. The theory Abelianises, i.e. the gauge group is Higgsed $SU(N) \to U(1)^{N-1}$, due to a non-vanishing VEV of the gauge field A_4 around the compact direction, so that the Wilson loop becomes

$$\Omega(x) = \mathcal{P}\mathrm{e}^{i \int dx_4 \, A_4} \quad \Rightarrow \quad \Omega(x) = \mathrm{e}^{iL\Phi}, \quad \Phi = \mathrm{diag}(\phi_1, \phi_2, \cdots, \phi_N).$$

Hence, the gauge field A_4 gives rise to the 3d adjoint scalar $\Phi = \Phi^a T^a$, the Higgs field, which is compact because it is circle-valued[2]. Each VEV correspond to one of the N vacua (supersymmetric in SYM), which are connected by Z_N transformations. After the Abelianisation, the colour non-diagonal components of the fermions and gauge fields become massive (W bosons), while the diagonal parts become photons and massless fermions. Perturbatively, an effective potential arises after the Kaluza-Klein (KK) modes with $k_n \sim \frac{2\pi n}{L_4}$ are integrated out

$$V_{\mathrm{pert}}[\Omega] = (-1 + n_f)\frac{2}{\pi^2 L_4^4} \sum_n \frac{1}{n^4} |\operatorname{tr} \Omega^n|^2,$$

which vanishes for SYM. Moreover, because of SUSY, the potential vanishes to all orders in perturbation theory. We focus now exclusively on SYM, although the more general $n_f > 1$ cases follow similarly, as the arguments will not rely on SUSY. Let's see now how a potential may arise non-perturbatively. Similar to the Georgi-Glashow model, we have $N - 1$ three-dimensional $SU(2) \hookrightarrow SU(N)$ BPS monopoles (monopole-instanton on the Euclidean cylinder). Since at $L_4 > 0$ the theory is still locally four dimensional and due to the compactness of the Higgs field, there is an additional so-called KK monopole-instanton[3]. The monopoles have the following magnetic and topological charges (mag,top)

$$\mathrm{BPS} : (1, 1/2), \quad \mathrm{KK} : (-1, 1/2)$$

$$\overline{\mathrm{BPS}} : (-1, -1/2) \quad \overline{\mathrm{KK}} : (1, -1/2).$$

---

[2]Note that this feature is unlike the SM Higgs, which is $\mathbb{R}$-valued.
[3]If one thinks of the BPS monopoles as connecting the vacua $\phi_1 \to \phi_2, \cdots, \phi_{N-1} \to \phi_N$, the KK monopole connects $\phi_N \to \phi_1$, because of the compactness of the Higgs.

Because of the index theorem, each monopole creates two fermionic zero modes[4]. Let us ignore for a while the fermions. In the semi-classical approximation, one writes the partition function as a sum over well separated monopoles $e^{S_{\text{mono}}}$ and their Coulomb-like interactions (dilute monopole gas). Because of the Abelian duality in 3d QED, the interactions can be written by means of the scalar dual photon σ through operator insertions $e^{i\sigma(x)}$. This results in a sine-Gordon-like effective Lagrangian of the form

$$\mathcal{L}_\sigma = \frac{1}{2}(\partial_\mu \sigma) - ce^{-S_0}\cos(\sigma),$$

where e^{-S_0} is the 1-instanton amplitude and c is a constant. Thus, in the absence of fermions, monopole-instantons generate a mass for σ. The story is different when massless fermions are included, since the instantons always come along with two zero modes each:

$$e^{-S_0}\cos\sigma \quad \rightarrow \quad e^{-S_0}\det\lambda_0\lambda_0(\cos\sigma).$$

As a consequence, the $\cos(\sigma)$ term is not part of the bosonic potential. In Ref. [125], it was proposed that only objects with vanishing topological charge can contribute to the bosonic potential. These objects appear at order e^{-2S_0} in the semi-classical expansion. To order e^{-2S_0}, the effective bosonic Lagrangian is

$$\mathcal{L}_\sigma = \frac{1}{2}(\partial_\mu \sigma) - be^{-2S_0}\cos(2\sigma),$$

where b is a constant. The 2σ term signals that the contributions to the potential come from objects carrying two times the monopole charge. These are precisely pairs (or molecules) of monopoles-antimonopoles, e.g. BPS·$\overline{\text{KK}}$. They are called *magnetic bions*. This bosonic potential generates a mass term for σ, which then generates confinement through Debye screening. The dual-photon mass is proportional to the confinement string tension. The pairing of the monopoles forming the bions is stable due to an effective attractive force, which arises through two-fermion exchange. This force overcome the repulsive magnetic force between them.

Magnetic bions thus explain confinement in SYM on the cylinder at small L_4, through the generation of a centre-stabilising effective potential. It is now natural to ask what happens beyond the range of validity of the semi-classical expansion $L\Lambda \ll 1$ and at $m_g \neq 0$. In general one probes the phase structure as function of L_4 and the gaugino mass m_g by means of the partition function, which for periodic boundary conditions is

---

[4]In $\mathbb{R}^4$ we have that BPS instantons are associated to $4n_f$ zero modes, because their topological charge is $n = 1$.

the graded (non-thermal) sum

$$\tilde{Z}(L_4, m_g) = \mathrm{tr}\left[\mathrm{e}^{-L_4 \hat{H}(m_g)}(-1)^F\right]. \tag{9.1}$$

In massless SYM, only the zero-modes contribute and thus equation 9.1 reduces to the Witten index $I_W = N$, which is independent of L_4 and correspond to the N supersymmetric vacua labelled by the VEV of A_4. This independence makes clear that, in the massless limit, there should be continuity between the small and large circle physics. For $m_g \neq 0$, i.e. for softly-broken SUSY, $\tilde{Z}$ is not an index, but it is a functional that "interpolates" between the Witten index and the thermal partition function of pure YM, where the fermion decouples as $m_g \rightarrow \infty$. Contrary to the massless case, a small mass not only breaks SUSY but also leads to a non-zero perturbative effective potential

$$V_{\mathrm{pert}}[\Omega] = -\frac{m_g^2}{2\pi^2 L_4^2} \sum_n \frac{1}{n^2}|\operatorname{tr}\Omega^n|^2,$$

which breaks the centre symmetry, and to corrections to the non-perturbative one. Then, in the different regions of the (L_4, m_g) plane, there is a competition among the different centre-stabilising and centre-destabilising contributions. As discussed in Ref. [123], within the range of validity of the semi-classics, centre symmetry is preserved if $m_g/8L_4 \ll 1$, where bion contributions dominate. Outside that range, e.g. at smaller L_4 and fixed m_g, destabilising monopole effects take over leading to deconfinement. From here follows an additional continuity conjecture, namely that on the (L_4, m_g) plane the deconfinement phase transition line smoothly connects SYM (m_g=0) and thermal YM theory ($m_g \rightarrow \infty$). A semi-classical prediction of the phase diagram of $SU(2)$ SYM is sketched in Fig. 9.1. Interestingly, this figure is compatible with our result of section 8.3.2, namely the ratio of deconfinement phase transitions $T_c(\mathrm{SYM}) = 0.8352\, T_c(\mathrm{YM})$.

9.2 Confinement of SU(3) SYM on the cylinder

The nice semi-classical picture explained above is very revealing and sheds light on the long-standing confinement problem. The continuity of this description up to the the $\mathbb{R}^4$ limit depends, as mentioned earlier, on the absence of phase transitions as $L_4 \rightarrow \infty$. Of course, taking this limit moves us of away from the weak coupling regime that is trackable through the semi-classical approximation. We can test the continuity by simulating the theory on the lattice.

In our discretisation, we employ a tree-level Symanzik improved gauge action and
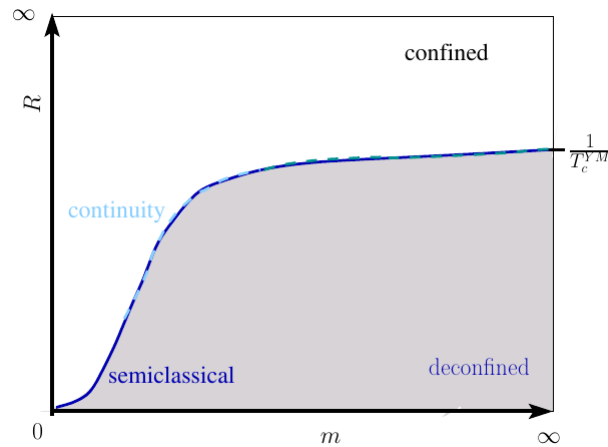
FIGURE 9.1: *Semi-classical prediction of the phase diagram of SYM on the cylinder. Figure taken from Ref. [129].*

one-loop clover-improved Wilson fermions. We test continuity by measuring the fundamental Polyakov loop at different compactification radii L_4. As for $SU(3)$ at finite temperatures, we set the bare gauge coupling $\beta = 5.5$. We analyse three different gaugino masses corresponding to the hopping parameters $\kappa = 0.165, 0.1667, 0.1673$, with the critical point being at $\kappa_c = 0.1684$. The different radii of the cylinder are achieved, at fixed β, by varying the number of points in that dimension, i.e. N_t. Moreover $\mathbb{R}^3$ is, as usual, approximated by choosing the other cycles of the lattice to be much larger than the compact time direction. We considered nine different radii $N_t \in \{4, \cdots, 12\}$. The results are summarised in figure 9.2, where we compare both boundary conditions.
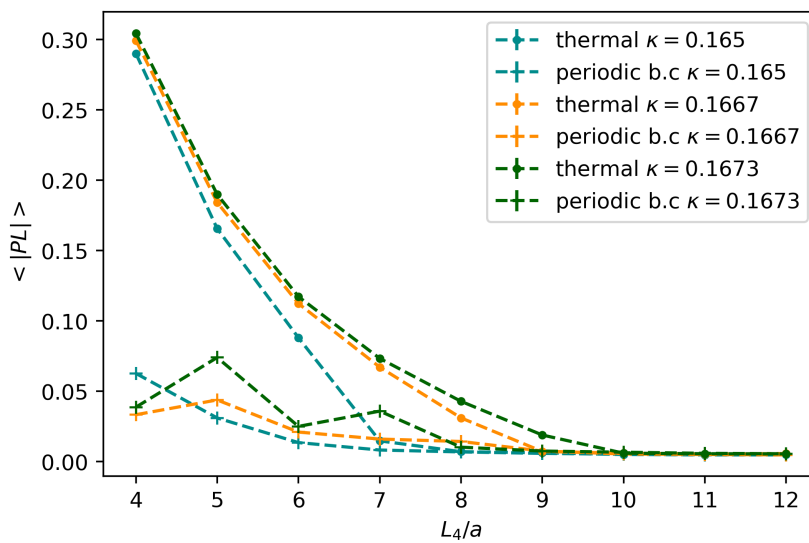
FIGURE 9.2: *Comparison of the Polyakov loop at different L_4 for both the thermal theory and the theory on the cylinder.*

We first see that for large radii (low temperature) $N_t = 10, 11, 12$, the theory is always confined, as expected from the limits $L_4 \to \infty$ and $T \to 0$. Then, for thermal boundary conditions, the centre symmetry gets broken already at large radii, signalised by a non-vanishing Polyakov loop VEV. The critical temperature of the phase transition $aT_c = 1/N_t^c$ is higher for larger bare fermion mass, and it is expected to reach the critical value for pure YM in the limit $m_g \to \infty$.
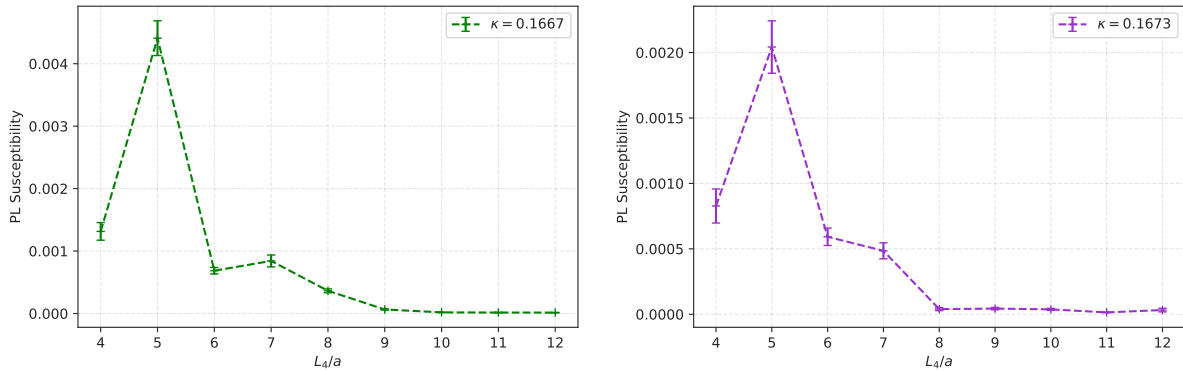

FIGURE 9.3: *Polyakov loop susceptibilities at* $\kappa = 0.1667$ *and* $\kappa = 0.1673$ *as function of* L_4. *A peak is observed at* $N_t = 5$.

For periodic boundary conditions, the theory remains confined up to smaller L_4. In Fig. 9.3 we see a peak in the susceptibility of the Polyakov loop at around $N_t^c = 5$ for the two largest κ values, which may be a signal of deconfinement. Hence, we already encounter a difference with respect to anti-periodic boundary conditions, where the peak of the susceptibility was found at $N_t = 9$. This difference tells us that the theory on the cylinder confines at least down to $N_t = 5$. Nevertheless, in order to be able to determine if there is actually a deconfinement phase transition, we need to take a closer look at the behaviour of the Polyakov loop near the peak, just as we did for finite temperatures. In Fig. 9.4 we see the density plots of the Polyakov loop in the complex plane. At $N_t = 9$ the theory is clearly confining. When the radius L_4 is reduced, the values of the Polyakov loop are distributed around a small region near to zero. A direct comparison of the plots at $N_t = 5$ for periodic and antiperiodic (Fig. 8.12) boundary conditions makes however evident that, on the cylinder, the non-vanishing value of the Polyakov loop is significantly smaller. An important observation is moreover that the distribution of the Polyakov loop is very broad at small compactification radii. This means that the effective potential at such radii is nearly flat, and its minimum is marginally shifted from the origin. This picture could however change if we would increase the statistics. We could namely see a clearer distribution around zero, i.e. confinement. The flatness of the potential together with the fact that finite size and volume effects become significant as $N_t \to 0$[5], make such

---

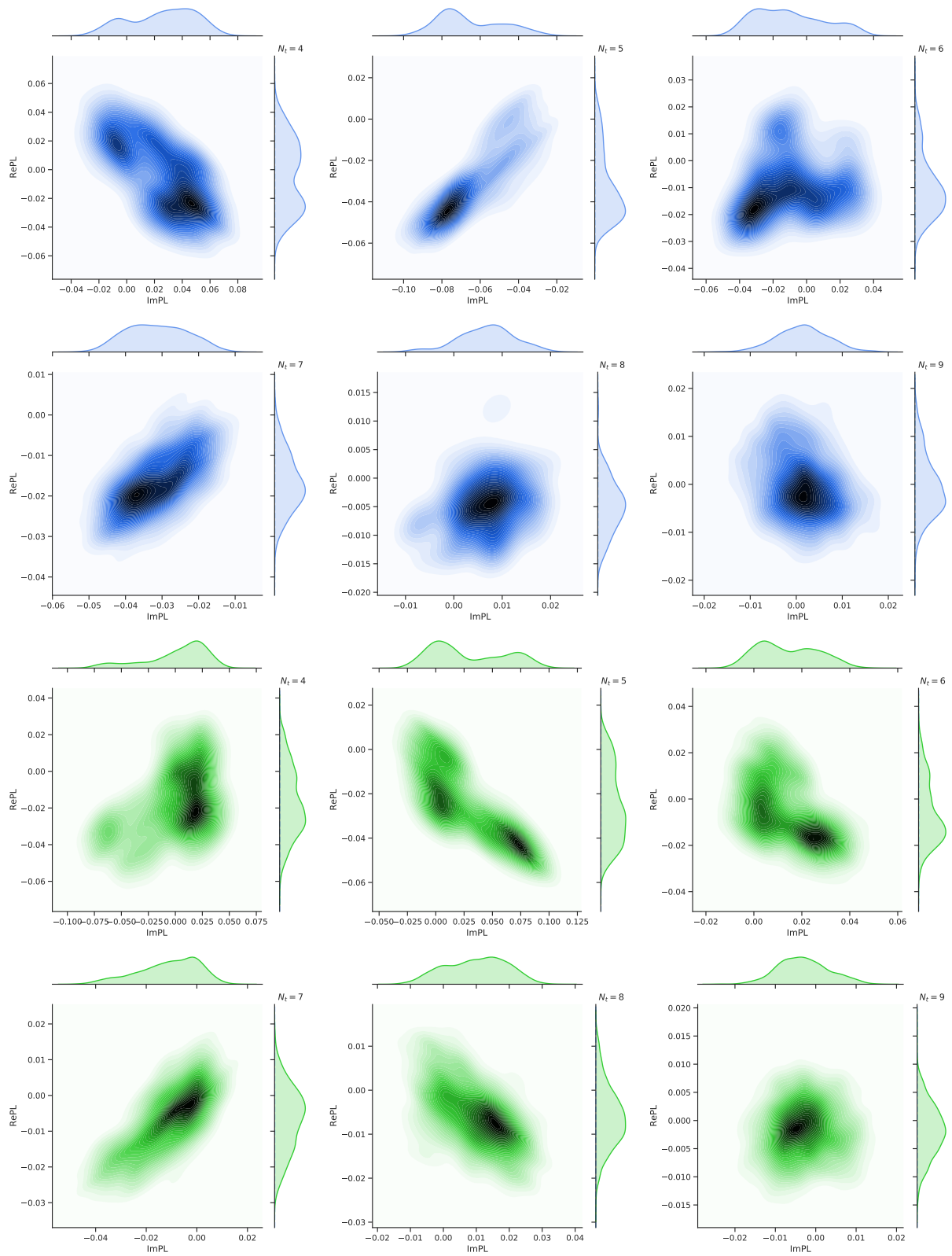[5]See Ref. [129, 130] for a thorough investigation of continuity in $SU(2)$ SYM.

FIGURE 9.4: *Polyakov loop histories at different L_4 for $\kappa = 0.1673$ (blue) and $\kappa = 0.1667$ (green).*

an analysis particularly difficult to perform and one may need to take into account a very large number of configurations. Thus, we don't have enough information in order to fully determine whether a deconfinement phase transition actually takes place or not at small L_4. Nevertheless, the proximity of the value of the Polyakov loop to zero and the broadness of the distribution may be a hint for the prevalence of confinement down to very small L_4. Clearly, a more thorough study is necessary in order to make this statement more precise. We plan to increase the statistics and to analyse different volumes. By doing so, one could confirm the continuity of the phase transition line as predicted by the semi-classical analysis. Accordingly, one should see that the critical L_4^c gets smaller as $m_g \to 0$. The main result of this section is nevertheless the big qualitative difference between thermal and periodic boundary conditions. We see that SYM with a periodic gaugino remains confined at least down to $N_t = 6$.

9.3   The Witten index in SU(3) SYM

If we go down to $m_g = 0$, the twisted partition function equals the Witten index, which tells us that SUSY is unbroken at all L_4. Hence, we can look for hints of continuity by measuring the Witten index at different masses. We should see that the Witten index smoothly becomes independent of L_4 in the massless limit. This measurement would allow us moreover to see how badly broken SUSY is for different lattice parameters, and whether it is recovered in the massless limit. From equation 9.1 follows that the Witten index is given by

$$\tilde{Z}(L_4) \equiv I_W = \sum_{\text{bosons}} e^{-L_4 E_i^B} - \sum_{\text{fermions}} e^{-L_4 E_i^F}, \tag{9.2}$$

and, as we already mentioned, $I_W = N$, the number of supersymmetric vacua. The energies $E_i^{B,F}$ are the eigenvalues of $\hat{H}$ on the graded Hilbert space. A direct measure of the Widen index on the lattice is difficult, as it implies knowing $\tilde{Z}$ and its normalisation factor. Luckily, we can easily measure derivatives of $\tilde{Z}$ on the lattice, as it is actually what we usually do when we measure correlators. We thus derive equation 9.2 with respect to L_4 to find the *graded energy density*

$$E_G(L_4) = \frac{\partial \tilde{Z}}{\partial L_4} = \sum_{\text{fermions}} E_i^F e^{-L_4 E_i^F} - \sum_{\text{bosons}} E_i^B e^{-L_4 E_i^B}. \tag{9.3}$$

We normalise it by subtracting the value in the limit of decompactification $\lim_{L_4 \to \infty} E_G(L_4) \equiv E_\infty$. If SUSY is unbroken, we must find $E_S(L_4) \equiv E_G(L_4) - E_\infty = 0$. In other words, E_S is sensitive to the mismatch between bosonic and fermionic excited

modes. The expectation is then to see that the subtracted energy density approaches zero at all compactification radii L_4 as we reduce the fermion mass.

Our approach to measure $E_S(L_4)$ is analogue to methods used to compute the equation of state in lattice QCD (see for example [131]). Note that in our isotropic lattice, i.e. with unique lattice spacing a in all dimensions, if we derive $\tilde{Z}$ with respect to L_4, we also have to take into account the variation with respect to the three-volume $V = (aN_s)$. Since the latter yields the pressure p, we are actually computing the trace of the energy-momentum, also called the interaction measure

$$\Delta = \frac{\epsilon - 3p}{T^4},$$

where ϵ is the energy density and $T = 1/L_4$. Following Ref.[131], we write

$$\epsilon - 3p = \frac{T}{V} a \frac{d\vec{b}}{da} \cdot \left\langle \frac{\partial S_L}{\partial \vec{b}} \right\rangle_{\text{sub}}, \tag{9.4}$$

where we make explicit that we subtract the correlator at zero temperature. S_L is the lattice action and $d\vec{b}/da$ the beta-functions of the lattice coupling parameters. In our case the couplings are just β and κ. It thus follows

$$\Delta = \frac{N_t^3}{N_s^3} \left[a \frac{\partial \beta}{\partial a} \left\langle \frac{\partial S_L}{\partial \beta} \right\rangle_{\text{sub}} + a \frac{\partial \beta}{\partial a} \frac{\partial m}{\partial \beta} \frac{\partial \kappa}{\partial m} \left\langle \frac{\partial S_L}{\partial \kappa} \right\rangle_{\text{sub}} \right]. \tag{9.5}$$

The first term is the action density, which is six times the average plaquette (see Fig. 9.5), while the second term requires the measuring of the condensate (see Fig. 9.6), since the mass is a source of the fermion bilinear (cf. equation 8.3). The derivative $\partial \kappa / \partial m$ follows from the definition of the hopping parameter and $\partial m / \partial \beta$ is obtained from the change of the critical mass with respect to β. Finally, the beta-function is computed through the NSZV beta-function (see 6.12), yielding

$$\frac{\partial \beta}{\partial a} = \frac{3}{4\pi^2} \frac{3N}{1 - \frac{Ng^2}{8\pi^2}}.$$

We measure Δ according to equation 9.5 on the same lattices as in previous section. The results for the three different gaugino masses are shown in Fig. 9.7. In Fig. 9.8 we compare the results to the finite temperature case. We observe that for the larger masses, Δ deviates towards positive values. This fact signals the explicit breaking of SUSY and thus an unbalance between bosonic and fermionic modes. The deviation from zero is greatly suppressed for the smallest mass, where the value is very near to zero at all L_4, consistent with an almost recovery of SUSY. This tendency shows that Δ actually vanishes in the limit of zero renormalised gaugino mass, where continuity along L_4 is expected.
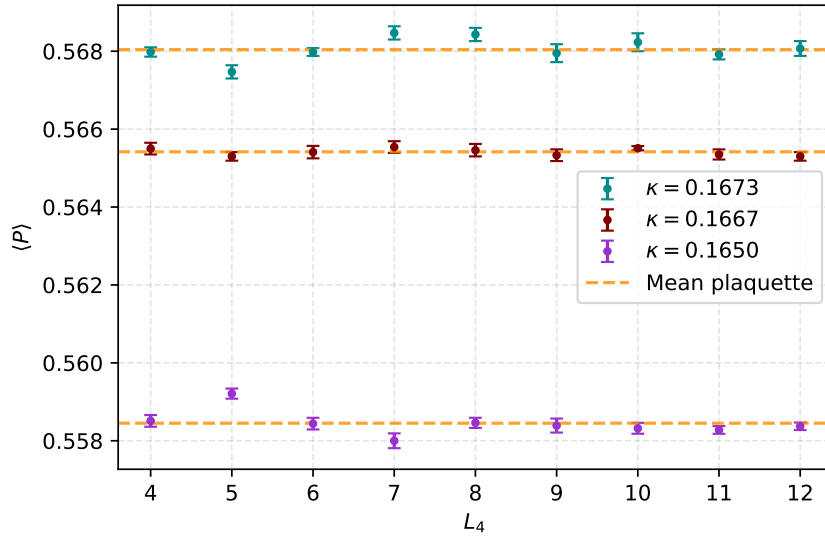
FIGURE 9.5: *Plaquette as function of L_4 for the three different fermion masses.*
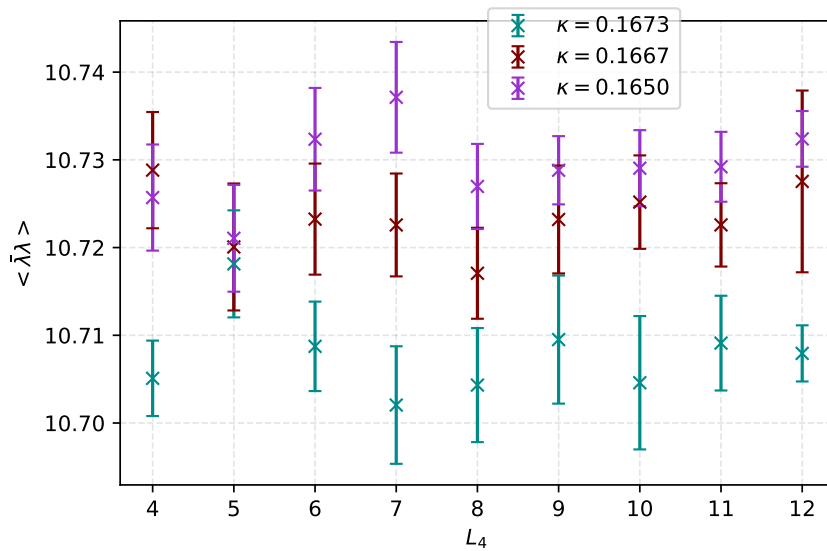
FIGURE 9.6: *Condensate as function of L_4 for the three different fermion masses.*
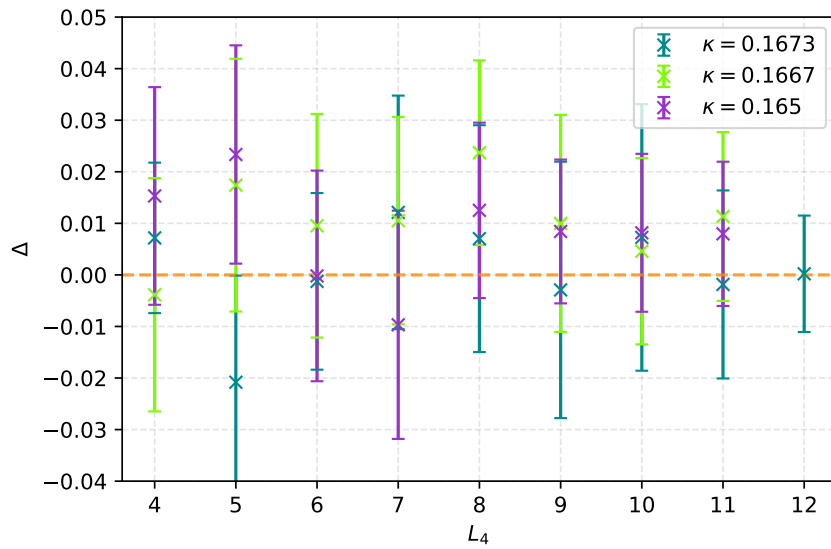
FIGURE 9.7: *Trace of the energy-momentum tensor as function of L_4 for the three different fermion masses.*
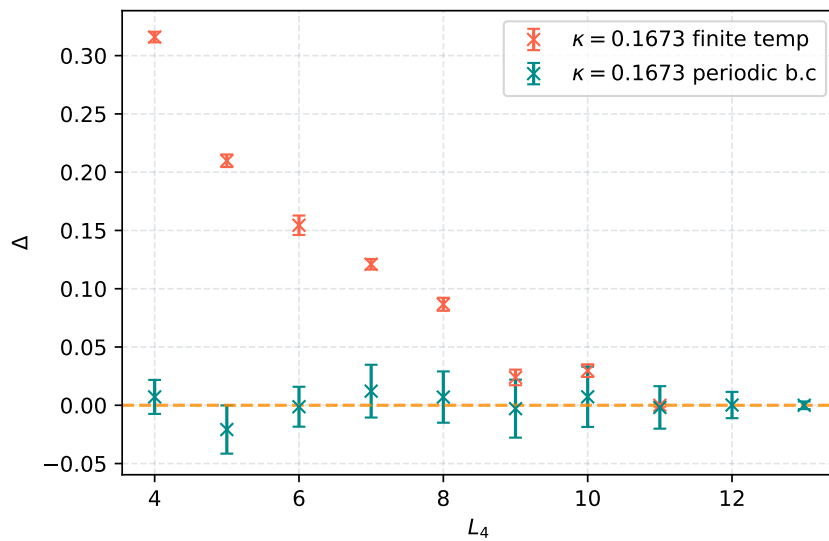

FIGURE 9.8: *Comparison of Δ for both periodic and antiperiodic boundary conditions at $\kappa = 0.1673$. For anti-periodic b.c. the breaking of SUSY is quite evident.*

Chapter 10

The conformal window of adjoint QCD

In this chapter we approach the problem of determining the IR phase of adjoint QCD by exploring whether the theory lies or not inside the conformal window. We have seen that analytical and numerical computations are able to describe the non-perturbative low-energy properties of $SU(N)$ SYM. Nevertheless, when we add more fermions to the theory, we break SUSY explicitly. With the loss of SUSY we also lose all the restrictions it puts on the dynamics, and thus we lose analytical predictability. We are left with a very limited number of available tools, namely semi-classical computations, like those we reviewed on the cylinder, and 't Hooft anomaly matching. However, semi-classical computations are only valid on the small circle and they can't tell us whether there are phase transitions in the decompactification limit. Moreover, anomaly matching conditions often don't provide a unique IR scenario. As we will see, lattice simulations are a well-suited tool to investigate the conformal window. The analysis focuses on the scaling of the mass anomalous dimension and profits from the relation between the GF and the RG transformations, as discussed at the end of section 7.4.

At this point, a brief remark is in order. Following our results of section 8.3, one may be tempted to employ Wilson fermions to measure the flowed condensate in adjoint QCD, in order to see whether the theory is conformal, or if it breaks chiral symmetry through fermion condensation. We have tried this naive approach in $N_f = 1$ adjoint QCD. However, we quickly noticed that it is not practicable. The reason is that this theory should be in or very near the lower edge of the conformal window. This can be seen from Fig. 10.1, where $t^2 E(t)$ (cf. Eq. 7.7) varies very weakly with t at finite gaugino mass. As a consequence, we are unable to determine the scale t_0, contrary to the SYM case (cf. Fig. 6.3). Therefore, we are not able to perform any consistent measurements of the condensate. Such a study would require the implementation of Ginsparg-Wilson fermions. This is a study we leave for the near future.

The study of conformal and near-conformal theories on the lattice is difficult, since the discretisation imposes UV and IR cut-offs, and it normally requires fermions to have
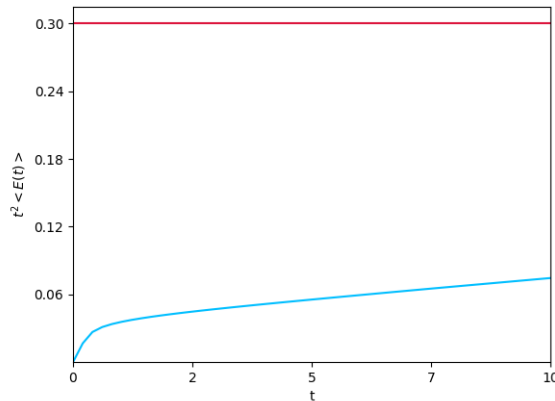
FIGURE 10.1: *t dependence of $t^2\langle E(t)\rangle$. $N_f = 1$ adjoint QCD on $24^3 \times 48$ lattice at $\beta = 1.75$, $\kappa = 0.1663$.*

a mass. In other words, the lattice naturally puts a scale in the system, breaking conformal symmetry explicitly. Nevertheless, exploring the conformal window has been an active research area within the lattice community, not only because of pure theoretical reasons but also motivated by BSM theories of electroweak symmetry breaking, e.g. technicolour models (see Ref. [132] for an overview). These theories are candidates to explain the dynamical breaking of the electroweak symmetry through an additional strong interaction. Consistency with experiments requires the new strong sector to be near-conformal and to have a large critical mass anomalous dimension $\gamma_* \sim 1$[1]. In this regard, several methods have been employed in order to determine if a theory is conformal or near-conformal, and especially to compute the value of γ_*. The fact that for fermions in higher representations the conformal window is already achieved at small N_f, makes adjoint QCD especially interesting.

A widely used method is to extract γ_* from the bound state spectrum. Accordingly, all masses M of the theory should scale to zero with the renormalised fermion mass m_g as $M \approx m_g^{1/(1+\gamma_*)}$ [133, 134]. A more precise method relies on the scaling of the integrated spectral density of the Dirac operator, the mode number (for details see Ref. [135]).

In this work we compute γ_* from the scaling of the mass anomalous dimension γ_m, as we vary the energy. In the end of this chapter we show results for $SU(2)$ adjoint QCD with $1/2 \leq N_f \leq 2$ Dirac flavours. Hereby, our main focus lies on $N_f = 2$, since there is enough evidence for this theory to lie within the conformal window. Moreover, this model has caught the most attention within the high energy physics community, and thus there are many results in the literature we can compare ours to. Our purpose is, to a great extent,

---

[1]The upper bound of γ_* is 2, the maximal allowed value for a unitary CFT.

to probe the effectiveness of this new method, its goodness and limitations, before we pursue more ambitious goals.

10.1 The anomalous dimension from the gradient flow

The method we describe now was first proposed in Ref. [91] and it is built upon the main result of section 7.4, namely that at large distances the correlators of effective fields are equivalent to correlators of flowed bare fields. In section 7.4 we discussed the coarse-graining features of the GF. However, we didn't take into account the remaining steps of the RG, namely the dilations. To study the existence of a fixed point, we are in fact interested in making that scaling explicit. In the lattice regularisation, a RG transformation changes the couplings as[2] $g \to g'$, $m \to m'$ and the cut-off as $a \to a' = b\,a$. In analogy to equation 3.5, a 2-point function transforms as:

$$\langle \mathcal{O}(0)\mathcal{O}(x_0) \rangle_{g,m} = b^{-2(d_\mathcal{O}+\gamma_\mathcal{O})} \langle \mathcal{O}(0)\mathcal{O}(x_0/b) \rangle_{g',m'}, \tag{10.1}$$

where the operator $\mathcal{O}(x_0)$ is some lattice interpolator, which is in general a monomial of gauge and fermion fields. The correlator of the rhs is computed in the effective theory and, because of equation 7.9, we can express it through flowed fields. However, since the GF doesn't give us the wave function renormalisation constant of the fermions, the effective fields ϕ_b and the flowed fields ϕ_t only agree up to a normalising factor, which depends on the scaling dimension. We fix that by writing

$$\phi_b(x_0/b) = b^{d_\phi+\eta/2}\phi_t(x_0),$$

where d_ϕ is the classical and η the anomalous dimension. Note that this re-scales the coordinates on the rhs of 10.1 and now both correlators depend on the same insertion points. We notice moreover that equation 7.9 makes it natural to relate $\sqrt{t} \propto b$, as long as the operators are well separated. Putting all these observations together we write equation 10.1 in terms of the flowed operators as

$$\frac{\langle \mathcal{O}_t(0)\mathcal{O}_t(x_0) \rangle}{\langle \mathcal{O}(0)\mathcal{O}(x_0) \rangle} = t^{\Delta_\mathcal{O}-n_\mathcal{O}\Delta_\phi}, \quad \Delta_i = d_i + \gamma_i, \tag{10.2}$$

where $n_\mathcal{O}$ counts the powers of ϕ in $\mathcal{O}$. We see that $\gamma_\mathcal{O}$ is in the exponent of t. To extract it we have to get rid of Δ_ϕ. This can be achieved by multiplying the lhs of 10.2 with a similar ratio of correlators, where the operators $\mathcal{V}$ are protected from running by some symmetry, i.e. $\gamma_\mathcal{V} = 0$, and whose field content is the same as $\mathcal{O}$, so that the multiplication

---

[2]Here $b > 1$ is analogous to the parameter $s < 1$ in chapter 2

completely cancels Δ_ϕ. Assuming that such an operator can be found, one defines the ratio

$$\mathcal{R}_\mathcal{O}(t, x_0) = \frac{\langle \mathcal{O}(0)\mathcal{O}_t(x_0)\rangle}{\langle \mathcal{O}(0)\mathcal{O}(x_0)\rangle} \left(\frac{\langle \mathcal{V}(0)\mathcal{V}(x_0)\rangle}{\langle \mathcal{V}(0)\mathcal{V}_t(x_0)\rangle} \right)^{n_\mathcal{O}/n_\mathcal{V}} = t^{\gamma_\mathcal{O}/2 + d_\mathcal{O}/2 - (n_\mathcal{O}/n_\mathcal{V})d_\mathcal{V}/2}.$$

As we will see, our operators will satisfy $n_\mathcal{O} = n_\mathcal{V}$ and $d_\mathcal{O} = d_\mathcal{V}$. We then arrive to

$$\mathcal{R}_\mathcal{O}(t, x_0) = \frac{\langle \mathcal{O}(0)\mathcal{O}_t(x_0)\rangle}{\langle \mathcal{O}(0)\mathcal{O}(x_0)\rangle} \frac{\langle \mathcal{V}(0)\mathcal{V}(x_0)\rangle}{\langle \mathcal{V}(0)\mathcal{V}_t(x_0)\rangle} = t^{\gamma_\mathcal{O}/2} \tag{10.3}$$

Since the computation of the flowed correlators $\langle \mathcal{O}_t(0)\mathcal{O}_t(x_0)\rangle$ requires the integration of the computationally expensive adjoint fermion flow equation 8.6, we opt for determining instead $\langle \mathcal{O}(0)\mathcal{O}_t(x_0)\rangle$, i.e. we only flow the source. This adds an uncertainty $\mathcal{O}(a\sqrt{t}/x_0)$ in the measurement of $\mathcal{R}_\mathcal{O}$. As in Ref. [91], we extract the scaling of $\gamma_\mathcal{O}$ with the energy scale by means of the function

$$\gamma_\mathcal{O}(\bar{t}) = \frac{\log(\mathcal{R}_\mathcal{O}(t_1)/\mathcal{R}_\mathcal{O}(t_2))}{\log\left(\sqrt{t_1}/\sqrt{t_2}\right)}. \tag{10.4}$$

Note that in this equation $\mathcal{R}$ doesn't depend on x_0, as it is expected that $\mathcal{R}(t, x_0)$ approaches a constant (a plateau), at large x_0 values. Eq. 10.4 is the main result of this section and correspond to the quantity we will measure on the lattice. At this point it is important to make a remark. If the theory we are studying has an IR fixed point, then it should lie on the critical surface in theory space, so that the fixed point is reached at infinite flow-time. Relevant deformations would shoot us away from the critical trajectory. Moreover, we see that no relevant couplings were taken into account for deriving equation 10.3. This means that if such deformations are present, the value of $\mathcal{R}_\mathcal{O}$ would get extra corrections in form of complicated t-dependences. On the lattice, the fermion mass and the volume are relevant deformations that cannot be easily discarded, especially when using Wilson fermions. In order to minimise this problem, we will simulate lattices with the smallest masses we can achieve. Moreover, we will, in some cases, be able to compare two different volumes in order to have a sense of its effect.

10.2 The mass anomalous dimension of N_f adjoint QCD

We measured the anomalous dimension of the pseudo-scalar operator, which is related to the mass anomalous dimension as $\gamma_m = -\gamma_{PS}$, in adjoint QCD with $N_f = 1/2, 1, 3/2$ and 2. As mentioned earlier, our emphasis lied on the two-flavour case. From the analysed theories, only the SYM is known to lie outside the conformal window. The interpolator

of the pseudo-scalar operator is just the one given in equation 6.10. The choice of $\mathcal{V}$ was narrowed down to the vector current, as it is the simplest conserved current on the lattice. It is however important to notice, that the local (continuum) vector current $\mathcal{V}_\mu = \bar{\lambda}\gamma_\mu\lambda$ is not exactly conserved at finite lattice spacing. A thorough discussion on this issue can be found in Ref. [136]. In short, the vector operator entering the vector Ward identity is actually the non-local current, which is also known in the literature as point-split lattice vector current:

$$\tilde{\mathcal{V}}_\mu^a = \frac{1}{2}\left[\bar{\lambda}(x)(\gamma_\mu - 1)U_\mu(x)\frac{\tau^a}{2}\lambda(x + a\hat{\mu}) + \bar{\lambda}(x + a\hat{\mu})(\gamma_\mu + 1)U_\mu^\dagger(x)\frac{\tau^a}{2}\lambda(x)\right]. \qquad (10.5)$$

Here τ^a are the Pauli matrices. The correlator of $\tilde{\mathcal{V}}_\mu$ is computed in a similar way to the local operator, by applying Wick's theorem as in Eq. 6.10. Inserting the two-point function of $\tilde{\mathcal{V}}_\mu^a$ in Eq. 10.3 would allow us to completely remove the dependence of $\mathcal{R}_\mathcal{O}(t, x_0)$ on the anomalous dimension of the field λ. If we instead use the local current $\mathcal{V}_\mu$, we would still have some dependence on γ_λ, since $Z_\mathcal{V} \neq 1$. How much the renormalisation factor $Z_\mathcal{V}$ deviates from 1, is something one has to estimate directly from the lattice simulation. As we show in the next section, we actually perform the measurements of γ_{PS} with both currents for the $N_f = 2$ case.

Once γ_m is determined, we talk of IR conformal or near-conformal behaviour if γ_m stops running as the energy scale is changed. It gets frozen at its critical value γ_*. Since we can't go to very large flow-times because of finite size effects and oversmearing, we measure γ_m at intermediate flow-times. If we observe either freezing or a very slow walking of γ_m, we perform an extrapolation to the limit $t \to \infty$, where a theory lying on the critical surface should converge to the IR fixed point. In our results, we represent the energy scale μ through the flow-time as $\mu = 1/\sqrt{8\bar{t}}$, where $\bar{t}$ is just the average of two consecutive flow-times, in lattice units.

We considered the lattices shown in table 10.1. We employ a tree-level Symanzik improved gauge action and three-level stout-smeared Wilson fermions, except for the SYM configurations.

10.2.1 $N_f = 2$

In the specific case of $N_f = 2$, we have two different volumes, $V = 24^3 \times 64$ and $V = 32^3 \times 64$, for every lattice coupling, with $\beta = 1.5, 1.6$ and 1.7. In all cases we have measured $\mathcal{O}(100)$ well separated configurations. Although this may seem to be a small number, we have observed that it is sufficient. This can be inferred from the small statistical errors in

the figures below. Our results consider flow-times in the range $1 \leq t/a^2 \leq 9$. We have seen strong IR cut-off effects from $t/a^2 = 10$ on. For $\beta = 1.6$ and 1.7, we considered both $\mathcal{V}$ and $\tilde{\mathcal{V}}^3$. Analogue to Ref. [91], we use the following relation

$$\mathcal{R}_\mathcal{O}(g, s^4 t, s^2 L) = \mathcal{R}_\mathcal{O}(g, s^2 t, sL) + s^{-\gamma_\mathcal{O}} \left(\mathcal{R}_\mathcal{O}(g, t, sL) - \mathcal{R}_\mathcal{O}(g, t, L) \right) + O(g' - g), \quad (10.6)$$

in order to obtain data in a third effective volume $V = s^2 L \times 64$, where the volume effects should be very small. For the available lattices $s = 32/24$, i.e. $L_S \sim 42$. The first part of the analysis is to determine the ratios $\mathcal{R}_{PS}(t, x_0)$, which are easily obtained from the vector and pseudo-scalar operators at different flow-times. In Fig. 10.3 we show the ratio $\mathcal{R}_{PS}$ as a function of x_0 at different flow-times. We compare the results from both the local and non-local vector currents. We see that, for the local current, $\mathcal{R}_{PS}(x_0)$ rapidly reaches a plateau. The formation of a plateau is however not very clear when the non-local current is used instead. In other words, we observe that $\mathcal{R}_{PS}$ has some long-range fluctuations as a function of x_0. Although the figure shows $\beta = 1.7$, we observed this behaviour for all the volumes and β values we considered. Since Eq. 10.4 takes the asymptotic value of $\mathcal{R}_{PS}(t)$ at large distances, we take the average of $\mathcal{R}$ over the interval $x_0 \in [15, 20]$. In Fig. 10.4 we present $\gamma_{PS}(t)$ at $\beta = 1.7$ and spatial lattice size $L = 32$, computed with both kind of vector currents. We immediately see that the results are compatible, the uncertainties are however larger in the non-local current case. This arises from the fluctuations of $\mathcal{R}(t, x_0)$. Such a result suggests two things. First, the renormalisation factor of $\mathcal{V}_\mu$ doesn't seem to have a very important impact in the outcome. Second, one has to choose whether to use the local current, which is stable but not strictly conserved, or the non-local, which is conserved but noisy. For $N_f = 2$, we carry out the full analysis employing both currents, with the exception of $\beta = 1.5$. For all other measurements, we stick to $\mathcal{V}_\mu$. The running of γ_{PS} for all β values and lattice sizes $L = 24, 32$ can be seen in Fig. 10.5, for the local current case.

After γ_{PS} is computed, we utilise Eq. 10.6. Remember that the volume and the mass are relevant and they push us away from the critical surface. They tend to make the relation 10.3 not to be quite exact. From table 10.1 we see that the analysed masses are all very small and thus we expect our results to be dominated mainly by volume effects as we approach the infrared. The effective volume achieved through Eq. 10.6 allows us to minimise these effects. Since we don't have measurements at $t' = s^2 t$, as required by the volume formula, we obtain the term $\mathcal{R}_\mathcal{O}(g, s^2 t, sL)$ by interpolating the jackknife samples with an exponential function (see Fig. 10.6). The outcome of Eq. 10.6 can be seen in Fig. 10.7.

---

[3]The reason behind the lack of data for $\beta = 1.5$ with the non-local current is actually the reduced computing time available. We are planning to complete the analysis in the near future
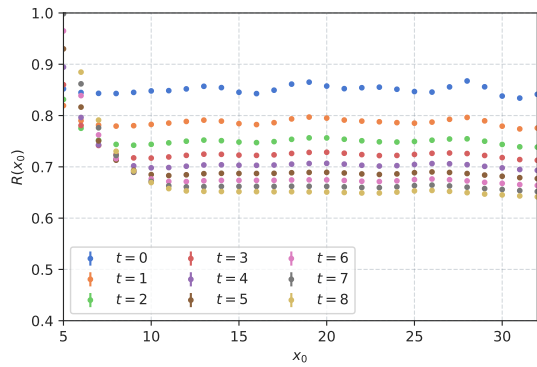
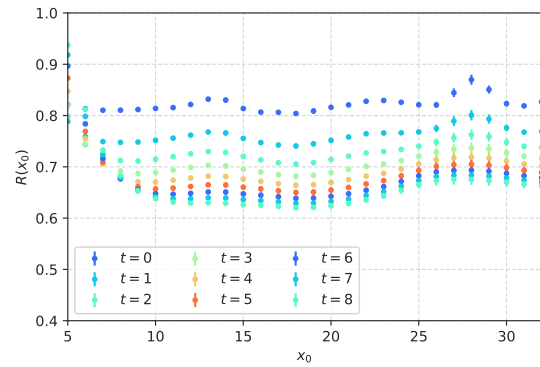FIGURE 10.2: $\mathcal{R}_{PS}(x_0)$ *from local current.*

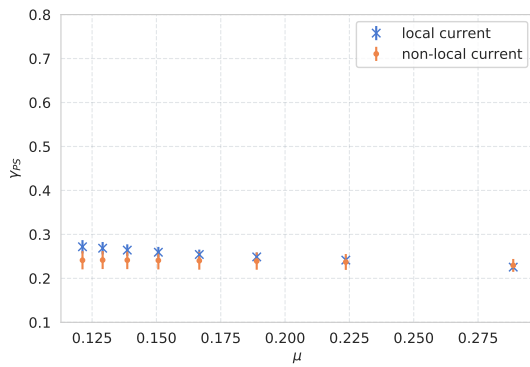FIGURE 10.3: $\mathcal{R}_{PS}(x_0)$ *from non-local current.*

FIGURE 10.4: *Comparison of γ_{PS} from local and non-local vector currents. $L = 32$, $\beta = 1.7$.*
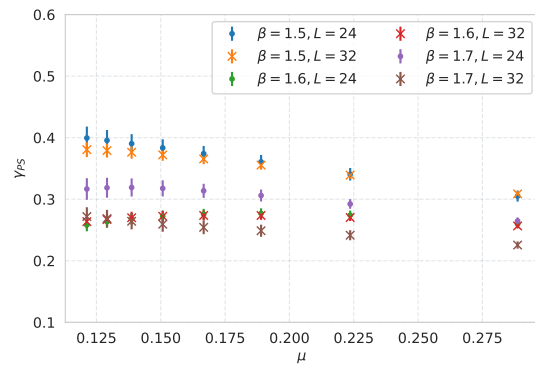

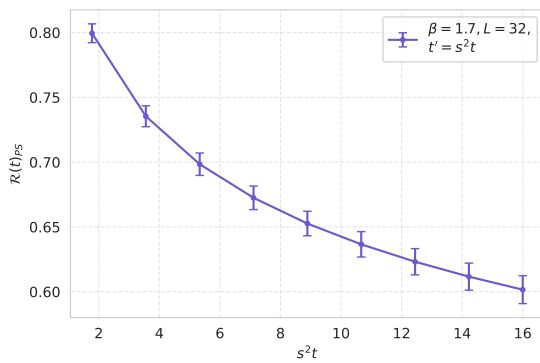FIGURE 10.5: *γ_{PS} obtained from the local current for all β and $L = 24, 32$.*

FIGURE 10.6: *interpolation of $\mathcal{R}_{PS}(s^2 t, L = 32)$.*
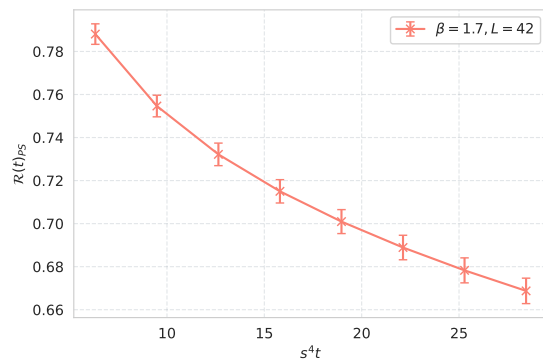

FIGURE 10.7: *$\mathcal{R}_{PS}(s^4 t, L = 42)$ from the volume formula.*

After obtaining $\mathcal{R}_{PS}(s^4 t)$ for $L = 42$, we directly compute $\gamma_{PS}(\mu)$. In Fig. 10.8 we show the final results for $N_f = 2$ using the local current, while the non-local current results follow in Fig. 10.9. We stress again that $\beta = 1.5$ was always computed with the local current. In both cases we only take into account the extrapolated values at $L = 42$, since they should be almost free of volume effects. In general we see that γ_{PS}, although not being strictly constant, shows a very weak scale dependence. This is a hint for an at least near conformal behaviour. At larger μ, we see that the different bare couplings yield distinct γ_{PS} values. As we move towards the infrared, however, the curves start to flow together. This is very clear when analysing $\beta = 1.6$ and 1.7, which overlap at $\mu \sim 0.08$. This behaviour is in fact what we expect to see in a near conformal system. Indeed, in the limit $\mu \to 0$, all bare couplings must yield the same universal value γ_*. To obtain the critical γ_* we performed a global (joint) fit to a cubic polynomial, where the parameter at $\mu = 0$, i.e. γ_*, was common to all data sets. The remaining fit parameters are allowed to vary. We see that the results obtained with both currents are compatible within their uncertainties.

In the literature, as mentioned before, there is a rather large number of studies focused on the computation of γ_* for $N_f = 2$ adjoint QCD. We emphasise on the results of Ref. [137], where the authors also explored $\beta = 1.5$ and 1.7 with the same lattice action we employed in this work. They get two different values for each bare coupling, namely $\gamma_* = 0.376(3)$ and $\gamma_* = 0.274(10)$ respectively. It is worth to mention that the fermion masses analysed in this thesis are much smaller and that we have an additional β, namely 1.6. Table 10.2 summarises our results and compare them to other studies found in the literature. From the table it can be seen that our findings are compatible with many of the studies performed in the last years. Moreover, since we get a unique γ_* value through the joint extrapolation, the gradient flow method might help to resolve the β dependence of γ_* in the deep infrared limit. We remark however on the fact that $\beta = 1.5$ is close to the bulk transition and thus a stronger β-dependence is expected there. Therefore, the goodness of the method in adjoint QCD should be further investigated through a more complete analysis by including more β values. It would be moreover important to see an overlap of $\gamma_{PS}(\mu)$ for all β values already before the extrapolation is performed, as it happens for $\beta = 1.6$ and 1.7.

10.2.2 $N_f < 2$

We performed the same measurements for all the others lattices of table 10.1. The analysis was done in the same way as in the $N_f = 2$ case. The only difference is that here we have notably less ensembles. In particular, for $N_f = 3/2$ we only have one β value. Although we employ the volume formula for this single β, we are of course not able
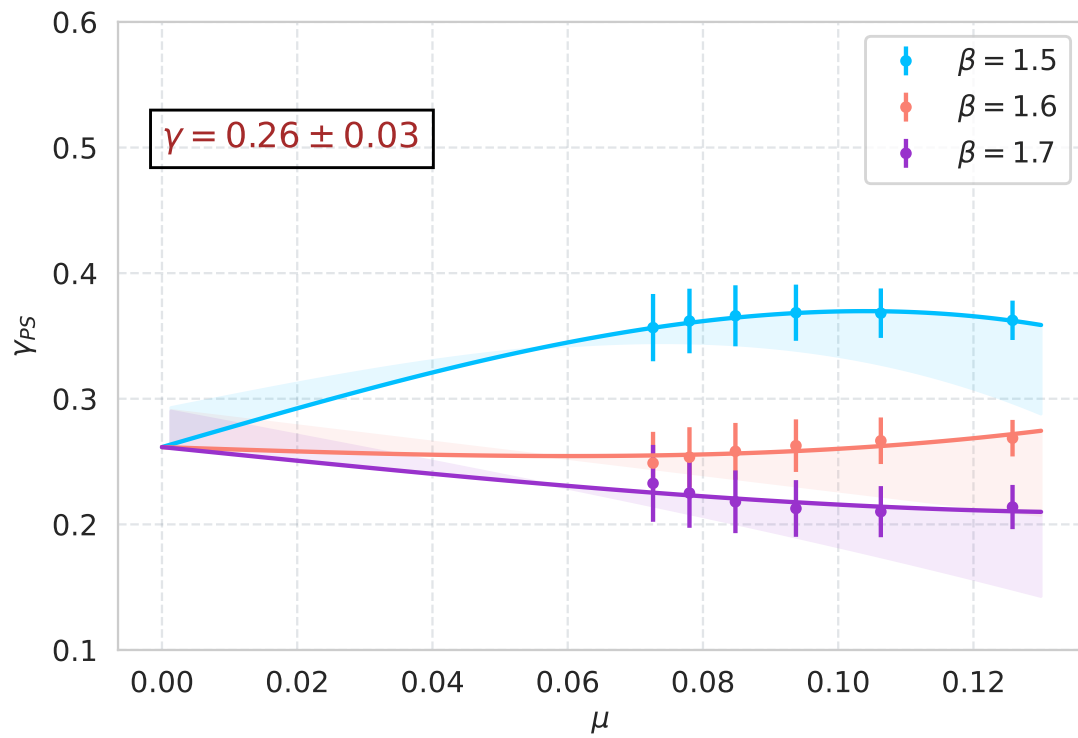
FIGURE 10.8: $N_f = 2$: *Extrapolation of γ_m to its critical value γ_* at $\mu \to 0$, from the local current.*
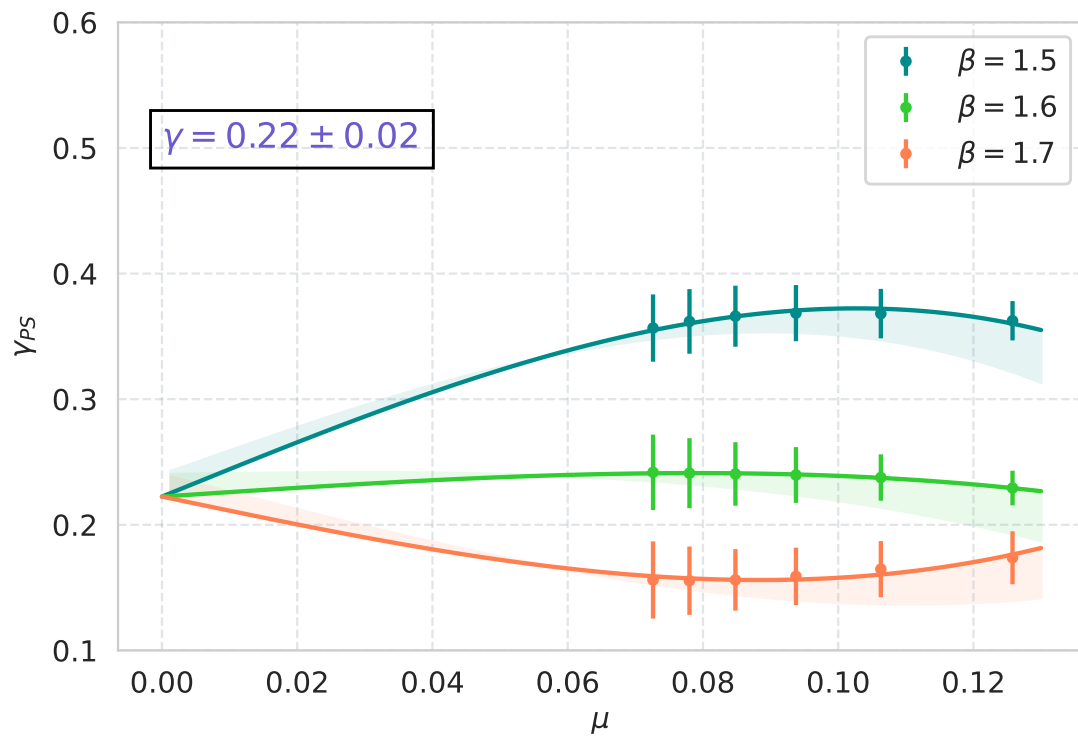

FIGURE 10.9: $N_f = 2$: *Extrapolation of γ_m to its critical value γ_* at $\mu \to 0$, from the non-local current.*

N_f	L_S	L_T	β	κ	am_{PCAC}
2	24	64	1.5	0.1350	0.03136(15)
2	32	64	1.5	0.1350	0.030414(45)
2	24	64	1.6	0.1340	0.00869(23)
2	32	64	1.6	0.1340	-
2	24	64	1.7	0.1328	0.00878(18)
2	32	64	1.7	0.1328	0.00894(13)
3/2	24	48	1.7	0.1340	-0.00097(22)
3/2	32	64	1.7	0.1340	-0.00052(11)
1	24	48	1.75	0.1663	-
1/2	32	64	1.75	0.1495	-

TABLE 10.1: *Lattice parameters.*

	γ_*
This study	*local:* 0.26(3)
	non-local: 0.22(2)
Ref. [137]	$\beta = 1.5:$ 0.376(3)
	$\beta = 1.7:$ 0.274(10)
Ref. [135]	0.371(20)
Ref. [138]	0.269(2)(5)
Ref. [139]	0.20(3)
Ref. [140]	0.31(6)
Ref. [141]	0.22(6)
Ref. [142]	0.50(26)

TABLE 10.2:
Comparison of our results to values found in the literature for $N_f = 2$.

to determine the β dependence of γ_*, as we did in the previous section. The results for $N_f = 3/2$ can be seen in Fig. 10.10. We clearly see that the anomalous dimension is almost a constant. This is a signal for the IR (near-)conformal behaviour of the theory. Hence, the system appears to lie inside the conformal window. We extrapolate to $\mu \to 0$ and obtain $\gamma_* = 0.38(2)$. As expected, the value of γ_* is larger than in the two-flavour case. Our result is in agreement with previous lattice investigations found in Refs. [134, 143, 144]. Especially, we get the same value as in Ref. [143], where the authors found $\gamma_* \sim 0.38$.

In the one-flavour case we only have one β and one volume. The results are shown in Fig. 10.11. Although for these parameters we are already able to see a (near-)conformal behaviour, i.e. a very weak change in γ_{PS}, the extrapolated value γ_* should be taken very carefully. Especially, it is considerably smaller than the results in Ref. [144], which is estimated to be $\gamma_* \sim 0.9$. It is however a valuable piece of information to see that it is likely for the theory to lie in or very near the conformal window.

Finally, in SYM, as expected, we don't see any freezing in the running of γ_m. This can be seen in Fig. 10.13. From Fig. 10.12 we see that no plateau is formed for $\mathcal{R}(x_0)$. If one insists in averaging over some x_0 interval, the resulting $\mathcal{R}(t)$ yields a $\gamma_{PS}(\mu)$ that seems to run without bounds as $\mu \to 0$. This result is indeed a signal for a system lying well below
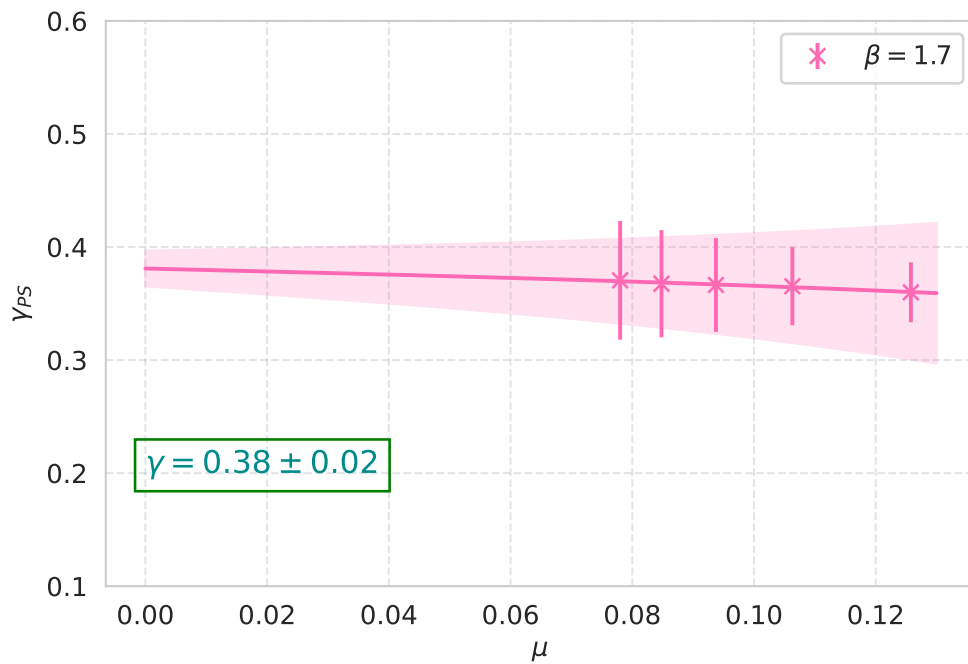
FIGURE 10.10: *Extrapolation of γ_{PS} to its critical value γ_*. $N_f = 3/2$, $L = 42$.*

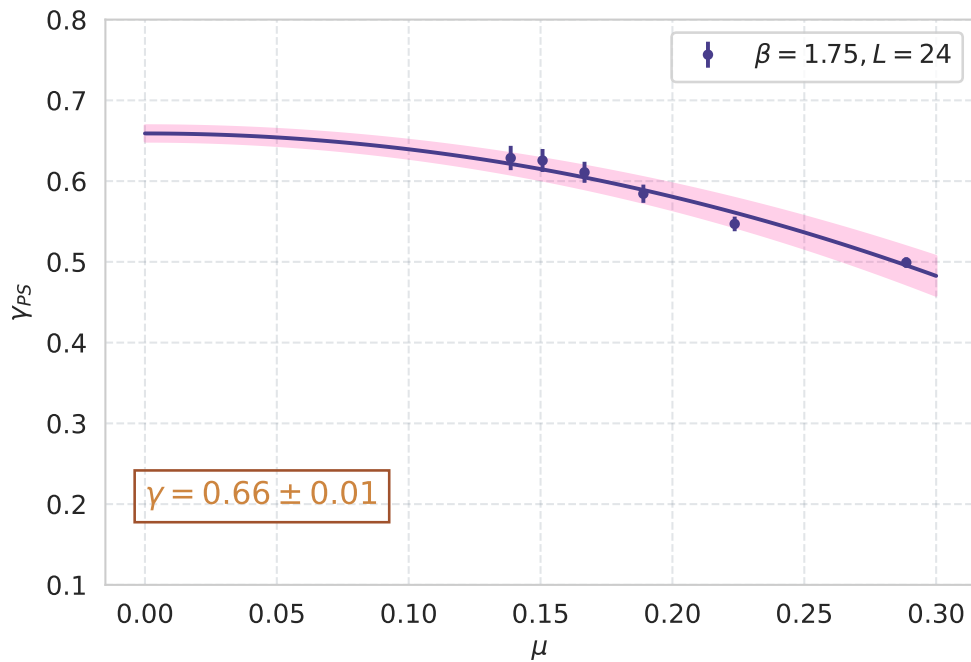the lower edge of the conformal window, as predicted for SYM.

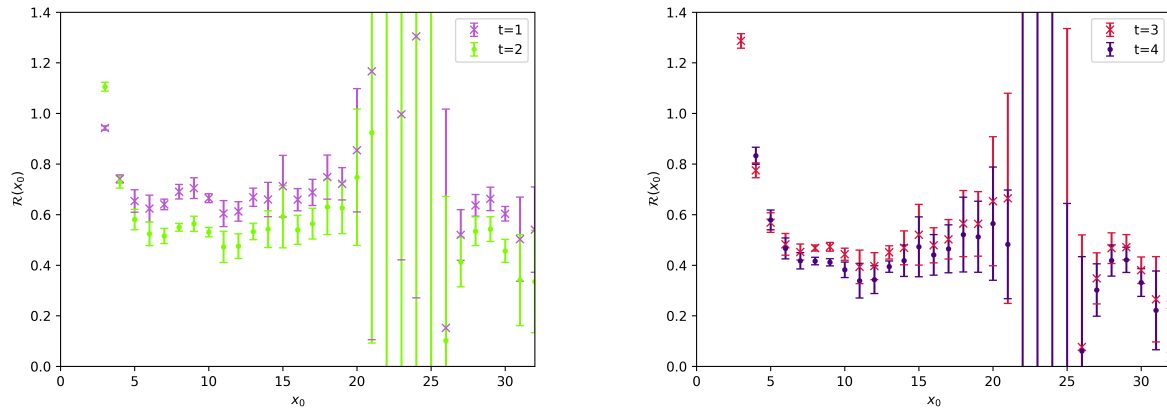FIGURE 10.11: *Extrapolation of γ_{PS} to its critical value γ_*. $N_f = 1$.*

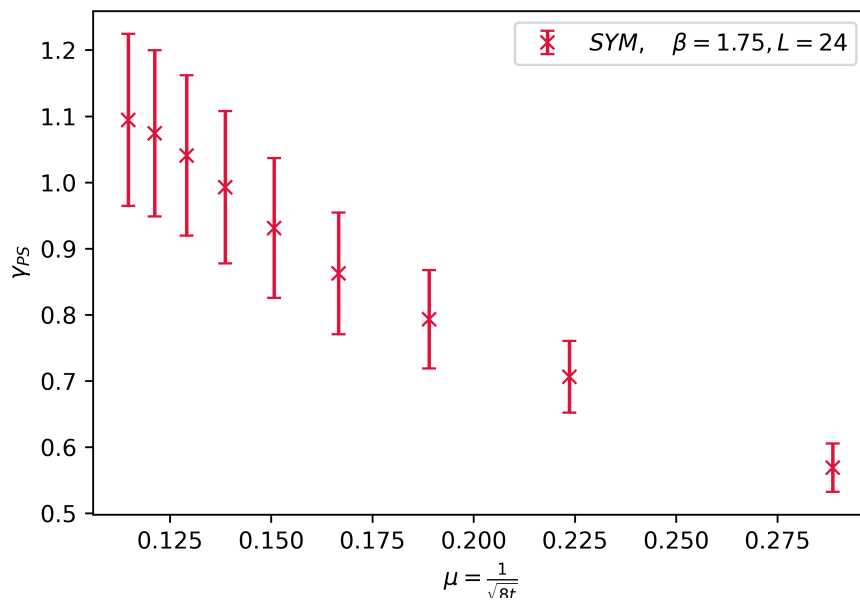FIGURE 10.12: $\mathcal{R}(x_0)$ *in SU(2) SYM. The ratio doesn't converge to a constant at large* x_0.

FIGURE 10.13: *Running of* γ_{PS} *in SU(2) SYM.*

Chapter 11

Summary and conclusions

In this thesis we have investigated the low-energy emergent behaviour of YM theory coupled to adjoint fermions, on the lattice. The Dirac-Wilson operator we use to discretise the fermion action explicitly includes a mass which has to be tuned to the critical point. This mass term poses, in general, a difficulty to the investigations of the chiral properties of the vacuum of the theory. For example, gaugino condensation, which is predicted from analytical computations, can't be proved at zero temperature because of this renormalisation constant. In theory, one would have to use lattice chiral fermions in order to measure this quantity. However, thanks to the gradient flow, the author has been able to measure, for the first time with Wilson fermions, the condensate of $SU(2)$ SYM at zero temperature and in the chiral/supersymmetric limit, which agrees with the condensates in other renormalisation schemes up to a constant factor. This has been possible because flowed fermions only renormalise multiplicatively and the gradient flow is regularisation scheme independent. The lattices we have employed were moreover shown in previous studies to have a very small breaking of SUSY, and thus the expected uncertainties arising from the finite lattice spacing are expected to be very small. Later, we have turned on a temperature and have measured the flowed condensate and the Polyakov loop, which in SYM is a true order parameter of the centre symmetry realisation. The author has found that the critical temperatures of deconfinement and chiral symmetry restoration agree up to very small uncertainties. It means that $SU(2)$ SYM has a single second order phase transition, which in the literature is predicted to be second order and to be in the universality class of the Z_2 Ising model. The coincidence of the critical temperatures is in agreement with the bound on critical temperatures $T_c^\chi \geq T_c^d$ predicted from anomaly matching conditions. Our results suggest however the saturation of the bound. Although this saturation was previously seen by other authors from semi-classical analysis, our findings arise non-perturbatively from the full theory. Such an observation is highly non-trivial and suggests that, at least in $\mathbb{R}^4$, chiral and centre symmetries are somehow intertwined. We have shortly discussed that a possible explanation for this may be found in the language of branes and strings as proposed by Witten. Namely that confining strings are fundamental strings, and that the domain

walls that connect the SUSY vacua are D-branes upon which the strings can end. The wall is then colour-charged and thus the Polyakov loop is non-zero and chiral symmetry is recovered in its core. However, it is still unclear how the string theory picture could explain the fate of the domain walls at the phase transition, as well as their interplay with the domain walls arising from the breaking of centre symmetry.

We have performed a similar work on the thermal phases of $SU(3)$ SYM. By using the gradient flow, the author found that the critical temperatures also coincide for this gauge group. The results are however not as clear as in the $SU(2)$ case. The problem lies on the determination of the order of the phase transition. To get a better idea about this, the Monte Carlo histories and 2d histograms of the Polyakov loop have been investigated at the critical N_t. The results give hints for a first order phase transition. Nevertheless, the coexistence of both confining and de-confining vacua is difficult to confirm with the available statistics and from the temperatures we can achieve within the fixed-scale approach. An important result is however that there is a clear correlation between the Polyakov loop and the flowed gaugino condensate, which supports the existence of a single phase transition.

The study of $SU(3)$ SYM was extended by investigations on the cylinder $\mathbb{R}^3 \times \mathbb{S}^1$, with periodic boundary conditions for the fermions. While in the case of antiperiodic boundary conditions the theory is thermal and thermal fluctuations break SUSY, the theory on the cylinder should preserve it as predicted by the Witten index. We have measured the Polyakov loop and have found no signal of deconfinement for compactification radii significantly smaller than the thermal critical radius. From the chiral susceptibility we see a possible deconfinement phase transition at very small radii, which could be expected provided we simulate at finite gaugino mass. Our results are however inconclusive with respect to the existence of this phase transition. The reason is that we see a nearly flat effective potential at small radii, signalised by a broad distribution of the Polyakov loop values in the complex plane. This distribution is moreover centred very near the origin. It is difficult to tell whether this observation is due to deconfinement or to lattice effects, which dominate the small radius regime. We have moreover measured the trace of the energy momentum tensor Δ at different radii. This quantity is computed as the derivative of the Witten index with respect to the volume, and is sensitive to the unmatch between fermionic and bosonic excited states. If $\Delta \neq 0$, then SUSY is broken. By analysing three different gaugino masses we have seen that Δ smoothly goes to zero in the chiral limit. This result explicitly shows how SUSY is recovered in that limit.

Finally we have discussed recent proposals in the literature about the relation between the gradient flow and the RG. Although the relation is not direct, since the gradient flow *is not* a RG because of its deterministic nature, the former can still be used to probe the long-distance properties of the theory, provided we only consider correlators of operators well separated in real space. We have identified an energy scale change b with the gradient flow-time t through $t \sim b^2$, at large distances. The author has performed the very first studies of the conformal window of adjoint QCD, where this relation between the gradient flow and the RG is exploited. We have compared ratios of correlators of the pseudo-scalar operator $\bar{\lambda}\gamma_5\lambda$ and of the vector current at different flow-times. From the flow-time dependence of those ratios we have extracted the running of the mass anomalous dimension $\gamma_m = -\gamma_{PS}$. The most complete study was carried out for adjoint QCD with two adjoint Dirac flavours. For that case, we have measured the scale dependence of γ_{PS} at three different β and at two different volumes. In order to avoid mass-effects, the fermion mass was chosen to be very small $am_{\text{PCAC}} \sim 0.008$. We have used the volume formula 10.6 in order to compute γ_{PS} at an effective lattice size $L = 42$, which is almost free of volume effects. In general we have observed a very weak dependence of the anomalous dimension on the energy scale. In other words, we see that at low energies γ_{PS} is almost constant. This is consistent with an IR conformal behaviour. We have extrapolated γ_{PS} to the limit $\mu \to 0$ in order to get the critical anomalous dimension γ_*, whose value is universal. This analysis, for the two-flavour case, was carried out using both the local and the point-split version of the vector current, where only the latter is strictly conserved at finite lattice spacing. We found that both results are compatible up to statistical errors. In the first case we found $\gamma_* = 0.26(3)$ and in the second $\gamma_* = 0.22(2)$. Our results are in agreement with several previous investigations found in the literature. However, from our analysis the β-dependence of γ_* is not quite resolved yet. Although we observe that all $\gamma_{PS}(\mu)$ tend to converge towards the IR, only the data from the two largest β actually overlap. The convergence to γ_* follows from the extrapolation. Especially $\beta = 1.5$ seems to be somewhat problematic, as it is near to the bulk transition. We plan to complete this study by analysing more intermediate β values.

The author has performed the same analysis for the $N_f = 1$, and $3/2$ theories. Also in these cases, hints for IR conformality have been observed, despite the fact that only one β value was available. It was found that γ_* grows as the number of flavours is lowered. As mentioned above, for $N_f = 2$ we have $\gamma_* \sim 0.26$. At $N_f = 3/2$, $\gamma_* \sim 0.38$ and $\gamma_* \sim 0.66$ at $N_f = 1$. At the end of this work also SYM theory was analysed, i.e. $N_f = 1/2$ adjoint QCD. For this theory no freezing of the running of γ_{PS} was observed. This is of course expected for SYM, which is known to lie outside the conformal window.

Appendix A

Data finite temperature SU(2) SYM

κ	t_0	N_t	$< \bar{\lambda}\lambda >$	Susceptibility	$B_4(P_L)$
0.1480	6.332(48)	8	0.002557(12)	0.000076(14)	0.65531(86)
		9	0.002738(20)	0.000082(6)	0.6417(27)
		10	0.002913(51)	0.000203(41)	0.5796(94)
		11	0.003289(16)	0.000073(13)	0.261(37)
		12	0.003334(46)	0.000214(48)	0.332(27)
		13	0.003614(34)	0.000165(34)	-0.051(66)
		14	0.003775(27)	0.000157(16)	0.031(27)
		15	0.003861(17)	0.000154(22)	-0.026(43)
		16	0.0039778(93)	0.000109(6)	0.012(26)
0.1490	9.851(32)	8	0.001374(21)	0.000031(5)	0.65851(49)
		10	0.001491(73)	0.000068(19)	0.6349(21)
		11	0.001557(32)	0.000077(11)	0.6110(33)
		12	0.001808(70)	0.000209(31)	0.530(15)
		13	0.001880(35)	0.000101(23)	0.377(37)
		14	0.002612(64)	0.000112(35)	0.079(38)
		16	0.002733(29)	0.000061(23)	0.031(43)
0.14925	10.545(69)	8	0.001144(12)	0.000025(2)	0.6581(3)
		10	0.001059(29)	0.000077(14)	0.6372(14)
		11	0.001254(23)	0.000102(24)	0.6244(18)
		12	0.001326(50)	0.000338(90)	0.5618(66)
		13	0.001742(121)	0.000450(78)	0.424(18)
		14	0.002013(92)	0.000155(21)	0.338(22)
		15	0.002533(28)	0.000108(11)	0.026(38)
		16	0.002564(57)	0.000116(17)	-0.026(35)

TABLE A.1: *Condensate, chiral susceptibility and Binder cumulant of the Polyakov loop at $\beta = 1.75$, $24^3 \times N_t$.*

κ	$am_{a-\pi}$
0.1480	0.4119(39)
0.1490	0.23780(97)
0.14925	0.1896(17)

TABLE A.2: *Adjoint pion masses for each κ value.*

Appendix B

The chiral anomaly

In this chapter we derive the chiral anomaly by means of Fujikawa's procedure [48]. This method consists in looking how the path integral transforms under chiral transformations. We already saw how the action transforms. Since the partition function Z is independent of the transformation parameter ω, i.e. $\frac{\delta Z}{\delta \omega} = 0$, if we assume that the measure is invariant, we quickly see from equation 5.4 that

$$\partial^\mu \langle \bar{\lambda} \gamma_\mu \gamma_5 \lambda \rangle = 0. \tag{B.1}$$

In other words, the invariance of the measure leads the current to be conserved also on the quantum level. This means that the anomaly must be hidden inside the transformation of the measure, which shouldn't be invariant after all. To analyse this, we start by looking at the orthonormal eigenstates of $\slashed{D}$ and $\bar{\slashed{D}}$

$$D^2 f_n \equiv \bar{\slashed{D}} \slashed{D} f_n = -\ell_n^2 f_n, \quad \slashed{D} f_n = \ell_n g_n, \tag{B.2}$$

$$D^2 g_n \equiv \slashed{D} \bar{\slashed{D}} g_n = -\ell_n^2 g_n, \quad \bar{\slashed{D}} g_n = -\ell_n f_n. \tag{B.3}$$

It is thus evident that the eigenstates f_n and g_n have opposite chiralities but share the same eigenvalues ℓ_n^2. This is however not necessarily the case when $\ell = 0$ and, as we will see, this fact will play the key role in the breaking of chiral symmetry. We move forward by expanding the gaugino fields in the basis of eigenstates

$$\lambda(x) = \sum_n a_n f_n(x), \quad \bar{\lambda}(x) = \sum_n b_n g_n(x),$$

where a_n and b_n must be Grassmannian, so that the Fermi statistics holds. In this basis the measure takes the form

$$\mathcal{D}\lambda \quad \rightarrow \quad \prod_{nm} da_n.$$

Now, under an infinitesimal local chiral rotation $\delta\lambda = -i\omega(x)\gamma_5\lambda$, the coefficients a_n would change as

$$\delta a_n = C_{nm}a_m,$$

and the measure transforms accordingly by

$$\prod_n da_n \to \det(\delta_{nm} + C_{nm})^{-1}\prod_m da_m,$$

where C is just the matrix representing the induced change of variables. Since the eigenfunctions f_n and g_n are an orthonormal basis, we can use their orthogonality relations

$$\int d^4x\, f_n^* f_m = \delta_{nm}, \quad \int d^4x\, g_n^* g_m = \delta_{nm}$$

to find that

$$C_{nm} = -\int d^4x\, i\omega(x)\gamma_5\, f_n^*(x)f_m(x).$$

Furthermore the identity

$$\det(1+C)^{-1} \approx \det(1-C) \approx \det e^{-C} = e^{-\operatorname{Tr} C}$$

allows us to write the Jacobian of the effective change of variables as

$$J = (\det C)^{-1} = \exp\left\{\left(i\int d^4x\, \omega(x)\mathcal{A}(x)\right)\right\}, \tag{B.4}$$

$$\mathcal{A}(x) = \operatorname{Tr}\sum_n f_n^*(x)\gamma_5 f_n(x).$$

The function $\mathcal{A}(x)$ is the anomaly, and it contains the physical information about how chiral symmetry is broken on the quantum level. We are, of course, interested in computing it explicitly. A complication arises by noticing that the expression is, in fact, ill-defined. The reason is that the number of eigenstates f_n, just as the measure itself, is infinite. We thus introduce a regulator function

$$\mathcal{A}(x) = \lim_{M\to\infty}\operatorname{Tr}\sum_n \exp\left\{\frac{\ell_n^2}{M^2}\right\}(f_n^*(x)\gamma_5 f_n(x)). \tag{B.5}$$

and use the completion relation

$$\sum_n f_n^*(x) f_n(y) = \delta(x - y)$$

to arrive to

$$\mathcal{A}(x) = \lim_{y \to x} \lim_{M \to \infty} \text{Tr} \left[\gamma_5 \exp\left\{ \frac{-D^2}{M^2} \right\} \right] \delta(x - y).$$

The square of the Dirac operator can be expanded as

$$D^2 = \frac{1}{2} [\gamma^\mu, \gamma^\nu] D_\mu D_\nu + \frac{1}{2} \{\gamma^\mu, \gamma^\nu\} D_\mu D_\nu$$

and, using $\{\gamma^\mu, \gamma^\nu\} = 2\delta_{\mu\nu}\mathbb{1}$ as well as $\sigma^{\mu\nu} = \frac{i}{2} [\gamma^\mu, \gamma^\nu]$ we find

$$D^2 = D^\mu D_\mu - i\sigma^{\mu\nu} D_\mu D_\nu = D^\mu D_\mu - \frac{i}{2} \sigma^{\mu\nu} [D_\mu, D_\nu] = D^\mu D_\mu + \frac{1}{2} \sigma^{\mu\nu} F^{\mu\nu}.$$

Where we have used the asymmetry of $\sigma^{\mu\nu}$ and the identity $-i[D_\mu, D_\nu] = F^{\mu\nu}$. Thus, the anomaly $\mathcal{A}(x)$ takes the form

$$\mathcal{A}(x) = \lim_{y \to x} \lim_{M \to \infty} \text{Tr} \left[\gamma_5 \exp\left\{ \frac{-D^\mu D_\mu - \frac{1}{2}\sigma^{\mu\nu} F^{\mu\nu}}{M^2} \right\} \right] \delta(x - y).$$

The only terms which will finally contribute to $\mathcal{A}(x)$ are those which don't depend on the cut-off M. If we expand the exponential, it is clear that terms with powers of the gauge field greater than two will die out as $M \to \infty$. One power of the gauge field would still vanish, as $\text{Tr}(\gamma_5 \sigma^{\mu\nu}) = 0$. We are only left with the term independent of A_μ, namely $e^{-\partial^2/M^2}$ and a term proportional to $(\sigma^{\mu\nu} F_{\mu\nu})^2$. We use the Fourier transformation of the delta distribution and write

$$\mathcal{A} = \lim_{M \to \infty} \text{Tr} \left[\gamma_5 \frac{1}{2} \left(\frac{\sigma^{\mu\nu} F_{\mu\nu}}{2M^2} \right)^2 \right] \int \frac{d^4k}{(2\pi)^4} \, e^{-k^2/M^2} \tag{B.6}$$

$$= \lim_{M \to \infty} \frac{1}{8M^4} \text{Tr}\left(\gamma_5 \sigma^{\mu\nu} \sigma^{\alpha\beta}\right) \text{Tr}(F_{\mu\nu} F_{\alpha\beta}) \frac{M^4}{16\pi^2}$$

$$= \frac{1}{32\pi^2} \epsilon^{\mu\nu\alpha\beta} \, \text{Tr}(F_{\mu\nu} F_{\alpha\beta})$$

$$= \frac{1}{16\pi^2} \text{Tr}\left(\tilde{F}_{\mu\nu} F_{\mu\nu} \right),$$

where $\tilde{F}_{\mu\nu} = \frac{1}{2} \epsilon^{\mu\nu\alpha\beta} F_{\alpha\beta}$ is the dual of the field strength tensor and the final trace runs over colour space. To arrive to the result the identity $\text{Tr}\left(\gamma_5 \gamma^\mu \gamma^\nu \gamma^\alpha \gamma^\beta\right) = 4\epsilon^{\mu\nu\alpha\beta}$ was employed. This results leads to the conclusion that the measure is not invariant under chiral rotations

but it changes as

$$\mathcal{D}\lambda \quad \rightarrow \quad \exp\left\{\frac{1}{16\pi^2}i\int d^4x\,\omega(x)\,\mathrm{Tr}\left(\tilde{F}_{\mu\nu}F_{\mu\nu}\right)\right\}\mathcal{D}\lambda$$

and thus we have to include the anomaly in the naive Ward identity B.1

$$\partial^\mu\langle\bar{\lambda}\gamma_\mu\gamma_5\lambda\rangle = \frac{1}{16\pi^2}\,\mathrm{Tr}\left(\tilde{F}_{\mu\nu}F_{\mu\nu}\right). \tag{B.7}$$

With this result, we have shown that chiral symmetry is broken on the quantum level. Moreover, since the integral of the anomaly looks just like the action of an instanton (cf. chapter 2), it becomes clear why the anomaly is an instanton effect. Indeed, Eq. B.7 tells us that an instanton creates an unbalance between right and left handed fermions. In other words, they interact with fermions by flipping their chirality[50]. But the chiral anomaly is not only related to the topology of the gauge field. From equation B.5 the regularised integral of the anomaly reads

$$\int d^4x\,\mathcal{A}(x) = \lim_{M\to\infty}\sum_n e^{\ell_n^2/M^2}\,\mathrm{Tr}\int d^4x\,f_n^*(x)\gamma_5 f_n(x). \tag{B.8}$$

Since it holds that $\{\slashed{D},\gamma_5\} = 0$, it follows that f_n^* and $\gamma_5 f_n$ are orthogonal eigenstates for $\ell_n \neq 0$. As a consequence, only the zero modes of $\slashed{D}$ will contribute to the anomaly B.8

$$\int d^4x\,\mathcal{A}(x) = n_+ - n_-, \quad \frac{1}{8\pi^2}\int d^4x\,\mathrm{Tr}\left(\tilde{F}^{\mu\nu}F_{\mu\nu}\right) = n_+ - n_- \equiv n, \tag{B.9}$$

Here n_+ and n_- are the number of zero modes for each chirality. As mentioned in the main text, this equation relates the index of the Dirac operator and the instanton winding number. It is an example of the Atiyah-Singer index theorem.

Let us finally comment on a very interesting fact, which is related with the power of the index theorem. Along our discussion on the chiral symmetry of SYM, we have seen that the chiral anomaly is given by the non-triviality of the YM bundle. But, what if we have extra geometrical structure? this would be the case if the base manifold of our theory is non-flat, i.e. if we have a background gravitational field. We can answer this by noting that our Dirac operator would include, besides the gauge connection, the spin connection. Comparing to our result in equation B.6, we would then expect an anomaly depending on the Riemann tensor. Indeed, it can be shown that [47]

$$\mathcal{A} \sim \epsilon^{\mu\nu\alpha\beta}R_{\mu\nu\lambda\sigma}R^{\lambda\sigma}_{\alpha\beta}.$$

Appendix C

Nielsen-Ninomiya theorem

As we saw in section 6.2, the lattice explicitly breaks the chiral symmetry by creating equal amounts of right and left-handed fermions, even when we start out with a single Weyl fermion in the continuum. In this appendix we will see that the reason behind this is topological and is encapsulated in the *Nielsen-Ninomiya theorem* [145][146]. The theorem is nicely derived by Witten in Ref. [147]. An additional proof is given in [148]. The Hamiltonian of a single Weyl fermion in $3 + 1$ dimensions is, in general, given by

$$H = b_i(k)\sigma^i + \epsilon(k),$$

where k is the spatial momentum, living in the Brillouin zone. Because of the Pauli matrices, one says that the Hamiltonian has two bands and, in the case at hand, the two bands have crossing points at some degenerated points k^*, i.e. where the Hamiltonian eigenvalues coincide. Here we set $\epsilon(k^*) = 0$, so that the band crossing coincides with the top of the Dirac sea. The points k^* are found when all $b_i(k) = 0$. Expanding the Hamiltonian around k^*

$$H = a_{ij}(k - k^*)_j\sigma^i + \mathcal{O}((k - k^*)^2), \quad a_{ij} = \frac{\partial b_i}{\partial k_j}$$

we can see that the chirality of a mode near the points is given by

$$\text{chirality} := \text{sign } \det\left(\frac{\partial b_i}{\partial k_j}\right).$$

We remember that, due to the periodicity in k, the Brillouin zone is actually a torus. The Hamiltonian tells us that for every k in this zone we have two states, corresponding to each band, and that Dirac sea contains the lower (negative) energy. Let us focus on the Dirac sea. There one has $H|\psi(k)\rangle = -|\psi(k)\rangle$. The phase of the wavefuncion is however not fixed. We consider now a $U(1)$ fibre bundle with base space the Brillouin zone. If we transport a fermion along some path, its wave function $|\psi(k)\rangle$ changes by a phase. This is

the Berry phase. The corresponding $U(1)$ Berry connection and curvature are defined as

$$A_i(k) = -i\langle\psi(k)|\frac{\partial}{\partial k^i}|\psi(k)\rangle, \quad F_{ij} = \frac{\partial A_j}{\partial k^i} - \frac{\partial A_i}{\partial k^j}$$

This similar to electrodynamics but with the base space being the momentum space. If we transport $|\psi(k)\rangle$ around a loop and we get a total change in the phase, then the bundle is not flat and the phase is physical. We learnt before, that the non-trivial topology of the YM bundle is reflected in the second Chern number c_2, which is the integral of $\mathrm{tr}(F_{YM}^2)$. Here we can do something similar, namely compute the first Chern number $c_1 \sim \int F$. If we integrate F on a sphere S_α^2 around a degenerated point k^*, we get the winding number

$$n_\alpha = \frac{1}{2\pi}\int_{S_\alpha^2} F = \pm 1.$$

The sign of the winding number is the chirality of the mode. Applying Stoke's theorem, the bulk is given by the Brillouin zone with the degenerated points k_i^* removed. We get

$$\frac{1}{2}\int_{\mathrm{bulk}} dF = \frac{1}{2\pi}\sum_\alpha \int_{S_\alpha^2} F = \sum_\alpha n_\alpha = 0.$$

The integral on the bulk vanishes because $dF = 0$. We thus see that the sum of all winding numbers has to vanish. In other words, there has to be an equal number of left and right modes. Another way to look at this is through the Hopf-Poincaré theorem. Since the Brillouin zone is a torus, its Euler characteristic is zero and thus the sum of the winding numbers around the singular points must vanish. One can see $n_\alpha = 1$ as a magnetic monopole in momentum space. Since the base manifold is compact, the flux line can't go to infinity but always has to end in a sink with $n_\alpha = -1$.

Bibliography

[1] Kenneth G. Wilson. "The Renormalization Group: Critical Phenomena and the Kondo Problem". *Rev. Mod. Phys.* 47.4 (1975).

[2] C. N. Yang and R. L. Mills. "Conservation of Isotopic Spin and Isotopic Gauge Invariance". *Phys. Rev.* 96.1 (1954).

[3] Arthur Jaffe and Edward Witten. "QUANTUM YANG–MILLS THEORY".

[4] Juan Maldacena. "The Large N Limit of Superconformal Field Theories and Supergravity".

[5] Leonard Susskind. "Entanglement Is Not Enough". *arXiv:1411.0690 [hep-th, physics:quant-ph]* (2014). arXiv: `1411.0690 [hep-th, physics:quant-ph]`.

[6] Pasquale Calabrese and John Cardy. "Entanglement Entropy and Quantum Field Theory". *J. Stat. Mech.: Theor. Exp.* 2004.06 (2004). arXiv: `hep-th/0405152`.

[7] S K Donaldson. "Yang-Mills Theory and Geometry".

[8] M. Daniel and C. M. Viallet. "The Geometrical Setting of Gauge Theories of the Yang-Mills Type". *Rev. Mod. Phys.* 52.1 (1980).

[9] David Tong. "TASI Lectures on Solitons". *arXiv:hep-th/0509216* (2005). arXiv: `hep-th/0509216`.

[10] Kevin Iga. "What Do Topologists Want from Seiberg–Witten Theory? (A Review of Four-Dimensional Topology for Physicists)". *Int. J. Mod. Phys. A* 17.30 (2002). arXiv: `hep-th/0207271`.

[11] Timothy J. Hollowood. "6 Lectures on QFT, RG and SUSY". *arXiv:0909.0859 [hep-th]* (2009). arXiv: `0909.0859 [hep-th]`.

[12] Peter Kopietz, L. Bartosch, and F. Schütz. *Introduction to the Functional Renormalization Group*. Lecture Notes in Physics 798. Heidelberg: Springer, 2010.

[13] Andreas Wipf. *Statistical Approach to Quantum Field Theory: An Introduction*. Lecture Notes in Physics volume 864. Heidelberg ; New York: Springer, 2013.

[14] Holger Gies. "Introduction to the Functional RG and Applications to Gauge Theories". *arXiv:hep-ph/0611146* 852 (2012). arXiv: `hep-ph/0611146`.

[15] Zamolodchikov, A.B. "Irreversibility of the Flux of the Renormalization Group in a 2D Field Theory". *JETP Lett.* 43 (1986).

[16] Zohar Komargodski and Adam Schwimmer. "On Renormalization Group Flows in Four Dimensions". *J. High Energ. Phys.* 2011.12 (2011). arXiv: `1107.3987`.

[17] Joseph Polchinski. "Scale and Conformal Invariance in Quantum Field Theory". *Nuclear Physics B* 303.2 (1988).

[18] Anatoly Dymarsky, Zohar Komargodski, Adam Schwimmer, and Stefan Theisen. "On Scale and Conformal Invariance in Four Dimensions". *arXiv:1309.2921 [hep-th]* (2013). arXiv: `1309.2921 [hep-th]`.

[19] Yu Nakayama. "Scale Invariance vs Conformal Invariance". *arXiv:1302.0884 [cond-mat, physics:hep-th]* (2014). arXiv: `1302.0884 [cond-mat, physics:hep-th]`.

[20] Luigi Del Debbio, Mads T. Frandsen, Haralambos Panagopoulos, and Francesco Sannino. "Higher Representations on the Lattice: Perturbative Studies". *J. High Energy Phys.* 2008.06 (2008). arXiv: `0802.0891`.

[21] Edward Witten. "Supersymmetric Yang-Mills Theory On A Four-Manifold". *Journal of Mathematical Physics* 35.10 (1994). arXiv: `hep-th/9403195`.

[22] N. Seiberg and E. Witten. "Monopole Condensation, And Confinement In N=2 Supersymmetric Yang-Mills Theory". *Nuclear Physics B* 426.1 (1994). arXiv: `hep-th/9407087`.

[23] R. Flume, L. O'Raifeartaigh, and I. Sachs. "Brief Resume of Seiberg-Witten Theory". *arXiv:hep-th/9611118* (1996). arXiv: `hep-th/9611118`.

[24] B. Sakita. "Supermultiplets of Elementary Particles". *Phys. Rev.* 136.6B (1964).

[25] Sidney Coleman and Jeffrey Mandula. "All Possible Symmetries of the S Matrix". *Phys. Rev.* 159.5 (1967).

[26] Golfand, Yu.A. and Likhtman, E.P. "Extension of the Algebra of Poincare Group Generators and Violation of p Invariance". *JETP Lett.* (1971).

[27] Rudolf Haag, Jan T LOPUSZAIqSKI, and Martin Sohnius. "ALL POSSIBLE GENERATORS OF SUPERSYMMETRIES OF THE S-MATRIX".

[28] Andreas Wipf. "Non-Perturbative Methods in Supersymmetric Theories". *arXiv:hep-th/0504180* (2005). arXiv: `hep-th/0504180`.

[29] John Terning. *Modern Supersymmetry: Dynamics and Duality*. International Series of Monographs on Physics 132. Oxford: Oxford University Press, 2010.

[30] Edward Witten. "Constraints on Supersymmetry Breaking". *Nuclear Physics B* 202.2 (1982).

[31] Mikhail Shifman and Arkady Vainshtein. "Instantons Versus Supersymmetry: Fifteen Years Later". *arXiv:hep-th/9902018* (1999). arXiv: `hep-th/9902018`.

[32] Nick Dorey, Timothy J. Hollowood, Valentin V. Khoze, and Michael P. Mattis. "The Calculus of Many Instantons". *Physics Reports* 371.4-5 (2002). arXiv: `hep-th/0206063`.

[33] Jeff Greensite. *An Introduction to the Confinement Problem*. Lecture Notes in Physics 821. Berlin: Springer, 2011.

[34] Michael R. Douglas and Stephen H. Shenker. "Dynamics of $SU(N)$ Supersymmetric Gauge Theory". *Nuclear Physics B* 447.2-3 (1995). arXiv: `hep-th/9503163`.

[35] G. Veneziano and S. Yankielowicz. "An Effective Lagrangian for the Pure N = 1 Supersymmetric Yang-Mills Theory". *Physics Letters B* 113.3 (1982).

[36] G. R. Farrar, G. Gabadadze, and M. Schwetz. "On the Effective Action of N=1 Supersymmetric Yang-Mills Theory". *Physical Review D* 58.1 (1998). arXiv: `hep-th/9711166`.

[37] G. R. Farrar, G. Gabadadze, and M. Schwetz. "The Spectrum of Softly Broken N=1 Supersymmetric Yang-Mills Theory". *Physical Review D* 60.3 (1999). arXiv: `hep-th/9806204`.

[38] Sajid Ali, Georg Bergner, Henning Gerber, Pietro Giudice, Gernot Münster, Istvan Montvay, Stefano Piemonte, and Philipp Scior. "The Light Bound States of $\mathcal{N}=1$ Supersymmetric SU(3) Yang-Mills Theory on the Lattice". *arXiv:1801.08062 [hep-lat, physics:hep-th]* (2018). arXiv: `1801.08062 [hep-lat, physics:hep-th]`.

[39] Sajid Ali, Georg Bergner, Henning Gerber, Pietro Giudice, Simon Kuberski, Istvan Montváy, Gernot Münster, Stefano Piemonte, and Philipp Scior. "Supermultiplets in N=1 SUSY SU(2) Yang-Mills Theory". *arXiv:1710.07464 [hep-lat, physics:hep-th]* (2017). arXiv: `1710.07464 [hep-lat, physics:hep-th]`.

[40] Georg Bergner, Pietro Giudice, Istvan Montvay, Gernot Münster, and Stefano Piemonte. "The Light Bound States of Supersymmetric SU(2) Yang-Mills Theory". *Journal of High Energy Physics* 2016.3 (2016). arXiv: `1512.07014`.

[41] G. 't Hooft. "Naturalness, Chiral Symmetry, and Spontaneous Chiral Symmetry Breaking". In: *Recent Developments in Gauge Theories*. Ed. by G. 't Hooft, C. Itzykson, A. Jaffe, H. Lehmann, P. K. Mitter, I. M. Singer, and R. Stora. Boston, MA: Springer US, 1980.

[42] John C. Collins, Anthony Duncan, and Satish D. Joglekar. "Trace and Dilatation Anomalies in Gauge Theories". *Phys. Rev. D* 16.2 (1977).

[43] Kazuya Yonekura. "On the Trace Anomaly and the Anomaly Puzzle in $\mathcal{N} = 1$ Pure Yang-Mills". *J. High Energ. Phys.* 2012.3 (2012).

[44] Eduardo Fradkin and Stephen H. Shenker. "Phase Diagrams of Lattice Gauge Theories with Higgs Fields". *Phys. Rev. D* 19.12 (1979).

[45] K Osterwalder and E Seiler. "Gauge Field Theories on a Lattice". *Annals of Physics* 110.2 (1978).

[46] Davide Gaiotto, Anton Kapustin, Nathan Seiberg, and Brian Willett. "Generalized Global Symmetries". *Journal of High Energy Physics* 2015.2 (2015). arXiv: `1412.5148`.

[47] Jeffrey A. Harvey. "TASI 2003 Lectures on Anomalies". *arXiv:hep-th/0509097* (2005). arXiv: `hep-th/0509097`.

[48] Kazuo Fujikawa. "Path-Integral Measure for Gauge-Invariant Fermion Theories". *Phys. Rev. Lett.* 42.18 (1979).

[49] R. Jackiw and C. Rebbi. "Spinor Analysis of Yang-Mills Theory". *Phys. Rev. D* 16.4 (1977).

[50] G. 't Hooft. "Symmetry Breaking through Bell-Jackiw Anomalies". *Phys. Rev. Lett.* 37.1 (1976).

[51] M.A. Shifman and A.I. Vainshtein. "On Gluino Condensation in Supersymmetric Gauge Theories with SU(N) and O(N) Groups". *Nuclear Physics B* 296.2 (1988).

[52] N. Michael Davies, Timothy J. Hollowood, Valentin V. Khoze, and Michael P. Mattis. "Gluino Condensate and Magnetic Monopoles in Supersymmetric Gluodynamics". *Nuclear Physics B* 559.1-2 (1999). arXiv: `hep-th/9905015`.

[53] G. Dvali and M. Shifman. "Domain Walls in Strongly Coupled Theories". *Physics Letters B* 407.3-4 (1997). arXiv: `hep-th/9612128`.

[54] G. Dvali and M. Shifman. "Dynamical Compactification as a Mechanism of Spontaneous Supersymmetry Breaking". *Nuclear Physics B* 504.1-2 (1997). arXiv: `hep-th/9611213`.

[55] Christof Gattringer and Christian B. Lang. *Quantum Chromodynamics on the Lattice: An Introductory Presentation*. Lecture Notes in Physics 788. Berlin: Springer, 2010.

[56] K.G. Wilson. "The Origins of Lattice Gauge Theory". *Nuclear Physics B - Proceedings Supplements* 140 (2005).

[57] Kenneth G. Wilson. "Confinement of Quarks". *Phys. Rev. D* 10.8 (1974).

[58] K. Symanzik. "Continuum Limit and Improved Action in Lattice Theories". *Nuclear Physics B* 226.1 (1983).

[59] Leonard Susskind. "Lattice Fermions". *Phys. Rev. D* 16.10 (1977).

[60] Karl Jansen and Chuan Liu. "Implementation of Symanzik's Improvement Program for Simulations of Dynamical Wilson Fermions in Lattice QCD". *Computer Physics Communications* 99.2-3 (1997). arXiv: `hep-lat/9603008`.

[61] S. Musberg, G. Münster, and S. Piemonte. "Perturbative Calculation of the Clover Term for Wilson Fermions in Any Representation of the Gauge Group SU(N)". *J. High Energ. Phys.* 2013.5 (2013). arXiv: `1304.5741`.

[62] Georg Bergner and Simon Catterall. "Supersymmetry on the Lattice". *International Journal of Modern Physics A* 31.22 (2016). arXiv: `1603.04478`.

[63] David Schaich. "Progress and Prospects of Lattice Supersymmetry". *arXiv:1810.09282 [hep-lat, physics:hep-th]* (2018). arXiv: `1810.09282 [hep-lat, physics:hep-th]`.

[64] Joel Giedt. "Progress in Four-Dimensional Lattice Supersymmetry". *International Journal of Modern Physics A* 24.22 (2009). arXiv: `0903.2443`.

[65] Alessandra Feo, Robert Kirchner, Silke Luckmann, Istvan Montvay, and Gernot Münster. "Numerical Simulations of Dynamical Gluinos in SU(3) Yang-Mills Theory: First Results". *Nuclear Physics B - Proceedings Supplements* 83-84 (2000). arXiv: `hep-lat/9909070`.

[66] Simon Catterall, Raghav G. Jha, David Schaich, and Toby Wiseman. "Testing Holography Using Lattice Super-Yang–Mills on a 2-Torus". *arXiv:1709.07025 [hep-lat, physics:hep-th]* (2017). arXiv: `1709.07025 [hep-lat, physics:hep-th]`.

[67] Thomas Appelquist, Richard Brower, Simon Catterall, George Fleming, Joel Giedt, Anna Hasenfratz, Julius Kuti, Ethan Neil, and David Schaich. "LATTICE GAUGE THEORIES AT THE ENERGY FRONTIER".

[68] Mithat Unsal. "Twisted Supersymmetric Gauge Theories and Orbifold Lattices". *J. High Energy Phys.* 2006.10 (2006). arXiv: `hep-th/0603046`.

[69] David B. Kaplan and Mithat Unsal. "A Euclidean Lattice Construction of Supersymmetric Yang-Mills Theories with Sixteen Supercharges". *J. High Energy Phys.* 2005.09 (2005). arXiv: `hep-lat/0503039`.

[70] Simon Catterall and David Schaich. "Lifting Flat Directions in Lattice Supersymmetry". *J. High Energ. Phys.* 2015.7 (2015). arXiv: `1505.03135`.

[71] G. Curci and G. Veneziano. "Supersymmetry and the Lattice: A Reconciliation?" *Nuclear Physics B* 292 (1987).

[72] Sajid Ali, Georg Bergner, Henning Gerber, Istvan Montvay, Gernot Münster, Stefano Piemonte, and Philipp Scior. "Analysis of Ward Identities in Supersymmetric Yang-Mills Theory". *arXiv:1802.07067 [hep-lat]* (2018). arXiv: `1802.07067 [hep-lat]`.

[73] Gernot Münster and Hendrik Stüwe. "The Mass of the Adjoint Pion in N=1 Supersymmetric Yang-Mills Theory". *Journal of High Energy Physics* 2014.5 (2014). arXiv: `1402.6616`.

[74] Nicholas Metropolis, Arianna W. Rosenbluth, Marshall N. Rosenbluth, Augusta H. Teller, and Edward Teller. "Equation of State Calculations by Fast Computing Machines". *The Journal of Chemical Physics* 21.6 (1953).

[75] Simon Duane, A.D. Kennedy, Brian J. Pendleton, and Duncan Roweth. "Hybrid Monte Carlo". *Physics Letters B* 195.2 (1987).

[76] Georg Bergner and Stefano Piemonte. "The Running Coupling from Gluon and Ghost Propagators in the Landau Gauge: Yang-Mills Theories with Adjoint Fermions". *Phys. Rev. D* 97.7 (2018). arXiv: `1709.07367`.

[77] M. A. Clark. "The Rational Hybrid Monte Carlo Algorithm". *arXiv:hep-lat/0610048* (2006). arXiv: `hep-lat/0610048`.

[78] D R T Jones. "THE P-FUNCTION IN SUPERSYMMETRIC YANG-MILLS THEORY". *PHYSICS LETTERS* 136.4 (1984).

[79] V.A. Novikov, M.A. Shifman, A.I. Vainshtein, and V.I. Zakharov. "Exact Gell-Mann-Low Function of Supersymmetric Yang-Mills Theories from Instanton Calculus". *Nuclear Physics B* 229.2 (1983).

[80] Martin Lüscher. "Properties and Uses of the Wilson Flow in Lattice QCD". *J. High Energ. Phys.* 2010.8 (2010). arXiv: `1006.4518`.

[81] R. Narayanan and H. Neuberger. "Infinite N Phase Transitions in Continuum Wilson Loop Operators". *J. High Energy Phys.* 2006.03 (2006). arXiv: `hep-th/0601210`.

[82] Martin Lüscher. "Chiral Symmetry and the Yang–Mills Gradient Flow". *Journal of High Energy Physics* 2013.4 (2013). arXiv: `1302.5246`.

[83] Martin Lüscher and Peter Weisz. "Perturbative Analysis of the Gradient Flow in Non-Abelian Gauge Theories". *J. High Energ. Phys.* 2011.2 (2011). arXiv: `1101.0963`.

[84] Martin Lüscher. "Trivializing Maps, the Wilson Flow and the HMC Algorithm". *Communications in Mathematical Physics* 293.3 (2010). arXiv: `0907.5491`.

[85] Martin Lüscher. "Future Applications of the Yang-Mills Gradient Flow in Lattice QCD". *arXiv:1308.5598 [hep-lat, physics:hep-th]* (2013). arXiv: `1308.5598 [hep-lat, physics:hep-th]`.

[86] Alberto Ramos. "The Yang-Mills Gradient Flow and Renormalization". *arXiv:1506.00118 [hep-lat]* (2015). arXiv: `1506.00118 [hep-lat]`.

[87] Yoshihiko Abe and Masafumi Fukuma. "Gradient Flow and the Renormalization Group". *arXiv:1805.12094 [hep-lat, physics:hep-th]* (2018). arXiv: `1805.12094 [hep-lat, physics:hep-th]`.

[88] Hiroki Makino, Okuto Morikawa, and Hiroshi Suzuki. "Gradient Flow and the Wilsonian Renormalization Group Flow". *arXiv:1802.07897 [hep-lat, physics:hep-th]* (2018). arXiv: `1802.07897 [hep-lat, physics:hep-th]`.

[89] Hidenori Sonoda and Hiroshi Suzuki. "Derivation of a Gradient Flow from ERG". *arXiv:1901.05169 [hep-lat, physics:hep-th]* (2019). arXiv: `1901.05169 [hep-lat, physics:hep-th]`.

[90] Andrea Carosso. "Stochastic Renormalization Group and Gradient Flow". *J. High Energ. Phys.* 2020.1 (2020). arXiv: `1904.13057`.

[91] Andrea Carosso, Anna Hasenfratz, and Ethan T. Neil. "Non-Perturbative Renormalization of Operators in near-Conformal Systems Using Gradient Flow". *arXiv:1806.01385 [hep-lat, physics:hep-ph, physics:hep-th]* (2018). arXiv: `1806.01385 [hep-lat, physics:hep-ph, physics:hep-th]`.

[92] Daisuke Kadoh and Naoya Ukita. "Gradient Flow Equation in SQCD". *arXiv:1912.13247 [hep-lat, physics:hep-th]* (2019). arXiv: `1912.13247 [hep-lat, physics:hep-th]`.

[93] Daisuke Kadoh, Kengo Kikuchi, and Naoya Ukita. "Supersymmetric Gradient Flow in the Wess-Zumino Model". *Phys. Rev. D* 100.1 (2019). arXiv: `1904.06582`.

[94] Daisuke Kadoh and Naoya Ukita. "Supersymmetric Gradient Flow in N=1 SYM". *arXiv:1812.02351 [hep-lat, physics:hep-ph, physics:hep-th, physics:math-ph]* (2018). arXiv: `1812.02351 [hep-lat, physics:hep-ph, physics:hep-th, physics:math-ph]`.

[95] Sinya Aoki and Shuichi Yokoyama. "Flow Equation, Conformal Symmetry and AdS Geometry". *Progress of Theoretical and Experimental Physics* 2018.3 (2018). arXiv: `1707.03982`.

[96] Sinya Aoki, Kengo Kikuchi, and Tetsuya Onogi. "Geometries from Field Theories". *Prog. Theor. Exp. Phys.* 2015.10 (2015). arXiv: `1505.00131`.

[97] Davide Gaiotto, Anton Kapustin, Zohar Komargodski, and Nathan Seiberg. "Theta, Time Reversal and Temperature". *Journal of High Energy Physics* 2017.5 (2017).

[98] Zohar Komargodski, Tin Sulejmanpasic, and Mithat Ünsal. "Walls, Anomalies, and Deconfinement in Quantum Antiferromagnets". *Physical Review B* 97.5 (2018).

[99] Hiroyuki Shimizu and Kazuya Yonekura. "Anomaly Constraints on Deconfinement and Chiral Phase Transition". *Phys. Rev. D* 97.10 (2018). arXiv: `1706.06104`.

[100] Georg Bergner, Camilo López, and Stefano Piemonte. "Study of Center and Chiral Symmetry Realization in Thermal N = 1 Super Yang-Mills Theory Using the Gradient Flow". *Phys. Rev. D* 100.7 (2019).

[101] Georg Bergner, Camilo López, and Stefano Piemonte. "Study of Thermal SU(3) Supersymmetric Yang-Mills Theory and near-Conformal Theories from the Gradient Flow". *arXiv:1911.11575 [hep-lat, physics:hep-ph, physics:hep-th]* (2019). arXiv: `1911.11575 [hep-lat, physics:hep-ph, physics:hep-th]`.

[102] G. Bergner, P. Giudice, G. Münster, S. Piemonte, and D. Sandbrink. "Phase Structure of the N=1 Supersymmetric Yang-Mills Theory at Finite Temperature". *Journal of High Energy Physics* 2014.11 (2014). arXiv: `1405.3180`.

[103] Kenji Hieda and Hiroshi Suzuki. "Small Flow-Time Representation of Fermion Bilinear Operators". *Modern Physics Letters A* 31.38 (2016). arXiv: `1606.04193`.

[104] R. Kirchner, S. Luckmann, I. Montvay, K. Spanderen, and J. Westphalen. "Evidence for Discrete Chiral Symmetry Breaking in N=1 Supersymmetric Yang-Mills Theory". *arXiv:hep-lat/9810062* (1998). arXiv: `hep-lat/9810062`.

[105] Michael G. Endres. "Dynamical Simulation of N=1 Supersymmetric Yang-Mills Theory with Domain Wall Fermions". *Phys. Rev. D* 79.9 (2009). arXiv: `0902.4267`.

[106] Joel Giedt, Richard Brower, Simon Catterall, George T. Fleming, and Pavlos Vranas. "Lattice Super-Yang-Mills Using Domain Wall Fermions in the Chiral Limit". *Phys. Rev. D* 79.2 (2009). arXiv: `0810.5746`.

[107] G. Fleming, J. Kogut, and P. Vranas. "Super Yang-Mills on the Lattice with Domain Wall Fermions". *Phys. Rev. D* 64.3 (2001). arXiv: `hep-lat/0008009`.

[108] The JLQCD Collaboration, S.-W. Kim, H. Fukaya, S. Hashimoto, H. Matsufuru, J. Nishimura, and T. Onogi. "Lattice Study of 4d {\cal N}=1 Super Yang-Mills Theory with Dynamical Overlap Gluino". *arXiv:1111.2180 [hep-lat, physics:hep-ph]* (2011). arXiv: `1111.2180 [hep-lat, physics:hep-ph]`.

[109] S. Piemonte, G. Bergner, and C. López. "Monte-Carlo Simulations of Over-lap Majorana Fermions". *arXiv:2005.02236 [hep-lat]* (2020). arXiv: `2005.02236 [hep-lat]`.

[110] Alan M. Ferrenberg, Jiahao Xu, and David P. Landau. "Pushing the Limits of Monte Carlo Simulations for the 3d Ising Model". *Phys. Rev. E* 97.4 (2018). arXiv: `1806.03558`.

[111] Frithjof Karsch and Martin Lütgemeier. "Deconfinement and Chiral Symmetry Restoration in an SU(3) Gauge Theory with Adjoint Fermions". *Nuclear Physics B* 550.1-2 (1999). arXiv: `hep-lat/9812023`.

[112] Mohamed M. Anber and Benjamin J. Kolligs. "Entanglement Entropy, Dualities, and Deconfinement in Gauge Theories". *J. High Energ. Phys.* 2018.8 (2018). arXiv: `1804.01956`.

[113] Mohamed M. Anber, Scott Collier, Erich Poppitz, Seth Strimas-Mackey, and Brett Teeple. "Deconfinement in N=1 Super Yang-Mills Theory on R$\hat{3}$ x S$\hat{I}$ via Dual-Coulomb Gas and "Affine" XY-Model". *J. High Energ. Phys.* 2013.11 (2013). arXiv: `1310.3522`.

[114] Mohamed M. Anber, Scott Collier, and Erich Poppitz. "The SU(3)/Z_3 QCD(Adj) Deconfinement Transition via the Gauge Theory/"affine" XY-Model Duality". *J. High Energ. Phys.* 2013.1 (2013). arXiv: `1211.2824`.

[115] Mohamed M. Anber, Erich Poppitz, and Mithat Unsal. "2d Affine XY-Spin Model/ 4d Gauge Theory Duality and Deconfinement". *J. High Energ. Phys.* 2012.4 (2012). arXiv: `1112.6389`.

[116] Giancarlo Cella, Giuseppe Curci, Raffaele Tripiccione, and Andrea Vicerè. "Scaling, Asymptotic Scaling, and Symanzik Improvement: Deconfinement Temperature in SU(2) Pure Gauge Theory". *Phys. Rev. D* 49.1 (1994).

[117] Pietro Giudice and Stefano Piemonte. "Improved Thermodynamics of SU(2) Gauge Theory". *Eur. Phys. J. C* 77.12 (2017). arXiv: `1708.01216`.

[118] Gwendolyn Lacroix, Claude Semay, and Fabien Buisseret. "The Deconfined Phase of ${\cal N}=1$ SUSY Yang-Mills: Bound States and the Equation of State". *arXiv:1408.4979 [hep-lat, physics:hep-ph, physics:hep-th]* (2014). arXiv: `1408.4979 [hep-lat, physics:hep-ph, physics:hep-th]`.

[119] Edward Witten. "Branes And The Dynamics Of QCD". *Nuclear Physics B* 507.3 (1997). arXiv: `hep-th/9706109`.

[120] A. Campos, K. Holland, and U.-J. Wiese. "Complete Wetting in Supersymmetric QCD or Why QCD Strings Can End on Domain Walls". *Physical Review Letters* 81.12 (1998). arXiv: `hep-th/9805086`.

[121] Mohamed M. Anber and Erich Poppitz. "On the Global Structure of Deformed Yang-Mills Theory and QCD(Adj) on $\mathbb R\hat{3} \times \mathbb S\hat{I}$". *arXiv:1508.00910 [hep-lat, physics:hep-th]* (2015). arXiv: `1508.00910 [hep-lat, physics:hep-th]`.

[122] Mohamed M. Anber, Erich Poppitz, and Tin Sulejmanpasic. "Strings from Domain Walls in Supersymmetric Yang-Mills Theory and Adjoint QCD". *Physical Review D* 92.2 (2015). arXiv: `1501.06773`.

[123] Erich Poppitz, Thomas Schaefer, and Mithat Unsal. "Continuity, Deconfinement, and (Super) Yang-Mills Theory". *Journal of High Energy Physics* 2012.10 (2012). arXiv: `1205.0290`.

[124] Erich Poppitz and Mithat Unsal. "Seiberg-Witten and "Polyakov-like" Magnetic Bion Confinements Are Continuously Connected". *J. High Energ. Phys.* 2011.7 (2011). arXiv: `1105.3969`.

[125] Mithat Unsal. "Magnetic Bion Condensation: A New Mechanism of Confinement and Mass Gap in Four Dimensions". *Physical Review D* 80.6 (2009). arXiv: `0709.3269`.

[126] Mikhail Shifman and Mithat Unsal. "QCD-like Theories on R_3\times S_1: A Smooth Journey from Small to Large r(S_1) with Double-Trace Deformations". *Phys. Rev. D* 78.6 (2008). arXiv: `0802.1232`.

[127] Mithat Unsal. "Abelian Duality, Confinement, and Chiral Symmetry Breaking in QCD(Adj)". *Physical Review Letters* 100.3 (2008). arXiv: `0708.1772`.

[128] Mithat Unsal and Laurence G. Yaffe. "Center-Stabilized Yang-Mills Theory: Confinement and Large N Volume Independence". *Phys. Rev. D* 78.6 (2008). arXiv: `0803.0344`.

[129] Georg Bergner, Stefano Piemonte, and Mithat Ünsal. "Adiabatic Continuity and Confinement in Supersymmetric Yang-Mills Theory on the Lattice". *arXiv:1806.10894 [hep-lat, physics:hep-th]* (2018). arXiv: `1806.10894 [hep-lat, physics:hep-th]`.

[130] G. Bergner and S. Piemonte. "Compactified N=1 Supersymmetric Yang-Mills Theory on the Lattice: Continuity and the Disappearance of the Deconfinement Transition". *J. High Energ. Phys.* 2014.12 (2014). arXiv: `1410.3668`.

[131] Shinji Ejiri, Kazuyuki Kanaya, and Takashi Umeda for WHOT-QCD Collaboration. "Ab Initio Study of QCD Thermodynamics on the Lattice at Zero and Finite Densities". *arXiv:1205.5347 [hep-lat]* (2012). arXiv: `1205.5347 [hep-lat]`.

[132] Christopher T. Hill and Elizabeth H. Simmons. "Strong Dynamics and Electroweak Symmetry Breaking". *Physics Reports* 381.4-6 (2003). arXiv: `hep-ph/0203079`.

[133] Georg Bergner, Pietro Giudice, Istvan Montvay, Gernot Münster, and Stefano Piemonte. "Lattice Simulations of Technicolour Theories with Adjoint Fermions and Supersymmetric Yang-Mills Theory". *arXiv:1511.05097 [hep-lat]* (2015). arXiv: `1511.05097 [hep-lat]`.

[134] Georg Bergner, Pietro Giudice, Istvan Montvay, Gernot Münster, and Stefano Piemonte. "Spectrum and Mass Anomalous Dimension of SU(2) Gauge Theories with Fermions in the Adjoint Representation: From $N_f=1/2$ to $N_f=2$". *arXiv:1701.08992 [hep-lat]* (2017). arXiv: `1701.08992 [hep-lat]`.

[135] Agostino Patella. "A Precise Determination of the $\psi\,\bar{}\,\psi$ Anomalous Dimension in Conformal Gauge Theories". *Phys. Rev. D* 86.2 (2012).

[136] A. Vladikas. "Three Topics in Renormalization and Improvement". *arXiv:1103.1323 [hep-lat, physics:hep-th]* (2011). arXiv: `1103.1323 [hep-lat, physics:hep-th]`.

[137] Georg Bergner, Pietro Giudice, Istvan Montvay, Gernot Münster, and Stefano Piemonte. "The Spectrum and Mass Anomalous Dimension of SU(2) Adjoint QCD with Two Dirac Flavours". *Phys. Rev. D* 96.3 (2017). arXiv: `1610.01576`.

[138] Margarita García Pérez, Antonio González-Arroyo, Liam Keegan, and Masanori Okawa. "Mass Anomalous Dimension of Adjoint QCD at Large N from Twisted Volume Reduction". *J. High Energ. Phys.* 2015.8 (2015).

[139] Jarno Rantaharju, Teemu Rantalaiho, Kari Rummukainen, and Kimmo Tuominen. "Running Coupling in SU(2) Gauge Theory with Two Adjoint Fermions". *Phys. Rev. D* 93.9 (2016).

[140] Thomas DeGrand, Yigal Shamir, and Benjamin Svetitsky. "Infrared Fixed Point in SU(2) Gauge Theory with Adjoint Fermions". *Phys. Rev. D* 83.7 (2011).

[141] Luigi Del Debbio, Biagio Lucini, Agostino Patella, Claudio Pica, and Antonio Rago. "Infrared Dynamics of Minimal Walking Technicolor". *Phys. Rev. D* 82.1 (2010).

[142] Joel Giedt. "Anomalous Dimensions on the Lattice". *Int. J. Mod. Phys. A* 31.10 (2016).

[143] Georg Bergner, Pietro Giudice, Istvan Montvay, Gernot Münster, Stefano Piemonte, and Philipp Scior. "Low Energy Properties of SU(2) Gauge Theory with N_f = 3/2 Flavours of Adjoint Fermions". *Journal of High Energy Physics* 2018.1 (2018). arXiv: `1712.04692`.

[144] Andreas Athenodorou, Ed Bennett, Georg Bergner, and Biagio Lucini. "The Infrared Regime of SU(2) with One Adjoint Dirac Flavour". *Phys. Rev. D* 91.11 (2015). arXiv: `1412.5994`.

[145] H B Nielsen and M Ninomiya. "(I). Proof by Homotopy Theory".

[146] H B Nielsen and M Ninomiya. "ABSENCE OF NEUTRINOS ON A LATTICE".

[147] Edward Witten. "Three Lectures On Topological Phases Of Matter". *La Rivista del Nuovo Cimento* 39.7 (2016). arXiv: `1510.07698`.

[148] D. Friedan. "A Proof of the Nielsen-Ninomiya Theorem". *Commun.Math. Phys.* 85.4 (1982).

Acknowledgements

Ehrenwörtliche Erklärung

Ich erkläre hiermit ehrenwörtlich, dass ich die vorliegende Arbeit selbständig, ohne unzulässige Hilfe Dritter und ohne Benutzung anderer als der angegebenen Hilfsmittel und Literatur angefertigt habe. Die aus anderen Quellen direkt oder indirekt übernommenen Daten und Konzepte sind unter Angabe der Quelle gekennzeichnet. Ergebnisse, die in Zusammenarbeit mit den Mitgliedern des Theoretisch-Physikalischen Instituts in Jena und der DESY-Münster Kollaboration entstanden sind, sind in der Arbeit entsprechend benannt.

Weitere Personen waren an der inhaltlich-materiellen Erstellung der vorliegenden Arbeit nicht beteiligt. Insbesondere habe ich hierfür nicht die entgeltliche Hilfe von Vermittlungs- bzw. Beratungsdiensten (Promotionsberater oder andere Personen) in Anspruch genommen. Niemand hat von mir unmittelbar oder mittelbar geldwerte Leistungen für Arbeiten erhalten, die im Zusammenhang mit dem Inhalt der vorgelegten Dissertation stehen.

Die geltende Promotionsordnung der Physikalisch-Astronomischen Fakultät ist mir bekannt.

Ich versichere ehrenwörtlich, dass ich nach bestem Wissen die reine Wahrheit gesagt und nichts verschwiegen habe.

Jena, 8. Juni 2020

Juan Camilo López Vargas